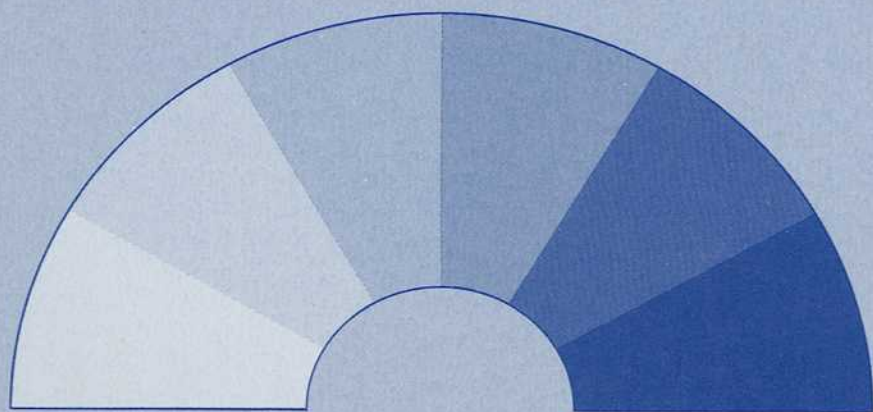


Review and Evaluation of Appearance

Methods and Techniques



Rennilson/Hale
editors

ASTM STP 914

REVIEW AND EVALUATION OF APPEARANCE: METHODS AND TECHNIQUES

A symposium sponsored by
ASTM Committee E-12 on
Appearance of Materials
Montreal, Canada, 23 May 1984

ASTM SPECIAL TECHNICAL PUBLICATION 914
J. J. Rennilson, Advanced Retro Technology,
Inc., and
W. N. Hale, Jr., Hale Color Consultants, Inc.,
editors

ASTM Publication Code Number (PCN)
04-914000-36



1916 Race Street, Philadelphia, PA 19103

Library of Congress Cataloging-in-Publication Data

Review and evaluation of appearance.

(ASTM special technical publication; 914)

"ASTM publication code number (PCN) 04-914000-36."

Includes bibliographies and index.

1. Materials—Sensory evaluation—Congresses.
 2. Materials—Appearance—Congresses.
 3. Specular reflectance—Congresses.
 4. Materials—Coloring—Congresses.
- I. Rennilson, Jay J. II. Hale, W. N. (William Nick), 1924- III. ASTM Committee E-12 on Appearance of Materials. IV. Series.
- TA418.5.R48 1986 620.1'1 86-7999
ISBN 0-8031-0480-4

Copyright © by AMERICAN SOCIETY FOR TESTING AND MATERIALS 1986
Library of Congress Catalog Card Number: 86-7999

NOTE

The Society is not responsible, as a body,
for the statements and opinions
advanced in this publication.

Foreword

The symposium on Review and Evaluation of Appearance: Methods and Techniques was presented at Montreal, Canada, 23 May 1984. The symposium was sponsored by ASTM Committee E-12 on Appearance of Materials. J. J. Rennilson, Advanced Retro Technology, Inc., served as chairman of the symposium and is coeditor of the resulting publication. W. N. Hale, Jr., Hale Color Consultants, Inc., is coeditor of the publication.

Related ASTM Publications

Sensory Evaluation of Appearance of Materials, STP 545 (1973),
04-545000-36

Compilation of ASTM Standards on Color and Appearance Measurement,
1984, 03-512083-14

A Note of Appreciation to Reviewers

The quality of the papers that appear in this publication reflects not only the obvious efforts of the authors but also the unheralded, though essential, work of the reviewers. On behalf of ASTM we acknowledge with appreciation their dedication to high professional standards and their sacrifice of time and effort.

ASTM Committee on Publications

ASTM Editorial Staff

Susan L. Gebremedhin
Janet R. Schroeder
Kathleen A. Greene
William T. Benzing

Contents

Overview	1
The Modes of Appearance and Their Attributes— RICHARD S. HUNTER	5
Psychometric Scaling of Gloss— FRANCIS X. D. O'DONNELL AND FRED W. BILLMEYER, JR.	14
Recent CIE Work on Color Difference Evaluation— ALAN R. ROBERTSON	33
A Colorimetric Determination of Dye Content on 100% Polyester Fabrics— LAURIE A. HAUCH, SUSAN GLICKSBERG, AND KWAN-NAN YEH	40
Measuring the Appearance of Retroreflectors by Application- Oriented Goniophotometry— NORBERT L. JOHNSON	49
Measurement of Color on Foods: Some Experiences at INTI, Buenos Aires— DAVID JUNGMAN, ROBERTO D. LOZANO, AND CRISTINA MELCÓN DE BELLORA	62
Specifying the Appearance of Escalator Treads: How to Minimize the Disorientation Effect— THEODORE E. COHN	69
Visual Color Technology Development for Industrial Applications— JAMES T. DEGROFF	78
On the Specification of Heterochromatic Brightness— WILLIAM B. COWAN	92
Index	103

Overview

The evaluation of appearance is as broadly based as any subject addressed by ASTM, being applicable to practically every raw material and finished product. While the major focus is on the production of consumer items that must have acceptable appearance as to color and gloss, appearance evaluation is also used with many nonconsumer products. For example, air contamination is graded by the appearance of filters, while contaminants in liquids is judged both by the appearance of filters and of the product itself.

Color is frequently an indicator of some important attribute of a product or material. Many medical laboratory tests are color-related. Color is a critical factor in the assessment of disease or of maturity in numerous agricultural products. The color of skin or tissue is closely related to health in humans and animals. The efficacy of suntanning products is evaluated by color, whether they purport to promote tanning or prevent it. A color test kit tells us if our swimming pool water has been adequately treated.

The industrial and commercial evaluation of appearance is both visual and instrumental. The unaided eye of an experienced observer is a widely used instrument for making color and gloss decisions, especially where photoelectric instruments are not feasible because of cost or portability. Augmenting the eye with material color and gloss standards, or with sets of standards that define acceptable tolerances, greatly improves such visual assessments. ASTM recognizes the value of visual judgments and provides, in ASTM Practice for Visual Evaluation of Color Difference of Opaque Materials (D 1729), guidelines for making such judgments.

Color and gloss measuring instruments continue to be improved in accuracy, precision, and their ability to handle a greater diversity of materials. As our understanding of color vision and visual color space increases, we are able to specify color order systems based upon uniform color scales; the same is now becoming true for visual gloss scales. The capability of instruments, using onboard computers, to transform their responses into these visual color order systems simplifies the setting of acceptability tolerances for product color. This leads to the automatic correction of colorant input and mixture to insure that acceptability is maintained throughout the production run.

Still, with all of our new knowledge, certain aspects of visual perception are not completely understood. Because instruments do only what we tell them to do, further advances in our understanding of perception are necessary before instruments can be designed to address some continuing problems. This STP

may be viewed as the third in a series of ASTM publications designed to provide the reader with a basic knowledge of the specification and evaluation of various appearance phenomena, along with examples of specific application of this knowledge to real-world appearance problems. The first was *Sensory Evaluation of Appearance of Materials, STP 545*, published in 1973. A compilation published in 1984 *ASTM Standards on Color and Appearance Measurement*, references 108 general appearance standards, and actually includes 34 of them. In addition, there are many other ASTM standards that address very specific examples of appearance evaluation that are not of general interest.

Continuing progress in the evaluation of appearance involves both visual and instrumental methods. No matter how sophisticated our instrumental methods become, we are always cautioned to never fail to "look at it." The eye of the skilled observer is unsurpassed for many appearance tasks, and correlates very well with the opinion of the ultimate inspector, the consumer. Progress in technology allows us to continually improve our assessment of traditional materials, while the emergence of new materials (for example, fluorescent and retroreflectors) present challenges to devise ways to deal with new and unusual optical characteristics.

The purpose of this volume is to present the fundamentals of the science of appearance measurement, along with recent research dealing with basic problems that impact upon a broad range of color and gloss specification and measurement efforts. Coupled with this broad-based review and update are papers describing recent applications of both old and new technology to appearance problems in science, industry, and the arts. While the applications cited will be useful to a limited number of readers, the papers describing appearance fundamentals should be of interest to everyone concerned with these broader, more comprehensive matters.

The lead-off paper by Hunter is an all too brief summary of the basic facts of color and gloss evaluation. Many books have been written on this subject, one of the best being by this same author who shares with us his more than 50 years of experience in this field. His comprehensive understanding of the psychophysical aspects of the subject have resulted in the design of many of the workhorse instruments in use today: colorimeters, spectrophotometers, and glossmeters. A knowledge of the interaction of color and gloss is basic to visual and instrumental evaluation. This paper presents it in summary form and allows the reader to determine the direction of further study.

A large part of industrial color work revolves around the specification of color tolerances. How closely should a color match its specification? This question is asked during the design and manufacture of every consumer product and of many others as well. Its answer should result in a product appearance that satisfies the buyer, produced at a cost acceptable to the seller. Robertson has been in the forefront of this work as chairman of the Committee on Color Difference Evaluation of the International Commission on Illu-

mination (CIE), the international body that sets standards in the light and color fields. Such ASTM standards as Methods for Instrumental Evaluation of Color Differences of Opaque Materials (D 2244) and Recommended Practice for Selecting and Defining and Color Gloss Tolerances of Opaque Materials for Evaluating Appearance (D 3134) implement the findings of this and similar committees. Color difference specification and evaluation operate within the field of color order systems. Robertson describes how the several attributes of such systems can be treated mathematically to bring some order to color difference and color tolerance work and shows that we still have a long way to go to bring this order.

Cowan's paper explores the relationship between luminance and perceived brightness. As he discusses the many parameters of this subject one can appreciate its complexity. While Cowan limits his treatise to the theoretical aspects of the matter, there are many important practical concerns relating to the quick and accurate perception of brightness in such critical areas as signals on aircraft instrument consoles and in a variety of military applications where zero error is practically mandatory. A great deal of research continues to be done in this field, and we are gradually increasing our knowledge of this critical relationship.

The complex field of specular reflectance, or gloss, is the subject of the paper by O'Donnell and Billmeyer. Gloss is separated into its many aspects, each are defined, and scales displaying equal visual intervals are derived for each. Just as visual scales for color are important to the work described by Robertson, visual gloss scales are needed to adequately describe gloss differences and to prescribe gloss tolerances. The fundamental ASTM method for gloss measurement is ASTM Test Method for Specular Gloss (D 523), originally approved in 1939; the present work on psychometric gloss scaling represents a major contribution to the work begun so long ago.

In the second part of this volume are reports of specific applications of color technology to industrial and agricultural situations. The last paper describes the modification of a very old color mixture technique to color representation, which could be very useful in the design field. Even though the specific subject matter may be outside the area of interest of a particular reader, the way that color technology has been applied to these problems may have useful ramifications in other areas.

The successful application of instrumental measurements to materials depends upon making the measurements under a regimen that duplicates as nearly as possible the actual use situation. This frequently means that the instrument must have illuminating and viewing geometry and observer conditions identical to some specific combination of light source, object, and human observer. When the product has unusual optical characteristics, this identity of conditions may be of particular importance. Johnson is a specialist in the measurement of retroreflective materials used in highway signs. In his paper he discusses a sophisticated approach to the assessment of the optical

characteristics of this unique material which, as its efficiency is improved, provides a continuing challenge to make the accurate measurements needed to employ it to its full potential for safety purposes.

The report by Jungman et al on color measurement of food involves some current applications of this very old subject. Fruits and vegetables are bought and sold on the basis of color, among other attributes. Color is not only related to consumer preference, but also to disease, maturity, and other factors. Color standards for food products are included in the regulations of many nations as a method of policing the market. Several states (California and Florida) also publish such rules. Government inspectors enforce marketing orders between buyers and sellers, insuring that color and other appearance standards are met. Color is an important marketing factor in the textile industry, and color quality control is basic to a fabric dyeing operation. Hauch describes how colorimetric analysis can be substituted for more expensive and time-consuming analytical methods. The highly competitive nature of this industry, world-wide, continues to inspire research projects resulting in more economical methodology. Safety is also the focus of Cohn's paper on the appearance of escalator treads, and how such appearance can be modified to reduce accidents caused by the visual illusions created by the moving treads. This is a completely different type of appearance evaluation than discussed elsewhere in this volume, and emphasizes the human engineering approach.

The designer faced with the problem of selecting colors for a package or product needs the widest selection of color samples he can find. He often utilizes very expensive collections of color standards and still wishes for more. DeGroff describes how the century-old Maxwell disk-mixture device has been automated to permit the operator to see, under different light sources, an unlimited variety of colors, selected by the operator. Not only can the colors be seen, but they also can be specified in technical terms and communicated to others, whether they also possess the color simulator or not. The designer with 500 or 1000 colors knows he wants more; now that he has millions at his fingertips he can concentrate on how best to use them. Are there other important applications for this million-color generator?

Discussions of theory and fact, delineation of general principles, and product specific applications all generate ideas that may be pertinent to a problem at hand. We hope this book will, for the novice, serve as an introduction to this very interesting subject of appearance evaluation. Those already working in this field will find the new material timely and worthwhile. Committee E-12 on Appearance of Materials hopes to hold future symposia to report further advances in the state-of-the-art.

J. J. Rennilson

Advanced Retro Technology, Inc., La Mesa,
CA 92041; symposium chairman and coeditor.

Nick Hale

Hale Color Consultants, Inc., Phoenix, MD
21131; coeditor.

The Modes of Appearance and Their Attributes

REFERENCE: Hunter, R. S., "The Modes of Appearance and Their Attributes," *Review and Evaluation of Appearance: Methods and Techniques, ASTM STP 914*, J. J. Rennilson and W. N. Hale, Eds., American Society for Testing and Materials, Philadelphia, 1986, pp. 5-13.

ABSTRACT: To evaluate the appearances of objects and materials, it is necessary to assess both color and geometric attributes of appearance. Color stimuli can be synthesized by mixing proper amounts of three primary colored lights to match visually any unknown. Color is thus tridimensional. By contrast, the geometric attributes (gloss, texture, and distinctness-of-image) cannot be synthesized. Instead, different perceived attributes are selected on the basis of best correlation of measurement results with visual ratings. The best measurement methods are identified by ASTM and other organizations. In practice, however, only the most obvious sources of geometric appearance differences can be measured.

Complete analyses of geometric appearance, based on all directions of light distribution, would be too cumbersome to be usable.

KEY WORDS: colors, diffuse reflection, specular reflection, appearance, deflection factors

Dr. Deane B. Judd at the National Bureau of Standards (NBS) in 1934 proposed a classification of the optical attributes which combine to identify the appearances of objects and materials. In 1961, ASTM published Judd's proposal as STP 297 [1]. If optical measurements are to identify appearances of objects and materials, a reproducible system, such as Judd proposed for identifying the modes of appearance, will have to be developed.

The modes of appearance relate to the geometric conditions of illumination and view. The principal modes, which are illustrated in Fig. 1, are as follows:

1. *Aperture:* The color is seen through a hole so that the observer is unable to identify the illuminant or objects involved or both. He can measure only the distribution of energy passing through the aperture.

¹Chairman of the Board, Hunter Associates Laboratory, Inc., 11495 Sunset Hills Rd., Reston, VA 22090.

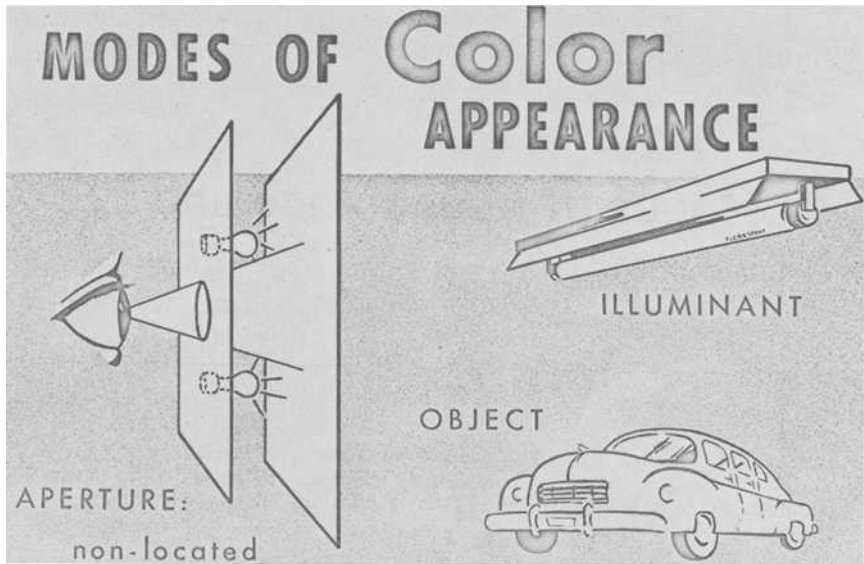


FIG. 1—The three modes of color appearance.

2. *Illuminant*: For lights and other self-luminous objects. Spectral and geometric distributions of light can be measured.

3. *Object*: The observer is conscious of both the object seen and its environment.

Our primary concern is with Mode 3, the object mode. Four submodes of the object mode are:

1. *Opaque, reflecting nonmetallic objects*: paint films, molded plastic objects, thick textile fabrics, papers, and so forth.

2. *Opaque metallic objects (bare metal surfaces)*: automobile bumpers and metallic trim.

3. *Translucent* (light-transmitting and reflecting) objects.

4. *Transparent* (clear) light-transmitting objects.

Table 1 [2] lists the appearance attributes of the four submodes (or classes) of objects and materials. It also gives their idealized geometric patterns of light distribution. Our concern, in the rest of this paper, will be with Submode 1, "Opaque, Reflecting Nonmetallic Objects," represented in Fig. 1 by the painted automobile.²

²Those who find and read the Judd reference [2] will note that Judd proposes five modes (whereas the present paper speaks of three modes and four submodes of the object mode) as follows: Modes listed by Judd are aperture, illuminant, volume, surface, and object. Modes listed by Hunter are aperture, illuminant, object, nonmetallic (opaque), metallic, translucent,

Thus, to describe the appearance of a painted automobile, the submode is opaque nonmetal, requiring assessment of color by diffuse reflection and high gloss by specular reflection. Although the object is primarily metal, optically it is the opaque coating over the metal that establishes the appearance and, therefore, its geometric submode, which is opaque nonmetal.

Geometric Conditions for the Measurement of Gloss and Color by Reflection

To explain the optical relationships between gloss and color of opaque non-metal surfaces, it is assumed that object-reflected light divides into two components:

1. First-surface or specular reflection. (Reflected light is projected in the direction or directions of mirror reflection.) The primary standard is the ideal perfect mirror.
2. Internal or diffuse reflection. (Reflected light is projected in all directions.) The primary standard is the ideal perfect white.

Specular reflection results from the initial contact of light with the surface of an object. Roughly, 4 to 10% of the incoming light is intercepted and reflected by the typical nonmetallic surface. This specular or mirror-like reflection is normally uncolored, that is, it is gray. The fraction of light reflected increases from about 4% at perpendicular incidence and average refractive index to perhaps 10% maximum. The fraction reflected will increase with an increase in refractive index or angle of reflection or both. It is significant that, even with dark objects, this initial-contact reflectance seldom drops below 4%.

The light that passes through the object skin or surface undergoes scattering or absorption within the body of the object. Some of this light returns to the surface and leaves as "diffuse reflection." By contrast with specular reflection factors, which do not vary markedly from light to dark objects, the internal or diffuse reflection factors run the whole range from zero (black) to almost 100% (white). Scattering (by small particles, fibers, pigments, and so forth) is responsible for the diffusion of light in all directions.

Directions in which beams of light strike an object, or leave the object toward a viewer, are measured from the perpendicular to the object surface. The directions of incidence come first; the directions of view follow. Thus, 45°/0° refers to a beam or beams incident on an object surface 45° from perpendicular; direction of object view is in the perpendicular (0°). The letter

and transparent. The writer's classification of modes is aimed at describing quantities that can be measured in order to identify appearances. It therefore lists individual modes by the groupings of attributes that will have to be measured to identify the appearances of specimens. The greatest difference between the Judd and Hunter classifications is the inclusion by Judd of the "Volume-Color" mode. Because procedures for measuring volume colors are not generally available, the writer failed to consider it in the present project.

TABLE 1—Idealized geometric distribution of light for four classes of objects and the major appearance attributes [2].

Object Class	Idealized Distribution of Light	Dominant Appearance Attribute	Other Appearance Attributes
Opaque non-metals Painted panel Ceramic tile Heavy fabric Pad of paper		Color (chromaticity and lightness): by diffuse reflection. Standard: Ideal white diffusor.	Gloss: by specular reflection. Standard: Perfect mirror.
Opaque metals Auto bumper Brass doorplate		Color (chromaticity and shininess): by specular reflection. Standard: Perfect mirror.	Haze or diffuseness: by diffuse reflection. Standard: Ideal white diffusor.
Translucent Plastic light enclosure Interior lighted sign		Color (chromaticity and lightness): by diffuse transmission. Standard: White diffuse transmission standard.	Gloss: by specular reflection and color by diffuse reflection. Standard: As above for opaque nonmetals.
Transparent Vegetable oil Sunglass lens		Color (chromaticity and transparency): by regular transmission. Standard: Clear air.	Gloss: by specular reflection; haze or turbidity by diffuse transmission. Standard: Perfect mirror.

“D” refers to uniform diffuse (hemispherical) incidence or projection. Uniform diffusion is normally achieved in instruments by exposure to the walls of a white-lined sphere. D_{SIN} refers to diffuse with specular included; D_{SEX} refers to diffusion with at least the central specular rays excluded.

Actually, directions of incidence and view may be interchanged without changing reflection factors, so long as both beam axes and cones of light spread within the beams are interchanged. This is sometimes referred to as the “Helmholtz reciprocal relation.”

If, as illustrated in Table 1, objects reflect light with either perfect diffusion or perfect specularity, appearance measurement reproducibility would be easy to achieve. In practice, most distributions of surface-reflected light show some approximations to the ideal geometries. However, they usually differ from the ideal significantly. Because of these departures from the ideal, one cannot expect reproducibility in measurements of either specular or diffuse reflection factors unless the measurements are made with identical geometries.

Normally, high-gloss surfaces are examined for color in manners that minimize specular projection of light to the eyes of the observer. Observers, examining such surfaces for color, will automatically position illuminant, object, and observer so that the surface’s uncolored specularly reflected light is not projected into the eyes. Under these conditions, the objects appear visually to be dark and saturated in color.

Conversely, low-gloss surfaces are likely to appear lighter and less saturated in color than high-gloss surfaces otherwise identical; because, with the low-gloss surfaces, some of the “specular reflected light” is spread so widely that it is added to the “diffuse.”

Choices of Geometry

The fraction of specular reflection in the total is much higher with dark colors than with light ones. Since this specular tends to be uncolored or gray, the chromaticities of dark objects are more changeable with change of geometric conditions of illumination and view than are the light ones.

D/0° Geometry versus 0°/45° for Diffuse Reflection

For the measurement of surface color, two geometric arrangements of incident and viewing directions are available. $D/0^\circ$ measures all of the light collected in the hemisphere of directions of reflection. Alternatively, the surface may be illuminated at 0° and viewed at 45° ($0^\circ/45^\circ$). The reciprocal conditions, 45° illumination and 0° viewing, are equivalent.

If one desires color measurements that represent normal visual practices, the $45^\circ/0^\circ$ geometry is preferred. The primary reason for the superiority of $45^\circ/0^\circ$ is that it seems to best represent the conditions normally selected by

technologists making visual intercomparisons of colors. It avoids, as far as possible, intrusions of any of the first-surface (specular) reflection.

On the other hand, one who is doing computer formulation of color by absorption and scattering coefficients, plus allowance for specular reflection, will probably choose the $0^\circ/D_{\text{SIN}}$ geometry. This is because the reflected light will include, as do most formulas for color by mixing ingredients, all of the reflected light, whether isolated in the specular (first contact) reflection or spread widely in the many diffuse directions.

The $D/0^\circ_{\text{(SEX)}}$ geometry is wholly free of specular only when the reflecting surface has high gloss and reflects all the specular light flux into the light trap. With most reflecting surfaces, some of the specular is included with the diffuse light. This added specular light makes measured colors lighter and less saturated than the colors of the same objects measured with $0^\circ/45^\circ$ geometry. Because of this changeable specular contribution, object color measurements should not employ the $D/0^\circ_{\text{(SEX)}}$ geometries for best reproducibility and correlation of instrument measurements with visual observations.

Experimental Verification of Gloss-Color Relationships

In order to demonstrate the variability of measured color with:

- (1) change of specimen gloss, and
- (2) change of instrument geometry,

eight molded plastic chips of eight different colors were measured. The two sides of each of the chips possessed the finishes shown in Fig. 2.

To make this figure, two dark green identical chips were chosen. With the dark color, it was possible to show (in a single photograph) both sides. One side of each chip was smooth and shiny, and one side had standard molded-in textures that made it low in gloss. Only the surface area with the lowest gloss was measured on the textured side.

Measurements were made with three instrument geometries on each side of each chip: $0^\circ/45^\circ$, $D_{\text{SIN}}/0^\circ$ (specular included), and $D_{\text{SEX}}/0^\circ$ (specular excluded). There were thus six color measurements of each chip.

The instruments used were a HunterLab D54 Spectrophotometer for D_{SIN} (specular included) and D_{SEX} (specular excluded) measurements. A Hunter LabScan I Spectrophotometer was used for $0^\circ/45^\circ$ measurements. The instruments were both programmed to give color in Hunter L , a , b . Results were plotted in a , b graphs, Figs. 3 and 4.

Note in Fig. 3 that, for each of the eight colors, the six a , b color values are located close to the respective straight-line radii from the 0,0 origin of the graph. Thus, the measured hue of each specimen remained nearly constant, while its saturation ($\sqrt{a^2+b^2}$) changed with changes of instrument geometry. Figure 4 shows only the measurements of the two most saturated colors, red and orange, in a small part of the a , b diagram. In this limited region of the a ,

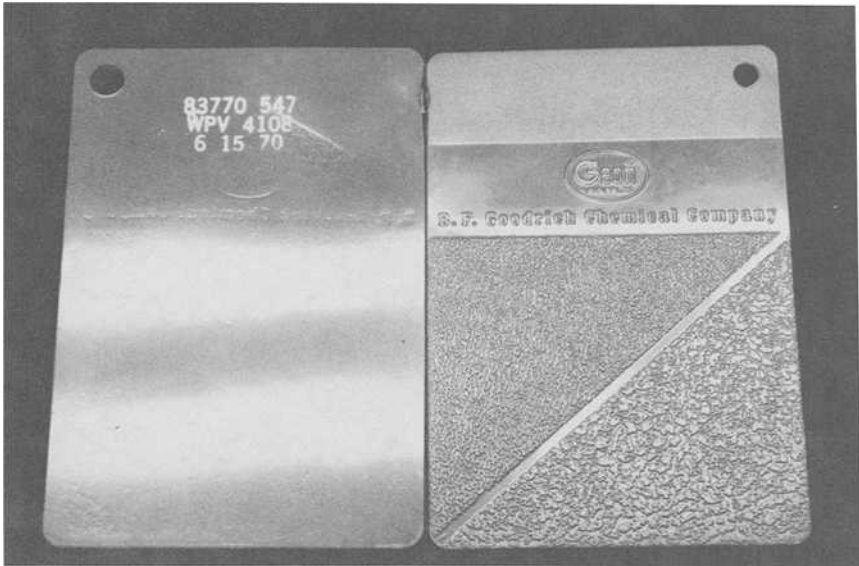


FIG. 2—Shiny (smooth) side and low-gloss (textured) side of molded plastic chips.

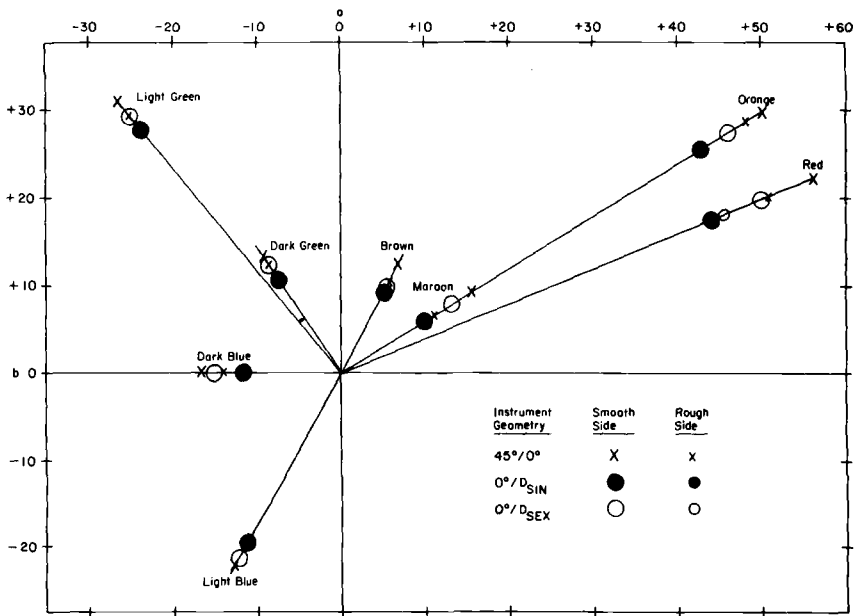


FIG. 3—Effect of spectrophotometer geometry on Hunter a, b color of eight molded plastic chips, each measured on glossy smooth side and on textured low-gloss side.

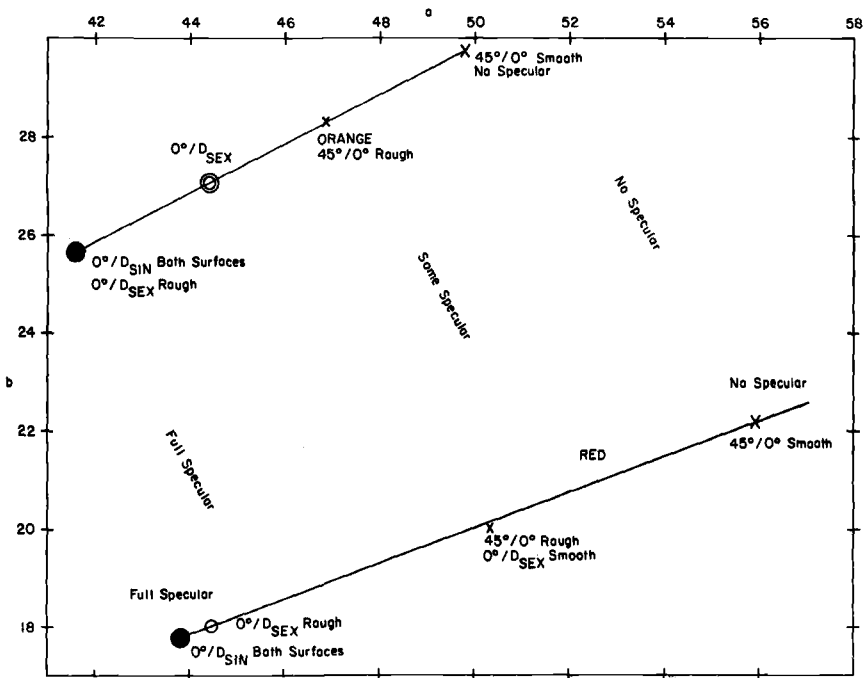


FIG. 4—Effect of spectrophotometer geometry on Hunter a , b color of red and orange molded plastic chips, each measured on glossy smooth side and on textured low-gloss side.

b diagram, the differences are magnified. Differences in a exceed twelve units for the saturated red and eight units for the saturated orange. These are large differences in measured color. For each colored plastic chip the color differences caused by geometry are greatest for dark saturated specimens.

Consistently, the $0^\circ/45^\circ$ values for glossy surfaces plot farthest from the gray center of the a , b diagram. The $0^\circ/45^\circ$ values for the corresponding matt surfaces plot closer to neutral, thus suggesting that a little specular gray light is being introduced as diffuse by the rough surface texture.

The $D_{SIN}/0^\circ$ values (specular included) show the full added contribution of gray specular reflection. Further, there were no significant differences between the two $D_{SIN}/0^\circ$ color values for the two sides of each chip. This suggests that, in spite of large gloss differences, the same amounts of light are reflected specularly from the two sides of each chip.

Conclusions

The optical measurements recommended for appearance identification of objects vary with the optical modes of the objects and the observing situation. With nonmetallic reflecting surfaces, which constitute the biggest fraction of

object-color measurements, $0^\circ/45^\circ$ geometry is recommended for best correlation with visual judgments of color.

$D_{\text{SIN}}/0^\circ$ geometry is widely used for color formulation by computation because of its insensitivity to gloss changes. With $D_{\text{SIN}}/0^\circ$ measurements, there is no need to change formulation equations as gloss is changed. However, appearance does change as gloss changes, suggesting that the $D_{\text{SIN}}/0^\circ$ measurements are not adequate for appearance measurement.

It must be remembered that precision decreases significantly where surfaces are dark in color and low in gloss. The $D_{\text{SEX}}/0^\circ$ geometry is not recommended for color measurement, because the light trap procedure for eliminating specular reflection fails with all but the glossiest surfaces to trap all of the specular reflection. In addition, small differences in focusing the 0° light beam are likely to introduce significant differences in specular inclusion and thus in measured color.

Diffuse color measurements by sphere with specular included (SIN) are easy to duplicate, even when surface gloss values differ. Visually, however, when compared for color, the $0^\circ/45^\circ$ values compare better to what is seen.

It appears that geometric variables are major contributors to the failures of color measurements to duplicate each other. If color and other appearance measurements are to be reproducible, tighter controls of the geometric conditions of illumination and view must be introduced.

The $D_{\text{SEX}}/0^\circ$ (diffuse, specular excluded) a , b values plot between the $0^\circ/45^\circ$ maximum saturation and the $D_{\text{SIN}}/0^\circ$ minimum saturation values. This intermediate color level indicates that the specular trap intended to collect all the specularly reflected light is, in fact, collecting only part of it. Where agreement between laboratories is required, $D_{\text{SEX}}/0^\circ$ should not be used.

References

- [1] Judd, B. J., *A Five-Attribute System of Describing Visual Appearance*, STP 297, American Society for Testing and Materials, Philadelphia, 1961.
- [2] Hunter, R. S., "Visually Perceived Attributes of the Appearance of Materials and ASTM Progress Toward Their Measurement," *Sensory Evaluation of Appearance of Materials*, STP 545. American Society for Testing and Materials, Philadelphia, pp. 18-34.
- [3] "Recommendations on Uniform Color Spaces, Color-Difference Equations, Psychometric Color Terms," Supplement No. 2 to CIE Publication No. 15 (TC-1.3), 1978, available from Klaus D. Mielenz, Secretary, USNC CIE, National Bureau of Standards, Washington, DC.

Psychometric Scaling of Gloss

REFERENCE: O'Donnell, F. X. D. and Billmeyer, F. W., Jr., "Psychometric Scaling of Gloss," *Review and Evaluation of Appearance: Methods and Techniques. ASTM STP 914*, J. J. Rennilson and W. N. Hale, Eds., American Society for Testing and Materials, Philadelphia, 1986, pp. 14-32.

ABSTRACT: Visual observations on gloss have identified approximately six types of gloss. To study the interrelations among these a method for the multidimensional scaling of gloss was devised. Two sets of painted specimens were examined. The first set covered a wide range of gloss using specimens that were a single grey color. The second set covered a more restricted range of gloss but consisted of black, grey, and white specimens. The results for these particular specimens under the particular viewing and illuminating conditions described yielded unidimensional interval scales. These interval scales were then correlated with the instrumental measurements obtained from the specimens. Equations relating the visual data to the instrumental data were derived.

KEY WORDS: gloss, senses, perception, psychometrics, multidimensional scaling, glossimetry

Visual observations on gloss have identified approximately six types of gloss [1,2]. These are as follows:

1. Specular Gloss. Perceived surface brightness associated with the luminous specular (regular) reflection from a surface. Because the eye cannot readily judge brightness in an absolute sense, specular gloss is usually judged by comparison between the brightness of the surface of interest and that of a reference surface, present either deliberately or fortuitously. Specular gloss is thus the result of an inter-specimen judgment. A small-area source of light against a dark background provides a suitable condition of illumination for judging specular gloss. The angles of illumination and viewing are not critical; any angle from 30° to 60° or over is generally satisfactory.

2. Sheen. Perceived shininess at a large angle of incidence seen in otherwise matte specimens.

¹Staff scientist, Diconix, a Kodak Company, P.O. Box 3230, Dayton, OH 45431.

²Consultant, 2121 Union St., Schenectady, NY 12309.

3. **Distinctness-of-Image Gloss.** The sharpness with which images are perceived after reflection from a surface. The conditions of illumination require a well-defined source with a black background. A black-velvet-backed fluorescent lamp with a coarse wire screen, as described by Hunter, provides suitable illumination [3].

4. **Contrast Gloss (Luster).** Perceived relative brightness of brighter and less-bright adjacent areas of the surface of an object, resulting from selective reflection in directions relatively far from those of specular reflection. Contrast gloss is thus an intra-specimen judgment of surfaces having low specular gloss. Suitable illuminating and viewing conditions are the same as those for specular gloss.

5. **Reflection Haze.** Perceived scattering of light reflected from a surface in directions near those of specular reflection. Reflection haze is observed in specimens with high specular gloss and, generally, high distinctness-of-image gloss. Often the haze appears bluish and the image reddish in comparison to similar areas of a haze-free specimen. A small-area source, either frosted or bare-filament, suspended in a darkened room, provides satisfactory illumination. The observer's eye should be focused on the specimen surface.

6. **Macroscopic Surface Properties.** Grouped under this heading are all the properties of a surface that can easily be seen without the aid of a high-power microscope. Surface properties, such as orange peel, directionality, and texture, are some examples of this type of phenomenon.

Specimen Selection

The task of scaling gloss can be extremely difficult because of the many variables that seem to contribute to the appearance of gloss. For this research several simplifying decisions were made:

1. No attempt would be made to scale the type of gloss associated with the macroscopic irregularities of a surface.

2. Only a single material system would be studied. The one chosen was a paint system as the gloss level could most easily be controlled with this system.

3. The paint was drawn down on aluminum plates, for greater usable lifetime, better flatness of the surface, and better stability compared to that of paper.

4. The color for the initial set of specimens was limited to grey. The second set consisted of a combination of black, grey, and white specimens. It was considered that the lightness component of a colored specimen would have the major effect on the perception of gloss, hence chromatic attributes were not considered.

Two sets of specimens were prepared. The first set consisted of 20 grey specimens varying from very low gloss to quite high gloss. The second set, which was prepared after some preliminary results were obtained with the

first set, consisted of 15 specimens. Five of the specimens were black, five were grey, and five were white. Four of the five grey specimens were ones used in the first experiment. The reasons for the reduced number of specimens in the second set were twofold. First, reducing the number of specimens by five halved the time to collect a complete set of data on them. Second, the preliminary results for the first experiment indicated that the range of gloss covered might be too large.

The paint used was Du Pont Lucite acrylic mixing lacquer. The gloss was controlled in two ways: the higher gloss specimens were produced by baking and the lower gloss ones by adding various amounts of flattening agent.

Experiment 1

In the first experiment the observer was presented all possible pair combinations of the grey specimens (190 pairs), a pair a time. From a duplicate set of specimens, prepared at the same time and from the same formulation as the 20 grey specimens, two specimens were chosen to act as an anchor pair. The purpose of the anchor pair was to increase the stability of the data by giving the observer a constant gloss difference to which to compare his or her judgments. The observer was shown the anchor pair and told to take the difference in gloss between its specimens as ten units. The grey test specimens were then presented to the observer, one pair at a time. The observer then gave an estimate of the gloss difference in the test pair, based on the difference seen in the anchor pair. If the difference in the test pair was less than that in the anchor pair, a number less than ten was given; if it was larger, a number greater than ten was given. Originally it was intended to use specimens at the ends of the chosen gloss range as the anchor pair, but the observers found the task of estimating the large gloss difference between them too difficult. The specimens finally chosen for the anchor pair had visually estimated gloss approximately one-third and two-thirds along the gloss range represented by the test specimens.

The specimens were viewed in a specially constructed booth using a modified desk lamp designed to help gloss judgements [3]. Eight sets of observations were obtained for this first experiment. The viewing and illuminating angles were fixed by setting the distance between the specimens and the lamp.

Experiment 2

The second experiment was similar to the first. The viewing and illuminating angles were set at 60° . The specimens used were the black, grey, and white set. This set exhibited a more restricted range of gloss, and so it was possible to select duplicates of the highest and lowest gloss specimens for use as the anchor pair.

Thirteen sets of observations were taken using these specimens.

Treatment of Data

The methods used to gather visual data on gloss in the past have been, for the most part, various forms of rank ordering. The task set for the observer was to arrange a set of specimens in order of increasing or decreasing glossiness. These methods usually only gave at best a one-dimensional ordinal scale. It was felt that the dimensionality of gloss should be investigated with the intention of obtaining a visual interval scale that would correlate well with the instrumental measurement of gloss. The technique chosen for this was that of multidimensional scaling (MDS).

MDS will optimally map similarity or dissimilarity data into spaces of various dimensionality. The programs are designed to minimize this dimensionality and will provide a measure of how well the solution in any particular dimension fits the data. The measure used is usually some form of a least-squares fit. The ones our programs used were called "stress" and "coefficient of alienation."

A simple example of what a MDS program is designed to do was given by Wish and Kruskal [4]. Given a map of the United States, it is a fairly trivial task to calculate the airline distances between the major cities. If, alternatively, one were given the airline distances for the major cities, but had no knowledge of what a map of the United States looked like, the task of reconstructing the map would be extremely difficult. MDS, given the airline distances, reproduces the map extremely well, except for a rigid rotation of the axes. That is, north and south, and east and west, may not lie on the y and x axes but may be rotated by some angle with respect to them.

Several different MDS programs were used in the analysis of the gloss data. These were KYST, MINISSA-1(M), INDSCAL, and PINDIS [5-9].

Results of the Analysis of the Visual Data

Grey Data Analysis

The first analysis performed on the data from Experiment 1 was that obtained by using MINISSA-1(M). The program was set to find the solution of least dimensionality for each of the eight data sets. All but two sets of data provided one-dimensional solutions. These two sets gave solutions in two and three dimensions. It is likely that in these two cases a one-dimensional solution is also the correct solution. The data were also analyzed by MINISSA-1(M) to provide solutions in three, two, and one dimensions. When the "stress" and "coefficient of alienation" were examined for the data sets that did not give one-dimensional solutions in the first analysis, the fit was found to be poor. There was no more information to be gained by going to solutions of higher dimensionality.

The eight data sets were then examined using the replicate option of

KYST. (In addition to analyzing a single data matrix, KYST will analyze several matrices together. It does this by taking the root-mean-square average of the dissimilarities over all matrices. It then analyzes this average matrix to find a space solution. The analysis of several matrices together is known as the replicate option.) Solutions were found in three, two, and one dimensions. The three-dimensional solution was found impossible to interpret in terms of gloss attributes. The two-dimensional solution, which was horseshoe-shaped, could be interpreted in terms of a high-to-low gloss dimension and a folded high-to-low gloss dimension (Fig. 1 and Table 1). The specimens in the figure are numbered 1 to 20 with 1 being the specimen of highest gloss and 20 being the specimen of lowest gloss. The ordering was based on the authors' own visual observations. In this case, by a folded gloss dimension we mean that in the plot shown in Fig. 1, the points may be split into two groups. On the negative side of dimension one, the samples 1 to 12 are ordered from high gloss to medium gloss, going from negative to positive in the direction of dimension two. The other samples, 13 to 20, are on the positive side of dimension one and descend from medium to low gloss in the negative direction of dimension two. It seems likely, however, that again the one-dimensional solution is the correct one.

INDSCAL was the next program used to examine the data. INDSCAL is a MDS program based on analysis of individual differences. It will analyze several input matrices. In addition to a group space solution, INDSCAL also provides a subject space solution. It allows each subject to attach dif-

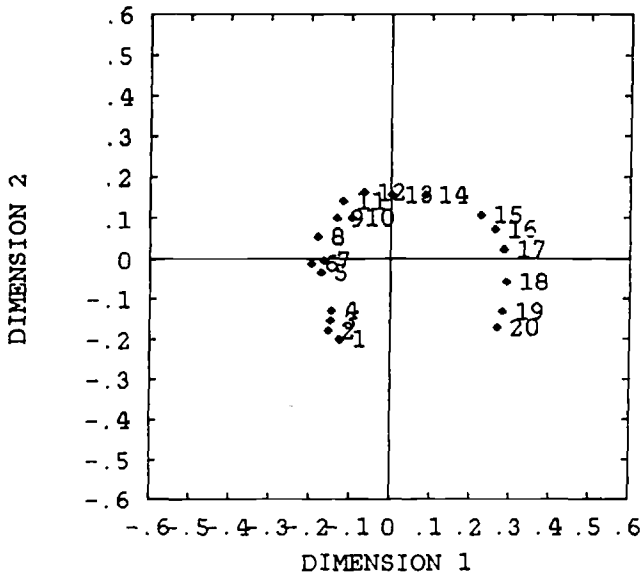


FIG. 1—Two-dimensional KYST group space solution for the data of the grey specimen set.

TABLE 1—Visual data for the grey specimen set, for the indicated MDS program, solution, and dimension.

Specimen	INDSCAL				KYST				PINDIS			
	2-Dimensional Solution		1-Dimensional Solution		2-Dimensional Solution		1-Dimensional Solution		2-Dimensional Solution		1-Dimensional Solution	
	Dim 1	Dim 2	Dim 1	Dim 2								
1	-0.262	-0.210	0.262	-0.201	-0.126	-0.201	0.289	-0.258	-0.111	0.284	0.284	
2	-0.256	-0.191	0.258	-0.180	-0.153	-0.180	0.276	-0.248	-0.092	0.270	0.270	
3	-0.240	-0.207	0.236	-0.155	-0.148	-0.155	0.256	-0.231	-0.073	0.249	0.249	
4	-0.213	-0.148	0.217	-0.130	-0.146	-0.130	0.240	-0.211	-0.079	0.238	0.238	
5	-0.151	0.003	0.181	-0.034	-0.172	-0.034	0.179	-0.178	-0.032	0.175	0.175	
6	-0.139	0.009	0.169	-0.012	-0.196	-0.012	0.166	-0.182	0.004	0.168	0.168	
7	-0.140	0.013	0.171	-0.004	-0.165	-0.004	0.154	-0.159	-0.011	0.153	0.153	
8	-0.113	0.051	0.147	-0.054	-0.181	-0.054	0.131	-0.145	0.015	0.135	0.135	
9	-0.062	0.119	0.103	-0.099	-0.133	-0.099	0.088	-0.098	0.040	0.086	0.086	
10	-0.052	0.111	0.090	0.100	-0.096	0.100	0.073	-0.078	0.038	0.074	0.074	
11	-0.046	0.114	0.083	0.141	-0.119	0.141	0.064	-0.075	0.048	0.067	0.067	
12	-0.012	0.133	0.048	-0.067	-0.067	0.162	0.028	-0.043	0.068	0.039	0.039	
13	0.028	0.130	-0.001	0.002	0.002	0.157	-0.015	0.003	0.036	-0.010	-0.010	
14	0.085	0.079	-0.082	0.086	0.086	0.156	-0.084	0.075	0.026	-0.076	-0.076	
15	0.178	-0.018	-0.216	0.226	0.226	0.107	-0.208	0.203	0.018	-0.203	-0.203	
16	0.224	0.006	-0.267	0.261	0.261	0.072	-0.250	0.248	0.025	-0.253	-0.253	
17	0.238	-0.032	-0.293	0.284	0.284	0.023	-0.285	0.278	-0.006	-0.282	-0.282	
18	0.258	-0.059	-0.324	0.291	0.291	-0.057	-0.329	0.321	0.026	-0.322	-0.322	
19	0.322	0.034	-0.377	0.281	0.281	-0.132	-0.375	0.379	0.013	-0.384	-0.384	
20	0.353	0.063	-0.405	0.269	0.269	-0.172	-0.397	0.399	0.045	-0.408	-0.408	

ferent significances (weights) to each dimension in the group space solution. INDSCAL gives an indication of how an individual's perception differs from the average for the group. If all the subject weights plot in the same region of the subject space, it may be assumed that the observers are attaching the same significance to each of the dimensions in the group space solution.

Solutions were obtained in three, two, and one dimensions. The three-dimensional solution was interesting in that it was possible to examine individual differences. The subject space solution (Fig. 2) indicates that, within the range of angles selected (30° , 45° , 60°), for these particular paint specimens, and under these particular illuminating and viewing conditions, the exact angle of view has little effect on the perception of gloss. It should be pointed out, however, that this is not the case for smaller angles, for instance less than 20° , or for larger angles, such as 75° or 85° . The numbers in the subject space refer to the following conditions: Numbers 1 and 8 were data sets obtained from the same observer, but Number 1 was obtained with viewing and illuminating conditions at 45° , while Number 8 was at 60° . Numbers 2 and 7 were data obtained at 30° and 60° , respectively, from a different observer. The other four were single sets obtained from different observers. Numbers 3, 4, and 6 were obtained at 30° , whereas Number 5 was obtained at 60° .

Although the INDSCAL two-dimensional group space solution is somewhat different in shape from the two-dimensional KYST solution, there are

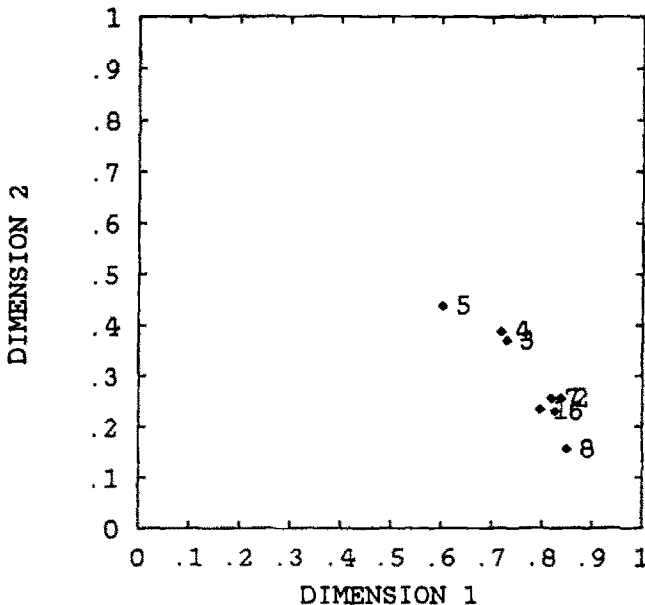


FIG. 2—Two-dimensional INDSCAL subject space solution for the data of the grey specimen set.

some similarities (Fig. 3). In both there is an area of medium-to-low gloss in which the solution seems to be unidimensional. The extremes of very high or very low gloss seem to provide the reason for the second dimension. Part of the output for the two-dimensional INDSCAL solution indicates that the two dimensions are not completely orthogonal. What this means is that the two dimensions are correlated with one another and that a solution of lower dimensionality is more appropriate. The one-dimensional solution from INDSCAL is very similar to the one-dimensional solution from the replicated KYST analysis. There is only one pair of specimens reversed in rank order, and these two specimens are perceptually very similar.

Finally, the eight solutions obtained from MINISSA-1(M) were examined using PINDIS (Fig. 4). The comparison to the INDSCAL and KYST group spaces shows a greater tendency to a single-dimensional solution. The deviations again occur with the high and low gloss specimens.

The one-dimensional PINDIS solution from the MINISSA-1(M) data was chosen for the comparison with instrumental data. It was chosen instead of the replicate KYST solution because KYST averages the various data matrices first and then finds the solution to this average data matrix. The MINISSA-1(M) and PINDIS combination finds the individual space solutions first and then finds the average of these for the group space. It was preferred to INDSCAL because INDSCAL makes the assumption that the input

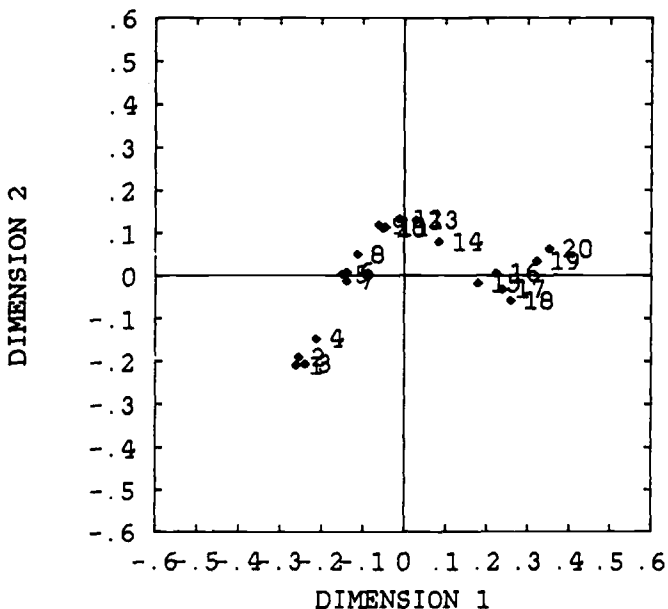


FIG. 3—Two-dimensional INDSCAL group space solution for the data of the grey specimen set.

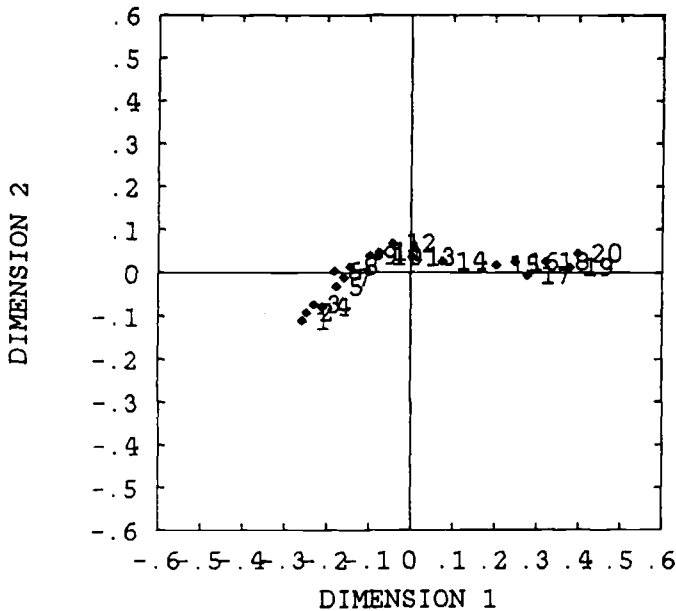


FIG. 4—Two-dimensional PINDIS group space solution for the data of the grey specimen set.

data are already in the form of an interval scale. The other programs, KYST and MINISSA-1(M), make the weaker assumption that the input data are ordinal scales. It should be noted that the solutions from all three programs may be regarded as interval scales.

Black, Grey, and White Data Analysis

The same analyses were performed on the 13 sets of data obtained from the black, grey, and white specimen set. The results are shown diagrammatically in Figs. 5 through 8 (see also Table 2). Figure 5 shows the two-dimensional solution obtained from the replicate KYST analysis. Specimens 1 through 5 were black with Specimen 1 having the highest gloss and Specimen 5 the lowest. Specimens 6 through 10 were grey, Specimen 6 having the highest gloss and Specimen 10 the lowest. Specimens 6, 7, 9, and 10 are the same as Specimens 9, 13, 16, and 17, respectively, used in the grey experiment. Specimens 11 through 15 were white, Specimen 11 having the highest gloss and Specimen 15 the lowest.

The two-dimensional KYST (Fig. 5) and INDSCAL (Fig. 6) solutions are similar to those of the grey set. It is interesting to note that with this particular black, grey, and white set of specimens there is no lightness dimension generated by the observers. This indicates that visual gloss judgements may sometimes be independent of lightness. It is certainly true for this particular set of

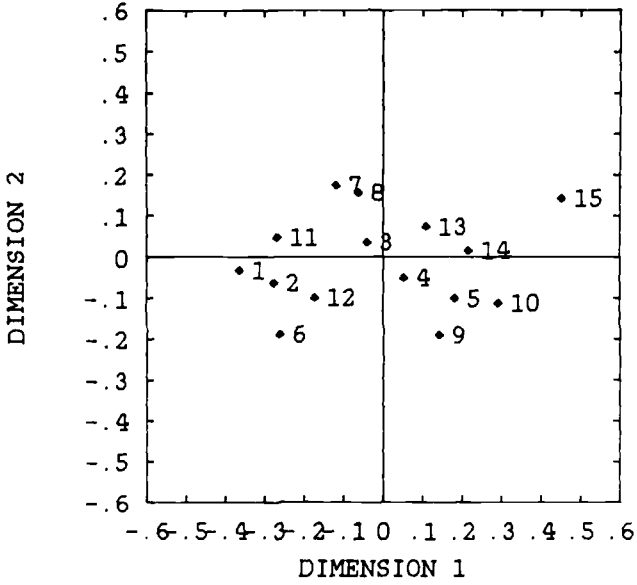


FIG. 5—Two-dimensional KYST group space solution for the data of the black, grey, and white specimen set.

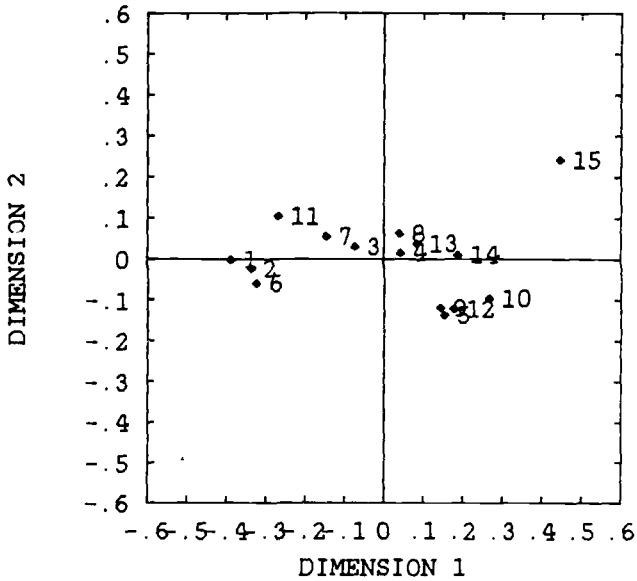


FIG. 6—Two-dimensional INDSCAL group space solution for the data of the black, grey, and white specimen set.

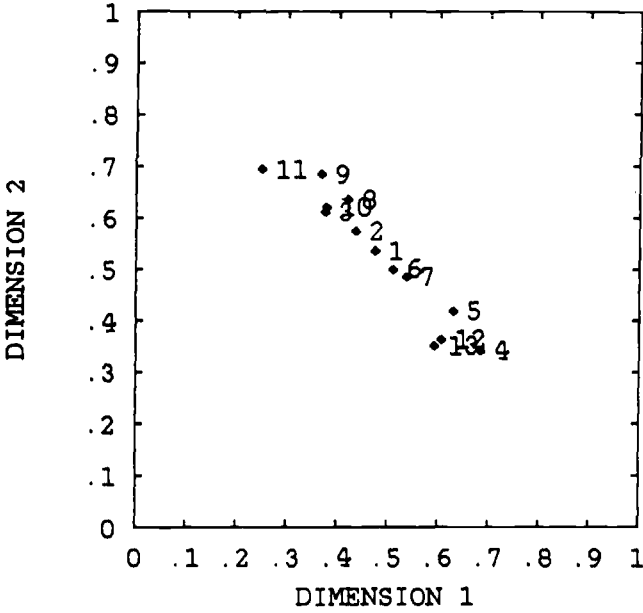


FIG. 7—Two-dimensional INDSCAL subject space solution for the data of the black, grey, and white specimen set.

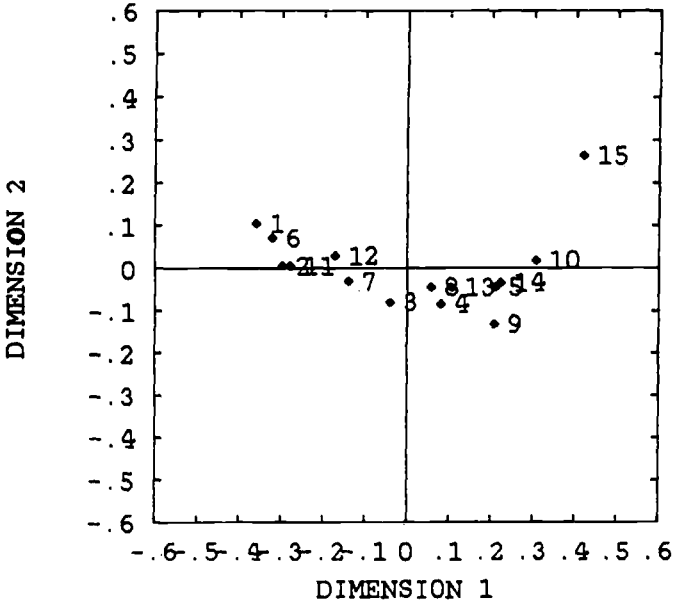


FIG. 8—Two-dimensional PINDIS group space solution for the data of the black, grey, and white specimen set.

TABLE 2—Visual data for the black, grey, and white specimen set, for the indicated MDS program, solution, and dimension.

Specimen	INDSCAL				KYST				PINDIS			
	2-Dimensional Solution		1-Dimensional Solution		2-Dimensional Solution		1-Dimensional Solution		2-Dimensional Solution		1-Dimensional Solution	
	Dim 1	Dim 2										
1	-0.388	-0.001	0.393	-0.364	-0.033	0.395	0.104	0.397	-0.359	0.104	0.397	0.397
2	-0.338	-0.023	0.339	-0.277	-0.063	0.302	0.005	0.304	-0.297	0.005	0.304	0.304
3	-0.074	0.030	0.055	-0.041	0.036	0.046	-0.080	0.035	-0.040	-0.080	0.035	0.035
4	0.042	0.016	-0.071	0.052	-0.050	-0.048	0.080	-0.077	0.080	-0.084	-0.077	-0.077
5	0.153	-0.137	-0.197	0.181	-0.102	-0.204	0.209	-0.203	0.209	-0.045	-0.203	-0.203
6	-0.325	-0.060	0.322	-0.263	-0.189	0.344	-0.321	0.338	-0.321	0.071	0.338	0.338
7	-0.147	0.055	0.136	-0.119	0.174	0.133	-0.140	0.141	-0.140	-0.031	0.141	0.141
8	0.039	0.062	-0.066	-0.063	0.156	-0.051	0.056	-0.051	0.056	-0.044	-0.051	-0.051
9	0.144	-0.119	-0.186	0.141	-0.191	-0.187	0.207	-0.184	0.207	-0.131	-0.184	-0.184
10	0.267	-0.096	-0.320	0.292	-0.113	-0.320	0.307	-0.326	0.307	0.018	-0.326	-0.326
11	-0.269	0.105	0.271	-0.269	0.047	0.263	-0.278	0.268	-0.278	0.005	0.268	0.268
12	0.177	-0.122	0.173	-0.173	0.099	0.177	-0.171	0.176	-0.171	0.029	0.176	0.176
13	0.084	0.038	-0.117	0.109	0.073	-0.102	0.105	-0.095	0.105	-0.045	-0.095	-0.095
14	0.188	0.011	-0.231	0.216	0.015	-0.231	0.222	-0.200	0.222	-0.034	-0.200	-0.200
15	0.445	0.241	-0.500	0.452	0.142	-0.516	0.420	0.523	0.420	0.263	0.523	0.523

specimens. Specimen 15 was the least glossy of the white specimens. We believe the reason it is set apart from the other specimens in the two-dimensional solutions is that little or no image was visible in this particular specimen. The other specimens all had at least some image visible. The two-dimensional INDSCAL solution again showed high correlation between the two dimensions.

The subject space for the two-dimensional INDSCAL solution is shown in Fig. 7. Data sets 6, 7, 9, 10, 11, and 13 were obtained with the anchor pair present when the judgement of the specimen pair was made. Data sets 1, 2, 3, 4, 5, 8, and 12 were data collected with the anchor pair removed before a judgement of the specimen pair was made. Data sets 1, 8, 9, and 10 were repeat data sets from a single subject. Sets 5 and 6, and Sets 4 and 7, were repeat data sets from two different subjects. The anchor pair was removed to test the effect the presence of the anchor pair had on the gloss judgement. From these results, the anchor pair is seen to have little effect, and therefore its presence is recommended as this makes the judgments easier for the observer.

The PINDIS analysis for the 13 individual two-dimensional analyses from MINISSA-1(M) again shows a great tendency toward unidimensionality (Fig. 8). Specimen 15 is again set apart from the other specimens. The solution from MINISSA-1(M) was again chosen for comparison with the instrumental data.

Instrumental Data

The grey set of specimens was measured with a 60° glossmeter (Table 3). The instrument used was a Pacific Scientific Gardner-Neotec Instrument Division Glossgard II 60° glossmeter. The highest measured gloss value was 82.87 and the lowest was 19.47. ASTM Test Method for Specular Gloss (D 523) recommends the use of the 60° glossmeter for the range between 70 and 10 gloss units. It was therefore decided to use the 60° glossmeter for comparison of these specimens with the visual scale. The 20° and 85° glossmeters would not be expected to produce a range of values as applicable as those from 60° instrument since they were designed for specific and limited gloss ranges.

The black, grey, and white specimens were also measured with the 60° glossmeter (Table 3). The highest measured gloss value in this case was 73.20 and the lowest was 37.23. The instrumental data are seen to be strongly dependent upon lightness. For example, Specimens 5 and 14 are seen by visual judgements (Table 2) to be very similar. Instrumental measurements, however, put them eight gloss units apart with the black specimen having the higher reading. Specimens 4, 8, and 13 show the same trend of being visually close but about 5 units apart by the 60° glossmeter measurements. Again, the black specimen had the highest reading and the white the lowest.

TABLE 3—*Instrumental data for the grey specimen set, the black, grey, and white specimen set, and their anchor pairs, for the indicated glossmeter.*

Grey Instrumental Data			<i>B, G, W</i> Instrumental Data		
Specimen	60° Glossmeter	Dori-gon D-o-I	Specimen	60° Glossmeter	Dori-gon D-o-I
1	82.87	91.54	1	73.20	73.44
2	82.00	92.92	2	68.50	54.90
3	79.03	86.27	3	60.80	30.60
4	76.27	90.80	4	55.43	19.90
5	64.23	87.07	5	50.00	8.03
6	65.07	83.12	6	58.97	63.47
7	65.80	80.32	7	57.10	34.93
8	62.67	73.14	8	50.63	23.67
9	58.57	63.90	9	47.93	9.85
10	61.87	57.77	10	41.33	6.70
11	62.03	56.17	11	56.87	64.35
12	56.60	47.02	12	53.70	44.22
13	56.67	35.12	13	44.90	18.07
14	53.33	26.57	14	42.17	10.43
15	48.37	16.23	15	37.23	4.25
16	47.67	9.82
17	41.03	6.67
18	34.10	3.15
19	27.80	1.53
20	19.47	1.20
				60° Glossmeter Dori-gon D-o-I	
	High gloss Grey anchor			55.13	40.72
	Low gloss Grey anchor			45.93	8.55
	Black <i>B, G, W</i> anchor			70.93	70.38
	White <i>B, G, W</i> anchor			37.37	4.65

Both sets of specimens were also measured using the Hunter Associates Laboratory Dori-gon (Model D47 R-6) distinctness-of-image gloss instrument. The readings are shown in Table 3. The Dori-gon readings used are those of distinctness-of-image gloss. It is also possible to obtain with this instrument measures of specular gloss at 30° and haze at 2°, 5°, and 15° from the specular angle. The distinctness-of-image gloss data reported in the table are those that gave the best rank ordering with the visual assessments.

Comparison of Visual Data with Instrumental Data

In Figs. 9 through 12, the Dori-gon and 60° glossmeter readings are plotted against the PINDIS one-dimensional visual solutions. The data for the black, grey, and white specimens may be fitted best with linear equations. No improvement was found by using polynomials of higher degree or by square-root or cube-root functions. A logarithmic function, likewise, gave no substantial improvement in the fit to the data. The fit to the Dori-gon data is greatly

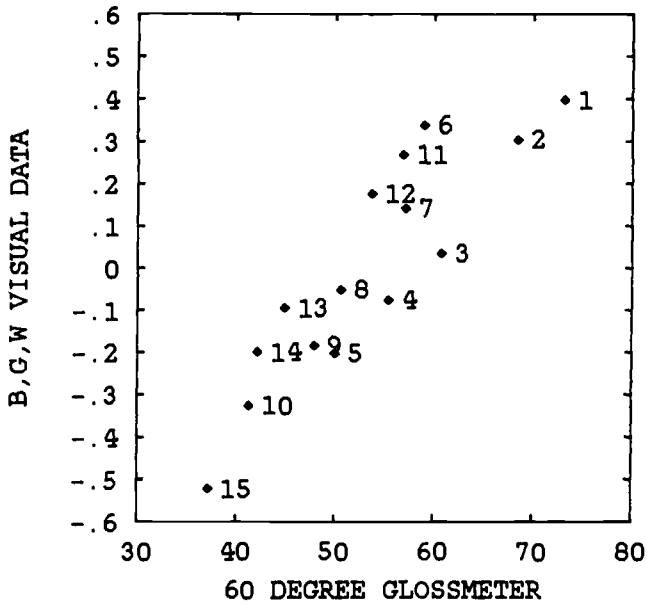


FIG. 9—PINDIS one-dimensional visual solution for the data of the black, grey, and white specimen set, plotted against the 60° glossmeter readings.

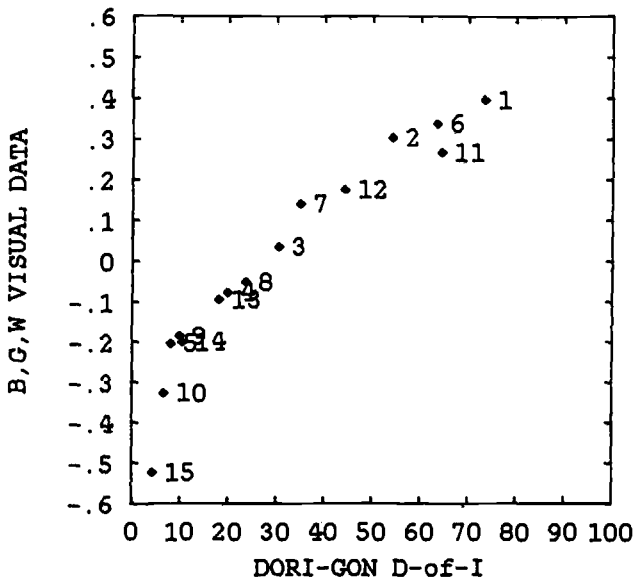


FIG. 10—PINDIS one-dimensional visual solution for the data of the black, grey, and white specimen set, plotted against the Dori-gon distinctness-of-image readings.

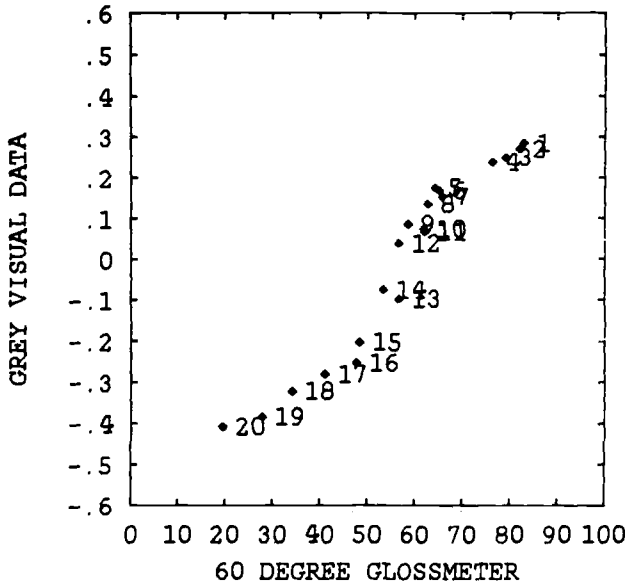


FIG. 11—PINDIS one-dimensional visual solution for the data of the grey specimen set, plotted against the 60° glossmeter readings.

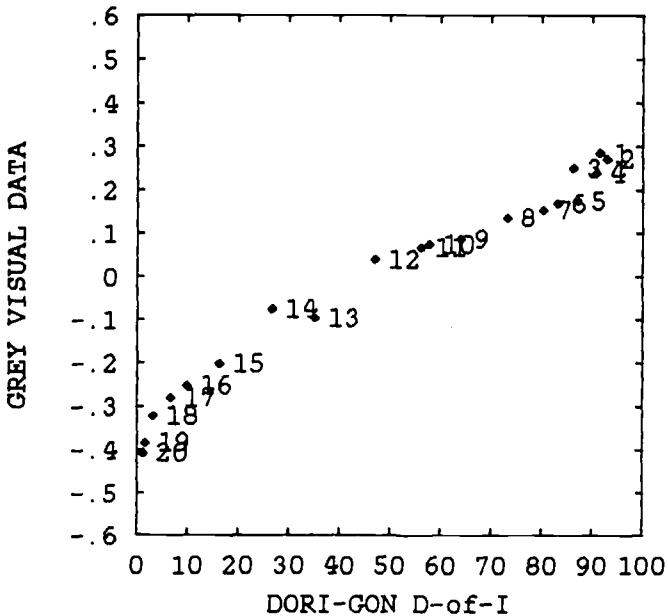


FIG. 12—PINDIS one-dimensional visual solution for the data of the grey specimen set, plotted against the Dori-gon distinctness-of-image readings.

improved if the data for Specimen 15 are excluded. This point is the one that was separated from all the other points in the two-dimensional visual solutions. The fit to the 60° glossmeter readings is not quite as good if a single linear equation is used, because of the separation of the specimens into black, grey, and white series. Three separate equations seem more appropriate for the fit to the visual data, one for each lightness level. The data for the white specimens are fit better if the data for Specimen 15 are again excluded.

The results with the wider gloss-range grey specimens are better fit with cubic polynomials, for reasons that are not clear. One explanation may be the nature of the anchor pair. The specimens used as the anchor pair were duplicates of Specimens 12 and 16. The specimens intermediate in gloss between these were probably judged relative to both of the anchors. The specimens with higher gloss than the anchor pair may only have been judged relative to the higher gloss anchor, and the specimens with lower gloss than the anchor pair may only have been judged relative to the lower gloss anchor. It is for this reason that the anchor pair should be picked at the upper and lower boundaries of the attribute to be scaled, if at all possible.

The equations for these solutions are given below. They were obtained using the BMDP series of statistical programs for the IBM 3033 computer. The numbers in parentheses at the end of the equations are the residual mean squares of the fit to the data.

For the black, grey, and white series, 60° gloss: $Y = B, G, W$ PINDIS one-dimensional solution; $X = B, G, W$ 60° glossmeter readings

$$Y = -1.145 + 2.174 \times 10^{-2} X (0.01502)$$

Black specimens only

$$Y = -1.557 + 2.676 \times 10^{-2} X$$

Grey specimens only

$$Y = -1.521 + 3.155 \times 10^{-2} X$$

White specimens only

$$Y = -1.589 + 3.012 \times 10^{-2} X$$

For the black, grey, and white series, distinctness-of-image gloss: $Y = B, G, W$ PINDIS one-dimensional solution; $X = B, G, W$ Dori-gon distinctness-of-image readings

$$Y = -2.876 \times 10^{-1} + 9.851 \times 10^{-3} X (0.00258)$$

For the grey series, 60° gloss: $Y =$ Grey PINDIS one-dimensional solution; $X =$ Grey 60° glossmeter readings

$$Y = + 2.182 \times 10^{-1} - 5.473 \times 10^{-2} X \\ + 1.397 \times 10^{-3} X^2 - 8.802 \times 10^{-6} X^3 (0.00147)$$

For the grey series, distinctness-of-image gloss: $Y =$ Grey PINDIS one-dimensional solution; $X =$ Grey Dori-gon distinctness-of-image readings

$$Y = - 4.096 \times 10^{-1} + 1.881 \times 10^{-2} X \\ - 2.783 \times 10^{-4} X^2 + 1.663 \times 10^{-6} X^3 (0.00048)$$

Conclusions

There are two areas in which this research has contributed to the study of gloss. These are the mathematical equations relating instrumental measurements to the visual observations and the methods by which they may be obtained.

The 60° glossmeter readings showed a lightness dependency, which means that three linear equations, one for each lightness level, were required to fit these readings to the visual data. The Dori-gon instrument does not show this lightness dependency, and so it would be the instrument of choice if the gloss of specimens with large lightness differences is to be compared.

The experimental method developed here gives a reliable method for obtaining a visual interval scale of gloss. The results obtained for these particular paint specimens and under these particular viewing and illuminating conditions indicate that their gloss may be regarded as unidimensional. The method but not necessarily the particular equations derived should be, however, equally applicable to other types of material specimens, such as paper or plastic. The only requirement is the capability of producing specimens covering a reasonable range of gloss in the particular material. It is hoped that future researchers will be able to use the methods we have developed to investigate different material systems.

Acknowledgments

We would like to express our appreciation to Hunter Associates Laboratory, Inc., and the Gardner-Neotec Instrument Division of Pacific Scientific for the loan of the gloss-measuring instruments, and to E. I. du Pont de Nemours and Co., Troy Laboratory, for supplying the paint used to make the specimens.

The funding for this research was provided by personal contributions from Mr. Richard S. Hunter, by the Gardner-Neotec Instrument Division of Pacific Scientific, and by Hunter Associates Laboratory, Inc., to all of whom we are very grateful.

This is Contribution 129 from The Rensselaer Color Measurement Laboratory, based on the Ph.D. thesis of F. X. D. O'Donnell, Department of Chemistry, Rensselaer Polytechnic Institute, Troy, NY, 1984.

References

- [1] Hunter, R. S., *Methods of Determining Gloss*, Proceedings 30, Part II, American Society for Testing and Materials, Philadelphia, 1936, pp. 738-806.
- [2] Christie, J. S., Chairman, "Evaluation of the Attribute of Appearance Called Gloss," CIE Technical Committee 2-07 on Gloss, Bureau Central de la CIE, Paris, 1986.
- [3] Hunter, R. S., *Appearance Attributes of Metallic Surfaces*, STP 478, American Society for Testing and Materials, Philadelphia, 1970, pp. 3-21.
- [4] Kruskal, J. B. and Wish, M., *Multidimensional Scaling*, Sage Publications, Beverly Hills, CA, 1981.
- [5] Kruskal, J. B., "Multidimensional Scaling by Optimizing Goodness of Fit to a Nonmetric Hypothesis," *Psychometrika*, Vol. 29, 1964, pp. 1-27.
- [6] Kruskal, J. B., "Nonmetric Multidimensional Scaling: A Numerical Method," *Psychometrika*, Vol. 29, 1964, pp. 115-129.
- [7] Lingoes, J. C., "An IBM-7090 Program for Guttman-Lingoes Smallest Space Analysis-1," *Behavioral Science*, Vol. 10, 1965, pp. 183-184.
- [8] Carroll, J. D. and Chang, J. J., "Analysis of Individual Differences in Multidimensional Scaling Via an N-Way Generalization of 'Eckart Young' Decomposition," *Psychometrika*, Vol. 35, 1970, pp. 283-319.
- [9] Lingoes, J. C. and Borg, I., "Procrustean Individual Difference Scaling," *Journal of Marketing Research*, Vol. 13, 1976, pp. 406-407.

Recent CIE Work on Color Difference Evaluation

REFERENCE: Robertson, A. R., "Recent CIE Work on Color-Difference Evaluation," *Review and Evaluation of Appearance: Methods and Techniques, ASTM STP 914*, J. J. Rennilson and W. N. Hale, Eds., American Society for Testing and Materials, Philadelphia, 1986, pp. 33-39.

ABSTRACT: Since the 1976 provisional recommendation of the CIELAB and CIELUV uniform color spaces and color difference formulae, a Committee of the Commission Internationale de l'Eclairage (CIE) has continued to work on the problem of color difference evaluation. In 1978 the committee published some guidelines in an effort to stimulate and coordinate research in the area. Following that, a number of studies were undertaken in which color difference ellipsoids were derived from observations of object colors. These studies have measured the effect (or lack of effect) of parameters such as the size of the color difference, the severity of the observer, and the type of dividing line between the samples. Other studies have shown that different relative weights for lightness, chroma, and hue indices may be needed for different viewing conditions and for different types of sample. Work planned for the next four years includes an attempt to assemble a single representative set of data with which color difference formulae can be tested.

KEY WORDS: colorimetry, CIE (International Commission on Illumination), color differences

Tristimulus values (X , Y , and Z) and chromaticity coordinates (x , y) in the Commission Internationale de l'Eclairage (CIE) system of colorimetry are used throughout the world to specify colors [1]. If two objects have the same CIE tristimulus values, an average observer will judge the colors of the objects to be the same. Unfortunately, if the two objects have different tristimulus values, there is no simple relationship between the differences in X , Y , Z and the perceived size of the difference in color. The distance, in CIE tristimulus space or in the CIE chromaticity diagram, between pairs of colors that are equally different from each other varies markedly with both position and direction in color space.

¹Senior research officer, Division of Physics, National Research Council, Ottawa, Ontario, Canada K1A 0R6.

Many experimental studies have been reported and recently reviewed [2,3] that provide data on how color discrimination varies through color space. Unfortunately, the studies do not always agree with each other, although exact comparison is made difficult by the rather large variability of the data.

In industrial applications, it is desirable to be able to calculate a number ΔE that represents the perceived size of the color difference between two objects whose tristimulus values are known. Many formulae (known as "color difference formulae") have been proposed for the calculation of ΔE , but even the best of the formulae are less accurate than is needed. Furthermore, it has not been possible to determine which of the many formulae is really the best because the experimental data, which the formulae are intended to fit, are very uncertain.

For many years the CIE has had a Committee on Color-Difference Evaluation. Currently, the committee is charged with stimulating and coordinating research on color difference evaluation so that eventually it will be possible to recommend a color difference formula that is significantly better than the currently recommended CIELAB and CIELUV formulae. The author has been chairman of this Committee since 1975.

CIE 1976 Color Difference Formulae

In 1976, in an attempt to promote uniformity of practice, the CIE recommended the use of two formulae [4,5] pending the development of a formula that would give substantially better correlation with visual judgments. The formulae are known as CIELAB and CIELUV and were chosen from among several of similar technical merit in the hope that the confusion caused by the simultaneous use of many different formulae could be overcome.

Unfortunately, the various industries and nations involved in the CIE could not agree on a single formula, but it was hoped that the recommendation of just two formulae of similar merit but different structure would go a long way towards unification of practice. It was predicted that preference for one or the other formula would be based mainly on convenience of use in particular industrial applications. This prediction has proved to be true. The CIELAB formula has been used widely in industries making colored products, such as paints, plastics, paper or textiles, whereas the CIELUV formula is used in the photographic, television, and video display industries mainly because it includes a chromaticity diagram in which additive mixtures of color stimuli plot on straight lines.

An advantage of both the CIELAB and the CIELUV formula is that quantities that correlate approximately with the subjective quantities lightness, chroma, and hue may be calculated easily. This allows a color difference to be broken up into three components, which correlate approximately with lightness, chroma, and hue differences. The total difference ΔE_{ab}^* in the CIELAB system is then given by

$$\Delta E_{ab}^* = [(\Delta L^*)^2 + (\Delta C_{ab}^*)^2 + (\Delta H_{ab}^*)^2]^{1/2}$$

where ΔL^* , ΔC_{ab}^* , and ΔH_{ab}^* represent differences in lightness, chroma, and hue, respectively. A similar equation exists in CIELUV with the subscript ab replaced by uv .

Since their recommendation in 1976, the use of CIELAB and CIELUV in industry has increased, and significant progress has been made towards the goal of unification of practice. Several authors [6-9] have compared the two formulae with each other, with other formulae, and with experimental data. These studies have confirmed that neither formula is ideal but have failed to provide any clear evidence that one is better than the other.

Guidelines for Coordinated Research

In 1978, the Color-Difference Committee of the CIE [10] published some *Guidelines for Coordinated Research* in the hope that researchers in the field would design their experiments to contribute in a coordinated way to the goal of the committee. Four steps were proposed and are being followed in the hope that they will lead eventually to a color-difference formula substantially better than CIELAB or CIELUV.

Step 1 is a study of methodology. Different methods are being used to collect and analyze data on color differences. Researchers are encouraged to include five particular colors in their experiments so that their results can be compared easily with each other.

Step 2 is the systematic study of the effect of different parameters. Parameters suggested for study are sample size, illuminance or luminance level, sample separation, texture, color of surround, luminance factor, size of color difference, observer variability, duration of observation, and monocular versus binocular viewing. Again, experimenters are encouraged to include five particular colors to facilitate comparison of their results.

Step 3 is a complete mapping of color-difference perception over the whole of color space for one set of viewing conditions.

Step 4 is the derivation of a formula to fit the data produced in Step 3, followed by field tests to validate the formula. It is anticipated that a successful formula will have to be based on a reliable theory of the visual system.

Ellipsoids and Ellipses for Object Colors

Data on color-difference perception are frequently presented as contours of equal perceived difference from selected test colors, plotted in a color space such as CIE x, y, Y space. These contours are usually assumed to be ellipsoidal in shape, and although this may not be exactly correct [11, 12], ellipsoidal contours are probably accurate enough for most practical purposes. In two-

dimensional cross sections of color space, such as the CIE chromaticity diagram, the contours are elliptical.

Several studies have been reported, both by members of the CIE committee and by others working independently, dealing with the derivation of ellipsoidal and elliptical contours from observations of object colors. These studies have contributed to Steps 1 and 2 of the "Guidelines."

Alder [13] investigated the distribution and number of test samples that are needed to determine a color-discrimination ellipse accurately. He concluded that 12 samples are enough if they are chosen carefully on the basis of preliminary experiments. On the other hand he found that less than half the data sets he studied from published reports were suitable for determining ellipses, nor do they test color difference equations as completely as may at first appear.

In a later report [14], Alder and coauthors described a series of studies involving gloss-paint and dyed-wool samples. They calculated chromaticity discrimination ellipses that form a fairly regular pattern in the x, y diagram. There are significant disagreements with other published sets of ellipses and with CIELAB.

Rich and Billmeyer [15] described the derivation of color difference ellipses for high-chroma blue and yellow acrylic lacquers. The ellipse orientations are independent of the size of the color difference from 0.5 to 1.5 CIELAB units.

Witt and Doring [16] described the derivation of a threshold ellipsoid based on observations of pairs of green acrylic-lacquer specimens by 25 observers. Different mathematical optimization techniques produced the same ellipsoids, but the ellipsoids of "severe" and "lenient" observers were found to differ slightly.

Strocka et al [17] used red dyed-acrylic-fabric specimens in a similar experiment. They reported that neither a black dividing line, the type of background (white or gray), nor the type of reference difference (gray or red in different directions of color space) affected the derived ellipsoid.

Weighting of Lightness, Chroma, and Hue Indices

Several attempts have been made to improve the correlation between the CIELAB formula and experimental data by changing the relative weighting of the lightness, chroma, and hue components. However, the optimum weightings vary from one study to another and appear to be a function of the type of sample being viewed. For example, McLaren [18] has suggested that, for textiles, CIELAB hue differences should be given the most weight and CIELAB lightness differences the least weight. This leads to a formula

$$\Delta E = [(\ell\Delta L^*)^2 + (c\Delta C_{ab}^*)^2 + (h\Delta H_{ab}^*)^2]^{1/2}$$

where $h > c > l$. However, for simulated object colors in a visual colorimeter, Robertson [9] found that ΔL^* should be given twice as much weight as ΔC_{ab}^* and ΔH_{ab}^* .

MacDonald [19] analyzed an extensive body of data on pass/fail decisions on textiles in terms of indices of lightness, chroma, and hue based on the ANLAB color difference formula. The ANLAB formula is sufficiently similar to CIELAB that McDonald's results would probably apply to CIELAB too. He found that ANLAB lightness tolerances varied with ANLAB lightness, that ANLAB chroma tolerances varied with ANLAB chroma, and that ANLAB hue tolerances varied with ANLAB chroma and ANLAB hue. He modified the ANLAB formula to produce an optimal fit to his data. McDonald's formula is known as "JPC79." It should be noted however that McDonald's study was of commercial acceptability rather than of perceptibility and that there is no general agreement over whether the two criteria are the same.

In a very recent paper, McLaren [20] has suggested some modifications (mainly smoothing and extrapolation) of the JPC79 formula and has given further evidence that different weightings of the lightness, chroma, and hue components are needed in different situations. He states that the modified formula is suitable for quantifying the perceptibility of small color differences.

Basic Research

Major improvements to the CIELAB and CIELUV system are likely to be achieved most readily by a formula based on a reliable theory of how the human visual system operates. For this reason, the CIE has continued to encourage basic research into color difference evaluation and the functioning of the visual system.

An example of such basic research is the work of Boynton and his colleagues [12], who analyzed chromaticity discrimination data in terms of absorptions in the three types of cone photoreceptors in the human retina. They found significant inter-observer differences that can be hidden or exposed by the method of plotting. They also found that the underlying components of color difference interact differently depending on their relative directions.

Future Work

During the next four-year CIE term (1983 through 1987), work will begin on Step 3 of the "Guidelines," the assembly of a representative set of data on color difference perceptibility covering the whole of object-color space. The committee will compare existing sets of data to determine whether they are

sufficiently compatible to be combined, and, if so, will merge them into a single representative set that can be used to test color difference formulae.

Conclusion

The CIE continues to work towards the recommendation of a color difference formula significantly better than the currently recommended CIELAB and CIELUV formulae. Progress is slow because the problem is a very complex one. Data on color discrimination are inconsistent because of imprecise techniques, because of the inherent variability of the visual process, and because of the influence of a large number of experimental parameters. Nevertheless, significant progress has been made in recent years and more is expected in the future.

The CIELAB and CIELUV formulae have become widely used, and the CIE's aim of unification of practice is being achieved. It is clear that both formulae are far from ideal and are of about equal technical merit as color difference formulae. Preference for one or the other in particular industries has been based on other considerations.

The CIE Color-Difference Committee has proposed a long-term four-step program towards the eventual derivation of a better formula. It is currently starting on Step 3, the specification of a representative set of data on color-difference perception.

References

- [1] Judd, D. B. and Wyszecki, G., *Color in Business, Science and Industry*, 2nd ed., Wiley, New York, 1975.
- [2] Robertson, A. R., *Die Farbe*, Vol. 10, 1981, pp. 273-296.
- [3] McDonald, R., *Journal of Oil Colour Chemistry*, Vol. 65, 1982, pp. 43-53 and 93-106.
- [4] *Official Recommendations on Uniform Color Spaces, Color-Difference Equations and Psychometric Color Terms*, CIE Publication 15, Supplement No. 2, Commission Internationale de l'Éclairage, Paris, 1978.
- [5] Robertson, A. R., *Color Research and Application*, Vol. 2, 1977, pp. 7-11.
- [6] Pointer, M. R., *Color Research and Application*, Vol. 6, 1981, pp. 108-117.
- [7] Ikeda, K., Nakayama, M., and Obara, K., *Journal of Light and Vision Environment*, Vol. 6, 1982, pp. 31-40.
- [8] Kuehni, R. G., *Color Research and Application*, Vol. 7, 1982, pp. 19-23.
- [9] Robertson, A. R., *Proceedings of the 18th Session CIE*, Paris, 1975, pp. 174-179.
- [10] Robertson, A. R., *Color Research and Application*, Vol. 3, 1978, pp. 149-151.
- [11] Kranda, K. and Kingsmith, P. E., *Vision Research*, Vol. 19, 1979, pp. 733-745.
- [12] Boynton, R. M., Nagy, A. L., and Olson, C. X., *Color Research and Application*, Vol. 8, 1983, pp. 69-74.
- [13] Alder, C., *Journal of the Society of Dyers and Colourists*, Vol. 97, 1981, pp. 514-517.
- [14] Alder, C., Chaing, K. P., Chong, T. F., Coates, E., Khalili, A. A., and Rigg, B., *Journal of the Society of Dyers and Colourists*, Vol. 98, 1982, pp. 14-20.
- [15] Rich, D. C. and Billmeyer, F. W., Jr., *Color Research and Application*, Vol. 8, 1983, pp. 31-39.
- [16] Witt, K. and Doring, G., *Color Research and Application*, Vol. 8, 1983, pp. 153-163.

- [17] Strocka, D., Brockes, A., and Paffhausen, W., *Color Research and Application*, Vol. 8, 1983, pp. 169-175.
- [18] McLaren, K., *Proceedings of the 18th Session CIE*, Paris, 1975, pp. 180-184.
- [19] McDonald, R., *Journal of the Society of Dyers and Colourists*, Vol. 96, 1980, pp. 372-376, 418-433, and 486-492.
- [20] McLaren, K., *Proceedings of the 20th Session CIE*, Paper D109, Paris, 1983.

A Colorimetric Determination of Dye Content on 100% Polyester Fabrics

REFERENCE: Hauch, L. A., Glicksberg, S., and Yeh, K.-N., "A Colorimetric Determination of Dye Content on 100% Polyester Fabrics," *Review and Evaluation of Appearance: Methods and Techniques, ASTM STP 914*, J. J. Rennilson and W. N. Hale, Eds., American Society for Testing and Materials, Philadelphia, 1986, pp. 40-48.

ABSTRACT: Colorimetric determinations of dye contents on polyester fibers evolved as a viable alternative to many hours of determining dye contents on fibers by Soxhlet extractions. Experimental work indicates a simple linear relationship between the amount of dye on the fabric and the color "appearance" of the fabric (as measured by a colorimeter). Varying dyeing procedures and dye carriers showed negligible effects on the correlation. Therefore, varying the penetration and fixation of the dye in the fiber were unimportant factors in this type of measurement. The established calibrations only relate to systems using identical fabric-dye combinations since both the dye and the fiber will affect colorimetric readings. The technique is applicable to any combination of fabric and dye (except pile fabrics), given the appropriate calibration. Where repeated determinations of dye contents on large quantities of similarly dyed fabrics will be required, colorimetric dye content determinations will save time and money.

KEY WORDS: colorimetry, polyester fabrics, disperse dyes, dye analyses, nondestructive tests

Existing dye analyses methods generally involve extraction of the dye from fabrics by a solvent and then measuring the dye concentration in solution by spectrophotometry. However, many disadvantages are associated with solvent extractions of this type. Consumption of time is the main drawback of extracting dyes with solvents. The accuracy of dye extractions can present prob-

¹Textile chemist, U.S. Army, Commander, CRDC, AMCCOM, DRSMC-CLW-PCA, Aberdeen Proving Ground, MD 21010.

²Building 9314, 7-Springs Apts., College Park, MD 20740.

³6-g Townridge Court, Baltimore, MD 21236.

lems depending on the given dye, solvent, or fiber. Also, dye extractions, such as soxlet extractions, usually destroy the entire sample.

The purpose of this study was to develop a nondestructive and time-saving method of determining dye contents on fabrics. Theoretically, there would be some type of relationship between the appearance of a fabric and the actual dye content on the fabric. This study shows that a direct relationship exists between the appearance of a fabric (as measured by a colorimeter) and the dye content on a fabric (as measured by a spectrophotometer). By using an established calibration for a particular dye, one may measure a fabric sample colorimetrically and then determine its dye content using an established equation.

Dyebaths of varying ingredients (including two different disperse dyes) were prepared to color the fabric samples. After dyeing, the colors of the samples were recorded on a colorimeter using the Hunterlab *L*, *a*, and *b* values. The dye was then removed from the fabric samples (using Janoušek's procedure, Ref 1) and their concentrations measured spectrophotometrically. Dye calibrations already exist for the Disperse Yellow 23 and Red 60 dyes used for this study. The dye concentrations were conveniently calculated using the acetone calibration formulas found in Tables 1 and 2. The entire procedure is simple, time-saving, and efficient.

Materials

Dyes and Fabric

Two commercial disperse dyes, Disperse Yellow 23 and Disperse Red 60, were used to dye a lightweight (140-g/m²) 100% spun polyester fabric.

TABLE 1—*Calibration of Yellow 23 in Acetone.*

Solution	Concentration, mg/l	Absorbance, 375 nm ^a
1	17.00	1.940
2	13.60	1.507
3	10.20	1.122
4	8.50	0.950
5	6.80	0.774
6	3.40	0.394
7	1.70	0.235
8	0.85	0.104

^a 375 nm, $C = (-.14) + 8.99 A$, m²/l; $1/ab = 8.99 \pm 0.13$; $Y = 0.9994$; $a = 111.23$ L/g·cm; and $E =$ molar extinction coefficient = 33.598 L/mole·cm.

TABLE 2—*Calibration of Disperse Red 60 in Acetone.*

Solution	Concentration, mg/L	A at 515 ^a	A at 550 ^b
1	0.80	0.028	0.024
2	1.81	0.067	0.057
3	2.66	0.101	0.085
4	5.32	0.202	0.171
5	6.98	0.300	0.252
6	10.64	0.406	0.343
7	13.30	0.503	0.424
8	15.95	0.606	0.511
9	18.61	0.705	0.593
10	21.27	0.803	0.678
11	23.93	0.903	0.759
12	26.59	1.008	0.851
13	29.25	1.110	0.936
14	34.57	1.296	1.096

^aAt 515, C (mg/L) = $1/ab(A) = 26.47(A)$; $1/ab = 26.47$; and coefficient = 0.99996.

^bAt 550, C (mg/L) = $1/ab(A) = 31.38(A)$; $1/ab = 31.38$; and coefficient = 0.99997.

Dye Carrier

Three commercial dye carriers were used throughout the study; two carriers contained varying amounts of biphenyl and the third carrier was composed of trichlorobenzene isomers.

Wetting Agent

The commercial wetting agent used for this study contained sodium-N-methyl-N-oleoyl-taurate.

Equipment

Two hundred sixty-six dyed fabric samples were evaluated by a Hunter Colorimeter (Model D252). The dye concentration on each fabric sample was measured by a Beckman Spectrophotometer (Model 25).

Sample Preparation

Two hundred sixty-six 30- by 22.5-cm fabric samples were scoured in water baths containing sodiumpyrophosphate. The samples were removed from the phosphate baths and rinsed with dilute acetic acid. After rinsing with acetic acid, the samples were rinsed with distilled water and left to air dry.

The disperse dye recipe used for this research simulates industrial atmospheric dyebaths. The dyebath ingredients and fabric samples were added accordingly to a 1-L water bath. The dyebath was boiled for approximately 45 min to allow penetration of the disperse dye into the fabric samples. After boiling, the dyebath was cooled to 71°C before the fabric samples were removed, scoured, rinsed, and then left to air dry.

Colorimetric Procedure

After dyeing, each air dried fabric sample was evaluated by a Hunterlab colorimeter in L , a , and b coordinates. The colorimeter was standardized by the Hunterlab yellow and pink reference tiles to obtain the smallest deviations from accepted reference levels for the yellow and red dyed fabric samples. According to the manufacturer, color values are accurate to a root-mean square deviation of 0.7 scale units only if deviations from the reference are small.

Every dyed fabric sample was measured three times to obtain individual average measurements. Each of the three measurements was taken at a different locality on the sample to eliminate dye leveling problems. The ΔE values reported for the samples originated from the recorded ΔL , Δa , and Δb values indicating the differences in individual color values between the dyed samples and the reference tiles.

Wet Chemistry Procedures

The quantity of disperse dye that penetrated each fabric sample was determined by Janoušeks dissolution procedure. A 2.5- by 2.5-cm² cut from each sample was weighed and then dissolved in a heated chlorobenzene/phenol solution. After cooling the solution, acetone was added to precipitate the polyester fiber. The clear acetone/dye solution was removed and the dye content measured by UV/VIS spectrophotometer. A spectrophotometric calibration was established for each dye, using the purified dye in acetone.

The concentration of dye on the fabric samples was calculated in the following manner:

1. Calculate average absorption value of the dye solution in the extraction flask.
2. Multiply the average absorption value by the calibration value for each dye to obtain the amount of pure dye in milligrams per litre.
3. Divide value from Step 2 by 20 to obtain the amount of pure dye in mg/50 m.
4. Subtract value from Step 3 from the weight of the 25.4- by 25.4-mm (1- by 1-in.) sample dissolved in the extraction flask to obtain the weight of the undyed 25.4- by 25.4-mm (1- by 1-in.) sample.

$$5. \frac{\text{Pure dye mg/50 ml}}{\text{undyed 1 by 1-in. sample weight (value from Step 4)}} = \frac{X}{\text{undyed fabric sample weight}}$$

X will equal the amount of pure dye per fabric sample.

6. Divide value from Step 5 or X by the weight of the undyed fabric to obtain the dye content in milligrams per gram.

Results and Discussion

Colorimetric Results

The total color difference ΔE between the dyed sample and the corresponding reference tile was calculated as $[(\Delta L)^2 + (\Delta a)^2 + (\Delta b)^2]^{1/2}$. As the color difference between the sample and the reference tile increases, ΔE increases.

TABLE 3—Dyebath average dye concentration of fiber (Disperse Yellow 23 dye) versus total color difference.

Bath	(D_f), mg/L	L	A	B	E	Dyebath Exhaustions, %
	0.0	78.2	-2.5	21.5	0.00	...
BP1	2.1	60.4	2.2	27.8	19.46	74.0
BP2	2.0	60.8	1.6	27.7	18.92	79.2
BP3	1.1	63.4	-2.9	23.4	14.93	29.4
BP4	1.6	62.1	-0.3	26.1	16.89	54.6
BP5	1.5	61.9	-0.5	26.3	17.11	47.5
BP6	2.1	58.9	2.9	27.5	20.92	72.1
PN6	1.5	62.2	0.1	26.0	16.82	63.8
BP8	2.0	61.0	1.2	27.6	18.62	69.5
BP9	3.1	58.0	5.8	29.9	23.40	94.5
BP11	3.1	58.1	5.4	29.8	23.14	94.1
BP12	2.9	57.8	6.6	30.2	23.97	93.1
BP13	3.0	58.1	5.9	29.6	23.24	93.3
BP14	3.0	58.0	5.4	29.4	23.08	90.0
TCB2	3.1	58.2	6.5	29.8	23.45	92.9
TCB3	2.6	59.3	5.3	29.4	21.92	92.6
TCBS-1	2.9	58.7	5.2	29.4	22.40	91.8
TCBS-2	2.7	59.6	4.8	29.6	21.56	91.2
TCBS-3	3.0	58.5	6.1	29.7	23.01	92.0
TCBG-3	3.0	58.4	5.3	29.3	22.67	93.1
TCBG-4	3.0	58.3	5.7	29.4	22.93	94.1
TCBG-5	3.1	58.4	5.6	29.3	22.77	94.8
TCBG-6	3.0	58.3	5.6	29.3	22.86	95.1
TCBG-7	3.4	58.3	6.0	29.4	23.04	94.3
TCBG-8	3.2	58.3	5.7	29.2	22.86	94.6
TCBG-9	3.0	58.2	5.6	29.3	22.94	92.9
TCBG-10	3.1	58.1	5.8	29.7	23.24	94.0
TCBG-11	2.9	58.5	4.8	29.2	22.38	93.3
TCBG-12	2.9	57.6	5.7	29.4	23.54	93.8

The calculated ΔE for each sample originated from the average L , a , and b values for each sample. Because of space limitations, only the dyebath average L , a , b , and ΔE values are shown in Tables 3 and 4 (note: the L , a , and b data for Disperse Red 60 dyed samples not available at this time). The dyebath average data shown in Tables 3 and 4 are the averaged colorimetric measurements of the four samples from each dyebath. According to Hunterlab, L defines the lightness of a color (on a scale of 0 to 100), a defines the redness-

TABLE 4—Dyebath average dye contents and total color differences Disperse Red 60 dye.

Dyebath	D_f	E
52	2.325	36.85
53	2.363	37.10
54	2.348	37.00
55	2.293	36.64
56	2.322	36.83
57	22.289	36.61
58	2.178	35.88
59	2.307	36.73
60	2.389	37.27
61	2.389	37.27
62	2.292	36.63
63	2.243	36.31
64	2.102	35.39
65	2.216	36.13
66	2.292	36.63
67	2.278	36.54
68	1.216	29.55
69	1.295	30.07
42	1.646	32.38
43	1.517	31.53
70	1.582	31.96
71	1.780	33.26
72	1.725	32.90
73	1.763	33.15
34	2.345	36.98
35	2.281	36.56
36	2.439	37.60
37	2.348	37.00
38	2.339	36.94
39	2.350	37.01
40	2.208	36.08
41	2.357	37.06
44	2.325	36.85
45	2.433	37.56
46	2.371	37.15
47	2.333	36.90
48	2.126	35.54
49	2.156	35.74
50	2.277	36.53
51	2.366	37.12

greenness of a color, and b defines the yellowness-blueness of a color. L values decrease, and a and b values increase as more dye exhausts onto the fabric sample. Also, as the colorimetric values increase, ΔE increases.

Dye Content on Fabrics

Dye contents on fabrics D_f (mg/g polyester fiber) are tabulated for the dyebath average values in Tables 3 and 4. The values for D_f were obtained using Janoušek's dissolution procedure followed by spectroscopic determinations of pure Yellow 23 and Red 60 dyes. The dyebath average D_f reflects the average dye content of the four samples per dyebath. More dye was exhausted onto the fabric samples at higher dyebath exhaustions (reflecting a higher D_f).

TABLE 5.—Regression of dyebath average data (disperse yellow dye) (D_f) = $A + B(\Delta E)$.^a

ΔE^b	D_{fC}	$D_f \text{ Calc}^d$	$D_f - D_f \text{ Calc}^e$	% Difference
19.460	2.100	2.150	-0.050	- 2.36
18.920	2.000	2.018	-0.018	- 0.88
14.930	1.100	1.042	0.058	5.29
16.890	1.600	1.521	0.079	4.93
17.110	1.500	1.575	-0.075	- 4.99
20.920	2.100	2.507	-0.407	-19.36
16.820	1.500	1.504	-0.004	- 0.27
18.620	2.000	1.944	0.056	2.79
23.400	3.100	3.113	-0.013	- 0.42
23.140	3.100	3.049	0.051	1.63
23.970	2.900	3.252	-0.352	-12.15
23.240	3.000	3.074	-0.074	- 2.46
23.080	3.000	3.035	-0.035	- 1.16
23.450	3.100	3.125	-0.025	- 0.82
21.920	2.600	2.751	-0.151	- 5.81
22.400	2.900	2.869	0.031	1.09
21.560	2.700	2.663	0.037	1.37
23.010	3.000	3.018	-0.018	- 0.59
22.670	3.000	2.935	0.065	2.18
22.930	3.000	2.998	0.002	0.06
22.770	3.100	2.959	0.141	4.55
22.860	3.000	2.981	0.019	0.63
23.040	3.400	3.025	0.375	11.03
22.860	3.200	2.981	0.219	6.84
22.940	3.000	3.001	-0.001	- 0.02
23.240	3.100	3.074	0.026	0.84
23.240	3.100	3.074	0.026	0.84
22.380	2.900	2.864	0.036	1.25

^a $N = 28$; Int (A) = -2.609; Slope (B) = 0.245; Coeff = 0.97346; (SD) Int = 0.244; and (SD) Slope = 0.011.

^b $\Delta E = X$.

^c $D_f = Y$.

^d $D_f \text{ Calc} = A + BX$.

^e $D_f - D_f \text{ Calc} = Y - (A + BX)$.

NOTE: Regression of individual data for disperse Yellow 23 dye: $N = 106$; Int (A) = 2.501; Slope (B) = 0.240; Coeff = 0.95345; (SD) Int = 0.161; and (SD) Slope = 0.007.

Dye Content on Fibers Versus Total Color Difference

The dyebath average data are summarized in Tables 3 and 4. All dyed samples were investigated for a D_f versus ΔE relationship. The average dyebath values and the individual values were tabulated and compared.

Linear regressions were performed on both the dyebath average and the individual average sample data. The data for the two dye systems were regressed in the form of $D_f = A + B(\Delta E)$ and are shown in Tables 5 and 6. The individual average values had lower standard deviations for the slopes. Overall, the difference between the standard deviations of the individual and dyebath average regressions were very small. All regressions performed during this study were found to have acceptable correlation coefficients, but the dyebath average D_f versus ΔE appears to have the slightly better correlation coefficient. Because the differences between the regressions were insignificant, either regression could be used.

The ΔE values for an undyed, white, control fabric were quite different compared to the ΔE s of the standard yellow and pink tiles. Comparing the ΔE values for the white control fabric to the ΔE values of the dyed samples is useless because of the extreme differences in color. The ΔE value shows only the color difference (in distance) between the two samples in a three-dimensional color space. The ΔE value does not indicate actual differences in color (shade) or color intensity unless the reference tile and the sample are the same shade of color. However, all the dyed samples are either yellow or red, so the resulting ΔE values indicate the total color differences between the sample as well as the color intensity among the yellow and red dye samples.

Summary and Conclusions

For each series of samples dyed with a given dye, a linear relationship was established between the dye content D_f and the total color difference ΔE .

TABLE 6—*Dye content versus total color difference (Disperse Red 60 dye).^a*

ΔE	D_f	D_f Calc	$D_f - D_f$ Calc	% Difference
29.300	1.150	1.177	-0.027	- 2.32
30.300	1.520	1.328	0.192	12.65
32.100	1.560	1.599	-0.039	- 2.52
32.900	1.660	1.720	-0.060	- 3.62
33.300	1.940	1.781	0.159	8.22
33.900	1.660	1.871	-0.211	-12.72
36.200	2.310	2.218	0.092	3.97
37.000	2.390	2.339	0.051	2.13
35.400	2.070	2.098	-0.028	- 1.33
32.300	1.500	1.630	-0.130	- 8.64

^a $N = 10$; Slope (B) = 0.151; INT (A) = -3.246; Coeff = 0.94746; (SD) INT = 0.601; and (SD) Slope = 0.018.

NOTE: $X = \Delta E$ and $Y = D_f$.

Using a least squares regression, a linear relationship $D_f = A + B(\Delta E)$, was obtained for both series of dyed samples. This empirical equation gave a standard deviation of ± 5 to 7% for both the yellow and the red dyed samples.

This simple and cost-effective procedure has been tested successfully using two dyeing systems. These equations may only be applied to systems with identical fabric, fiber, and dye combinations. Future applications of this colorimetric technique include studies on dye fastness, dyeing mechanisms, color-matching, and production control.

References

- [1] Janoušek, J., "Quantitative Determination of Disperse Dyes on Synthetic Fibers," *Textile Research Journal*, Vol. 40, 1970, p. 192.

Measuring the Appearance of Retroreflectors by Application-Oriented Goniophotometry

REFERENCE: Johnson, N. L., "Measuring the Appearance of Retroreflectors by Application-Oriented Goniophotometry," *Review and Evaluation of Appearance: Methods and Techniques, ASTM STP 914*, J. J. Rennilson and W. N. Hale, Eds., American Society for Testing and Materials, Philadelphia, 1986, pp. 49-61.

ABSTRACT: Evaluating the appearance of retroreflectors involves the application of the basic principles of appearance measurement. It is typical of many appearance measurement problems in that it involves a source (or sources) of illumination, a viewer, and an object or surface of concern. The objective is a numerical description of the appearance properties of the material. For such descriptions, the measurement geometry must be established, the spectral conditions considered, and meaningful appearance related quantities agreed upon.

In the measurement technique described here, computers are used to control the instrumentation for geometric and spectral analysis while simultaneously calculating appearance related quantities, along an appropriate application parameter. A shoulder mounted retroreflective road sign is the example considered, and the application parameter is the distance from vehicle to sign. Local viewing and illuminating geometry are translated into a laboratory measurement coordinate system. These transformations are made at distances corresponding to the incremental motion of a vehicle along the roadway. From these application-oriented measurements, intrinsic photometric results are calculated and displayed in terms of quantities such as coefficient of retroreflection. Once the material characteristics are measured, along the application parameter, additional analysis using the actual illuminating source can be completed. In the case of the retroreflector, the luminance in the direction of the viewer is an important result. Evaluation based on practical viewing conditions provides a useful insight into appearance without the necessity of completely describing the spectragoniophotometric properties of the retroreflector.

KEY WORDS: goniometers, retroreflectors, luminance, appearance, application parameter, coefficient of retroreflection, entrance angle, goniophotometry, observation angle, retroreflectance, retroreflection, rotation angle

¹Physics specialist, 3M Co., 3M Center 582-1-16, St. Paul, MN 55119.

Today the modern computer offers new opportunities to the appearance analyst. He is no longer limited to oversimplification in describing appearance properties and is potentially able to fully analyze the appearance characteristics of materials. So far the use of computers in appearance analysis in commercial instruments has been mostly limited to analysis of spectral data in terms of various color order systems. Programming is beginning to be developed to describe the geometric characteristics of materials such as the example of a retroreflective material presented here.

Even though this paper describes the procedures and outlines the programming steps necessary to analyze the appearance of retroreflectors, the same basic principles apply to goniophotometric measurements associated with appearance measurement of other materials. Attributes such as gloss, the metallic appearance of paint surfaces, textile texture appearance, and other geometric related properties are examples where application oriented goniophotometry can be potentially useful.

With the availability of low-cost computers and computer controlled goniometers, it is now possible to compute the geometric measurement conditions, execute the physical measurement, and transform this measurement into the final appearance characteristic of interest, all in a single instrument system. This is the technique described as "application oriented goniophotometry" in this paper. Such techniques offer a significant advance over conventional goniophotometric instrumentation and fixed geometry spectrophotometers, since more realism is achieved, and only measurements of actual interest to the end application need to be made.

General Principles of Appearance Measurement

The general principles of appearance measurement involve consideration of a number of factors. These include an understanding of the material properties (both geometric and spectral), an assessment of the source or sources of illumination, and an understanding of the observer or observers. Ideally the material properties should be understood in terms of spectral reflectance properties under all geometric conditions of illumination and viewing. The source of illumination needs be known spectrally and geometrically. The physical adaption (spectral responsivity), state of adaption, visual acuity, and other observer information is required. Measurement results can then be scaled in terms of appearance quantities, such as brightness, color, gloss, and even in more complex user appearance quantities such as legibility or target value for the retroreflective materials.

Geometric Systems

To describe the properties of a material, one must first specify the geometric system to be used. Generally a minimum of four angles are required. In

real measuring instruments one must also consider instrument apertures relative to source, receptor, and test materials.

Depending on the end application, the choice of the four angles needed may vary. For example, in typical color measurements of flat diffusing surfaces, a geometry in terms of the illumination, viewing, azimuthal, and rotation angles are defined (see ASTM Recommended Practice for Selection of Geometric Conditions for Measurement of Reflectance and Transmittance [E 179]). The geometry for measuring retroreflection in ASTM Practice for Describing Retroreflection (E 808) describes the entrance angle in two components, observation angle and rotation angle. National Bureau of Standards (NBS) Monogram 160 [1] describes these in the more general form of the bidirectional reflectance distribution function. One can generally transform between coordinate systems provided they are described completely.

Traditional Goniophotometry

In traditional goniophotometry, a geometric coordinate system is selected and then one of the angles is varied while the remaining three are fixed. ASTM Recommended Practice for Goniophotometry of Objects and Materials (E 167) shows typical reflectance curves as the viewing angle alone is varied. In abridged goniophotometry there is often a tendency to ignore the influence of certain angular parameters. In some cases this is because experience has shown them to be unimportant, in other cases they are simply assumed to be unimportant. Sometimes multiple scans are made at selected fixed settings for the remaining angles. To fully characterize the goniophotometric properties of complex materials, a tremendous number of measurements are required. For example, if only 20 points are measured along each of the four angular parameters, a total of $20 \times 20 \times 20 \times 20 = 160\,000$ data points are needed to fully describe the reflectance of the material. In practice, if reflectance is rapidly changing, 20 readings along any one angular parameter may not be sufficient. The number of readings may be reduced when it is certain that varying a particular angular parameter is not crucial. However, if we combine the 160 000 geometric settings with a minimum of 16 spectral measurements for color determination, the full material characterization requires over $2\frac{1}{2}$ million data points for a single specimen. This is a large amount of data by any standard and probably beyond the capability of small laboratory measurement computers to handle in a reasonable length of time.

Application-Oriented Goniophotometry

The concept of application-oriented goniophotometry provides a method for shortcutting the complete goniio-spectral characterization of the material when the material is to be used in a specific application. In application-oriented goniophotometry, instead of fully characterizing the material proper-

ties, the practical use application is analyzed in terms of a new single independent variable. In practice this generally involves the use of a local coordinate system suitable to the application. The local coordinate system describes the location of the source (or sources) of illumination, the observer position, and a point (points) on the test material surface. In the Cartesian coordinate system, three coordinates are required to locate the source, observer, and test point with additional sets of coordinates needed to express the orientation of the source, observer, or test specimen. Once the application geometry is determined a computer program may be written to transform the local application description into a set of coordinates suitable for measurement. Then the single application parameter is varied. In the example of the retroreflective material used here, this application parameter is the distance of a vehicle and driver from a retroreflective sign material measured along the center of the roadway. Now each of the four angles required for measurement become dependent variables as the application parameter is varied. This generates a series of angular parameters dependent on distance (the application parameter).

In a more general case, we can apply this technique to viewing a large surface, with the illumination source (sources) fixed and the viewer fixed. In this case the application parameter can be considered as a set of points on the surface covering the area of interest. Using these points as the independent application parameter, measurement angles can be calculated in terms of the geometry of the measuring goniophotometer, and the resulting reflectances determined for the specific application.

Applying the Concept

In applying this concept to retroreflective materials a small computer was employed. As the application parameter distance is varied, the program determines local coordinates, instrument measurement coordinates, and measures and records the photometric values. For complete analysis for each point, the spectral values are measured. This concept reduces the number of points needed to characterize a material's properties for a given application. Measurements are made only at the angular positions of interest in the application. Multiple applications may be required to describe the use of a given material. Even so, the total amount of data needed is greatly reduced. For example, if 20 different multiple application parameter sets of 20 points each are selected, this means that only 400 of the 160 000 combinations is required thus reducing 2½ million data points to a few thousand.

As the physical measurements are completed, visual appearance properties may be computed simultaneously, from the physical measurements.

Retroreflector Example

Historically in the goniophotometric analysis of retroreflectors, individual scans were made by varying a single angular parameter such as the observation angle α or the entrance angle β on a goniometer and the results plotted. The use of the application parameter provides a combined calculation of application angles and measurements as well as the resulting analysis in terms of luminance (brightness) as seen by the viewer in practice.

Retroreflector Local Coordinates

In the retroreflector example, a local coordinate system is established along the roadway. For simplicity of illustration, a straight roadway is used, but the techniques should not be considered limited to this straight case since motion along any shaped path can just as easily be used. In the example, a fixed shoulder mounted sign is analyzed, however, the same principles would apply to other types of retroreflectors. The vehicle considered is a midsize automobile. There are two sources of illumination, the two vehicle headlamps. The application parameter is measured as distance away from the sign plane.

The local coordinate system is located on the roadway with the y axis directed down the median line on the left of the vehicle, it is parallel to the centerline. The x axis is directed to the right side of the road and through the retroreflector. The z axis is directed upward vertically above the road, toward the sky originating in the center of the road at intersection of the x - y axes. Thus in this local coordinate system the application parameter is actually the distance in the negative direction along the y axis. This local coordinate system is illustrated in Fig. 1. In this case, three numbers are required to locate

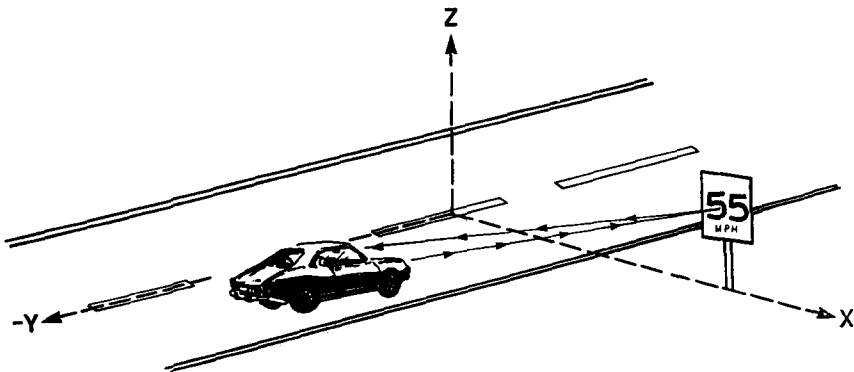


FIG. 1—Illustration of local Cartesian coordinate system showing the origin and directions of x , y , and z axes.

the observer, each light source, and the center of the sign. Additional coordinates are required to define the direction and rotation of the retroreflective sign surface. Also two more coordinates are needed to describe the direction of the central axis of the light sources (headlamps), if luminance calculation are desired.

Retroreflector Measurement Geometry

The computer program then moves the vehicle position along the roadway using the distance as the independent application parameter. As the distance is varied the measurement coordinates are calculated by transformations from the local geometry to the retroreflector test geometry as described in ASTM E 808. This transformation results in the four angular coordinates α , β , β_2 , and ϵ_1 shown in Fig. 2. A separate set of data is calculated for the left and right headlamps.

As each set of new angles for measurement are computed the automated measurement apparatus rotates the test material to these measurement coordinates. At the same time material characterization quantities are calculated. In the retroreflector these are coefficient of retroreflection R' and related quantities. Chromaticity coordinates are computed when spectral measurements are made. Thus this sequence of events has generated a series of application oriented material properties.

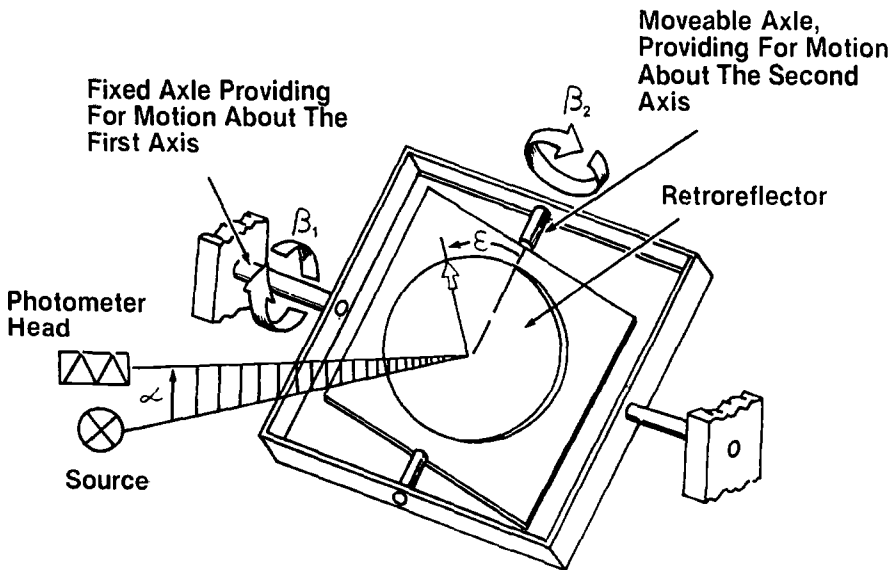


FIG. 2—Illustration of measuring geometry as described in ASTM E 808 and used in the example illustrated in this paper.

Visual Appearance of Retroreflector

The intrinsic material properties do not however describe how this particular retroreflective sign will appear to the user in this application. Additional calculations describing the sources of illumination are programmed to determine appearance of the material as seen by the observer. In fact the characteristics of the sources of illumination may also be measured using the application parameter technique. We then calculate the illuminance at the sample as a function of the application parameter. Intermediate steps include calculation of headlamp orientation (usually V and H angles) relative to sign position. The spectral distribution of the source in that direction may be used for spectral calculations. Previously compiled iso-candela data on the headlamps can provide sufficient information for determining the illumination on the sign.

An important appearance property for a sign is luminance, since this relates directly to how "bright" the retroreflective sign will appear to the observer. Once the illumination from each headlamp is determined and the material properties are known for the application parameter, sign luminance can be determined for the sum of the two headlight sources. Figures 3 through 11 illustrate calculation and measurement results for the shoulder sign as a function of the application parameter distance.

Sign luminance can be considered a final result of this measurement ap-

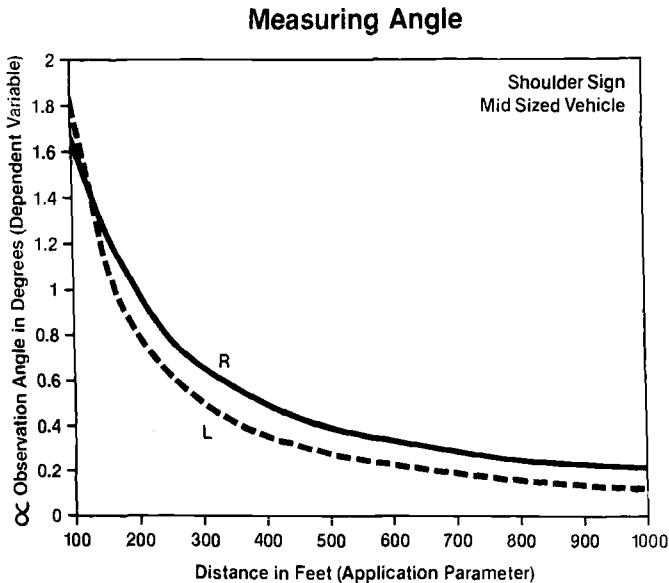


FIG. 3—Results of calculation of observation angle as the application parameter distance is varied. L is for the left headlamp and R is for the right headlamp.

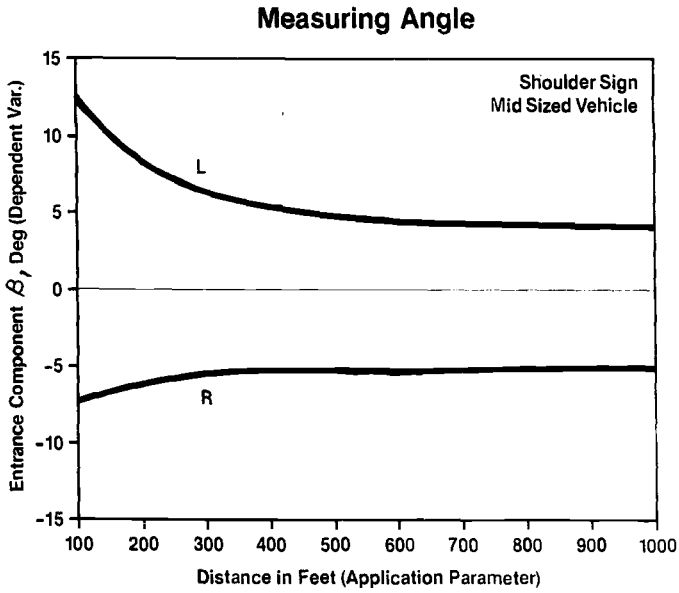


FIG. 4—Results of calculation of the first component of the entrance angle.

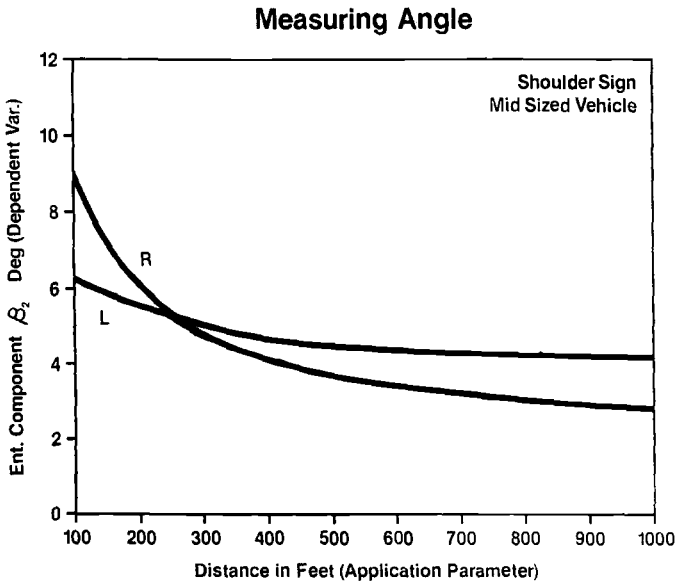


FIG. 5—Results of calculation of the second component of the entrance angle.

Measuring Angle

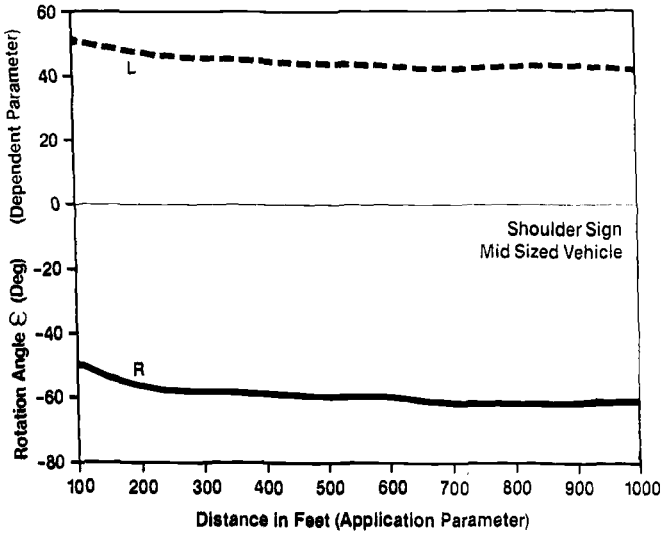


FIG. 6—Results of calculation of the rotation angle. The datum mark defined in ASTM E 808 is at the top of the sign.

Coefficient of Retroreflection

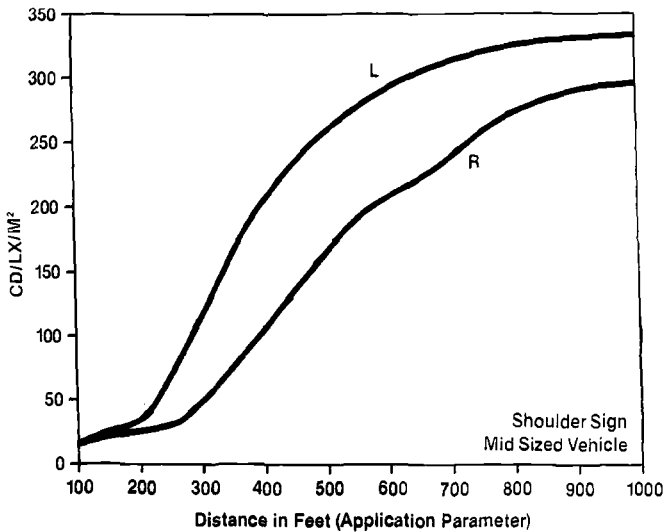


FIG. 7—Calculated output of coefficient of retroreflection as a goniometer positions the test specimen at the measuring angles corresponding to the application parameter distance. The coefficient of retroreflection is calculated as per ASTM Practice for Measuring Photometric Characteristics of Retroreflectors (E 809).

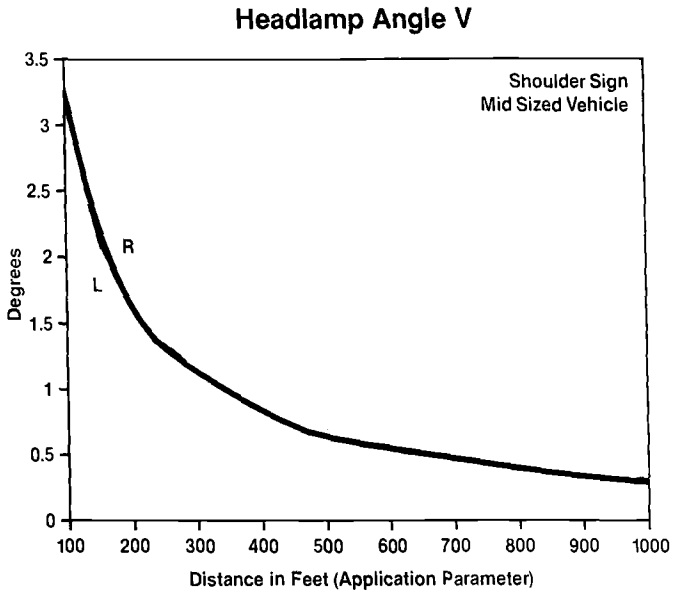


FIG. 8—Calculated vertical angle on headlamps. This angle shows the elevation of the sign above the central axis of the headlamp as described in *The Society of Automotive Engineers (SAE) Tests for Motor Vehicle Lighting Devices and Components (SAE J575)*.

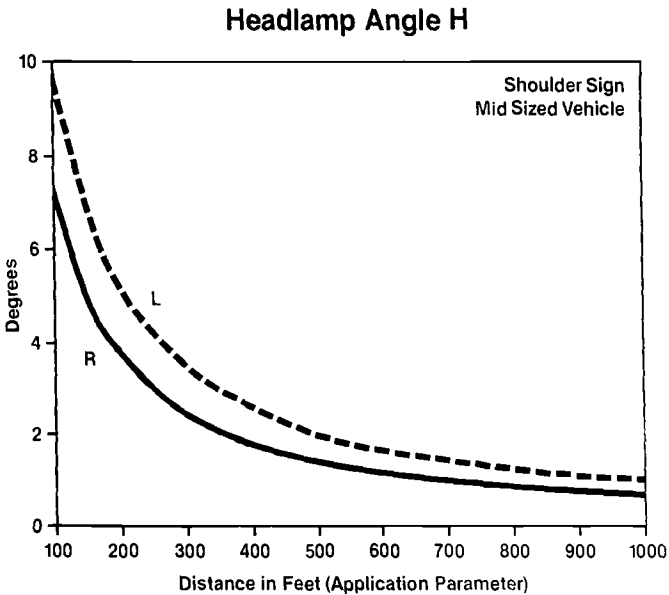


FIG. 9—Calculated horizontal angle on headlamps. This angle shows the laterals angle to the sign from the central axis of the headlamp as described in *SAE J575*.

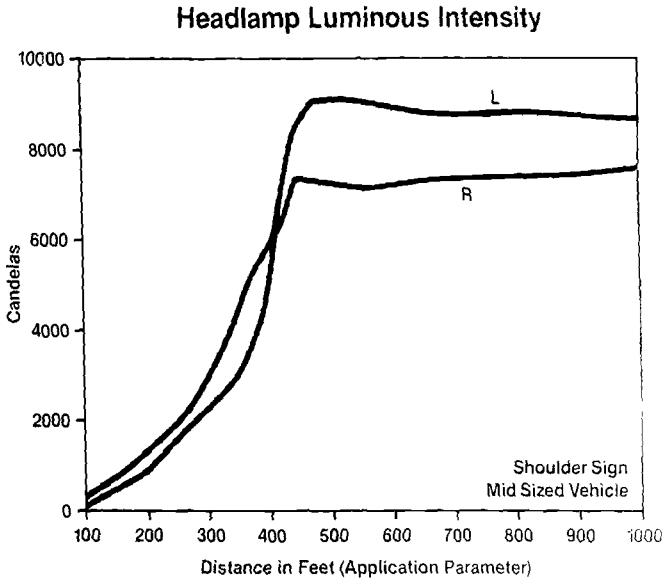


FIG. 10—Luminous intensity at the calculated vertical and horizontal angles for a low beam headlamp.

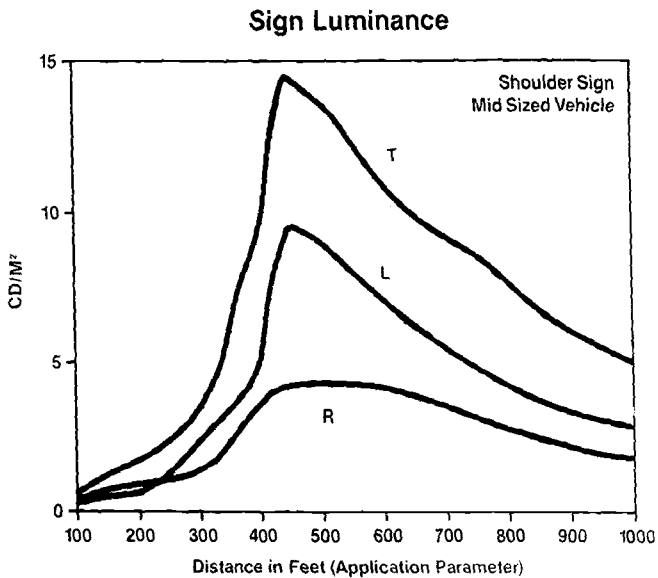


FIG. 11—Sign luminance calculated as a function of the application parameter distance. Luminance relates to how bright the sign appears for the test application.

proach. However, additional more complex appearance properties may also be calculated if the computer program is so programmed. An example is legibility of lettering on the sign or calculations of target value of the sign. Another example is allowing for the influence of background light level. These types of calculation are specific to the signing industry in most cases. Other specific calculations apply to other uses of application oriented goniophotometry.

Additional Considerations

In any measurement, one must be careful in interpreting the final results. For example, in this retroreflector example, in practice there may be other light sources such as the secondary reflection of the headlamps from the road surface and the headlamps from adjacent vehicles (when traffic is heavy) which influence appearance. Such complications need to be considered in the final interpretation of results.

Applications Other Than Retroreflection

Although this paper provided an example of an application oriented goniophotometric analysis of the appearance of retroreflectors, it should be emphasized this is not the only application. The principle of selecting a single independent parameter applies to other measurement problems. For example, the selection of a series of eye paths across a textile surface, which might be considered typical, could be used to characterize a textile or the selection of a series of points on a curved surface of metallic automotive paint could represent a typical appearance, graphically illustrating the geometric properties of these materials. It is apparent that full spectral-gonio measurement of materials requires millions of data points with little real understanding because of the mass of data. Selection of simplified application oriented measurement schemes can reduce measurement time and provide more meaningful information.

Conclusion

In conclusion, it is becoming more and more evident that the use of computer controlled goniophotometers offer new opportunities in measuring the appearance of many types of materials. In the past, traditional goniophotometry allowed for overly simplified geometric analysis. Full spectral-gonio measurements require so much data that time and interpretation are problems. The use of an application parameter and coordinate transformations allows for the more useful and realistic assessment of the geometric aspects of appearance. Such techniques should potentially be reducible to low-cost commercially available instrumentation in the future.

Reference

- [1] NBS Monograph 160, *Geometrical Considerations and Nomenclature for Reflectance*, U.S. Government Printing Office 003-003-01793, Washington, DC, 1977.

Bibliography

- ASTM Test Method for Coefficient of Retroreflection or Retroreflective Sheeting (E 810), *Annual Book of ASTM Standards*, Vol. 14.02.
- ASTM Practice for Measuring Colorimetric Characteristics of Retroreflectors Under Nighttime Conditions (E 811), *Annual Book of ASTM Standards*, Vol. 14.02.
- Johnson, N. L., "The Photometry of Retroreflectors Using a Computer-Controlled Four-Axis Goniometer," *Color, Research and Application*, Vol. 7, No. 4, pp. 319-326.
- Rennilson, J. J., "Definition, Measurement and Use of the Spectral Coefficient of Retroreflectance," *Color, Research and Application*, Vol. 7, No. 4, pp. 315-318.
- Venalbe, W. H. and Johnson, N. L., "Unified Coordinate System for Retroreflectance Measurements," *Applied Optics*, Vol. 19, No. 8, pp. 1236-1241.

David Jungman,¹ Roberto D. Lozano,¹ and
Cristina Melcón de Bellora¹

Measurement of Color on Foods: Some Experiences at INTI, Buenos Aires

REFERENCE: Jungman, D., Lozano, R. D., and Melcón de Bellora, C., “**Measurement of Color on Foods: Some Experience at INTI, Buenos Aires,**” *Review and Evaluation of Appearance: Methods and Techniques, ASTM STP 914*, J. J. Rennilson and W. N. Hale, Eds., American Society for Testing and Materials, Philadelphia, 1986, pp. 62-68.

ABSTRACT: Among problems studied by the Optical Division of The National Institute of Industrial Technology (INTI) in Argentina are efforts related to the food industry. A review of the most relevant projects includes: basic research on non-enzimatic browning, corned-beef, sausage meat, fish, wheat products (semoline, semoline noodles, and flour), tomatoes, and products derived therefrom, apples, apple juice, and yerba maté (*Ilex paraguayensis* or *Ilex theazans*). Some discussion is given in each case.

KEY WORDS: colors (materials), foods, meat, fishes, grains (food), fruits, nonenzimatic browning

The Optical Division of the Physics Department of the National Institute of Industrial Technology (INTI) is located in the suburbs of Buenos Aires, Argentina. Studies are being made on the modes of appearance of different materials.

Some work has been or is being done on whiteness [1-3], gloss [4-6], retro-reflective materials [7-19], and color [20].

In reference to this last item a continuing effort has involved the food industry. Different applications to fish, meat, vegetables, fruits, cereals, and honey have been studied. Basic research on nonenzimatic browning has been underway for several years.

A more detailed description of the problems involved and the results obtained follows.

¹ Researcher, head of optical division, and researcher, respectively, INTI, C.C. 157, 1650 San Martín (B.A.), Argentina.

Food constitutes Argentina's major production, and color is one of the most relevant organoleptic properties because consumers choose food mainly by its appearance. It is not only necessary that foodstuff have a "good" color, but that the color remains constant over long periods of time and among different samples on display. This is a basic requirement for export. Because of this and the need to open markets for Argentine products, some related industries are trying to avoid undesirable nonuniformities in the natural products, or to control the manufacturing process to keep uniform production within the limits of acceptability.

Some experiences with different products follow.

Color in Foods

Basic Research: Nonenzymatic Browning

This is part of a long-term project made in collaboration with the Scientific Research Council (CIC) of the province of Buenos Aires, which began three years ago.

The first part of this work deals with a liquid system model based on a solution of D-glucose, L-lisine, sodium chloride (NaCl) as a humectant and phosphate-buffer, the behavior of which has been studied for high water contents (>0.9) and storage temperatures of 35, 45, and 55°C. The results have been published elsewhere [21,22].

These results showed that a formula to predict changes in color in terms of CIE 1976 u , v saturation (S_{uv}) [23] is possible as follows:

$$\ln(S_{uv}) = 0.019 T + 0.126 T \ln(t) + 0.155 [\text{pH} \ln(T)] - 7.804$$

where T is the temperature in Celsius grads and t is the time in hours.

From this initial result more extended research is now being carried out using different carbohydrates (maltose, fructose, glucose, saccharose, and so forth) and amino acids (glicine, di-glicine, tri-glicine, and so forth).

Preliminary results are very interesting, and some of them will soon be published.

Meat Food Products

Corned-Beef—In this particular case, the color of the final product and its relation to the canning process has been studied [24-26].

The sterilization temperature was varied between 105 and 125°C. The variation of color in the CIELUV system [23] (ΔE_{uv}) in the function of temperature T in Celsius and time t in minutes may be expressed by

$$\ln(E_{uv}) = 1.005(10^{-2})T + 1.002(10^{-1}) \ln(t)$$

where ΔE_{uv} is the color difference between the initial color and the color of the sample after t time in terms of CIELUV units [23-26].

The study also shows that color changes during storage are small and that corned-beef color is mainly determined by the sterilization process.

Sausage Meat—This study is similar to the corned-beef study and is now in the final stage of statistical analysis of the variation of color through color parameter changes.

Fish

A study [27] on the process of maturation of salted anchovies (*Engraulis anchoita*) has been carried out.

In this case color may be used as an indicator of the state of ripeness of the material in process. Fresh fish has a brownish desaturated meat around the spine. The fish is set in barrels with salt and a weight to press it. An enzymatic process takes place. When it is over, after a variable period of 1 to 1.5 years, the meat has a good taste, is soft, and is more reddish around the spine because of the fact that hemoglobine has spread through it.

The investigation was carried out by taking samples at different time intervals from the fish and sectioning in a more or less systematic pattern. The results [27] have shown a clear correlation between the color of certain parts of the fish and processing time. The formula obtained is

$$f(t) = \log \left[\frac{2.5 a^*}{b^{*(2/3)}} \right]$$

where a^* and b^* are expressions of the CIELAB system.

Wheat

Different derivatives from the special type of wheat named "Candeal" (durum) have been studied [28]:

1. *Semolina*—In this case the normal tristimulus values, Hunter coordinates, yellowing index, and the diffuse spectral reflectance for 480 nm (R480) were correlated statistically with pigment content (expressed in ppm on a dry basis).

Results have shown a high multivariate correlation with the following expressions in which r is the correlation coefficient.

$$\begin{aligned} r &= 0.9693 \\ \ln(PC) &= -1.94 - 1.71 \ln(R480) + 1.06 \ln(IA) \\ r &= 0.9688 \\ PC &= -94.08 - 29.52 \ln(R480) + 19.11 \ln(Y) + 0.74 \ln(a) \end{aligned}$$

$$\begin{aligned}
 r &= 0.9688 \\
 PC &= -6.48 + 0.38 IA - 0.49 a - 11.53 \ln(R480) \\
 r &= 0.9687 \\
 \ln(PC) &= 2.43 - 3.22(R480) + 0.09 IA \\
 r &= 0.9648 \\
 PC &= 5.72 + 0.68 IA - 0.12 X
 \end{aligned}$$

where

PC = pigment content expressed in ppm on dry basis and
 $IA = 100(R480 - R550) =$ yellowing index.

This method avoids the rather cumbersome extraction of pigments to find how much is present, therefore contributing to a drastic reduction of time and cost of the determination.

2. When the color of semolina noodles is measured, correlation decreases and is less significant ($r < 0.89$), and this effect increases in the case of whole wheat flour where the correlations are markedly less significant ($r < 0.70$), probably because of the presence of grain shells in the mixture.

Fruits

Work has been done in the past with canned tomatoes and their derivatives, but our main efforts were dedicated to evaluating the production variability and standardizing the illumination and observational methods.

“Granny Smith” Apples—At the present time we are studying “Granny Smith” apples, and have very recently produced a color classification chart to begin with a classification method based on minimum requirements to secure a homogeneous classification between different producers and recollection places.

The second step will be to verify whether variations are introduced by characteristics of plants, different kinds of soils, or simply by normal variation.

Color is very critical for apples because of the fact that a chart is necessary to establish acceptance standards for product export. At the time of export they may have one color and after shipment to their destination they may have another. It is also important to preserve uniformity over different crops, and this is not possible without a systematic classification of the fruits by color and their control during storage.

We have measured the variability of 1983 production. The results showed a large color variation ellipsoid. The intersection points of the ellipse with its own major and minor axis, together with the center point, provides us with five points to build a color chart to classify the apple production.

Apple Juice—Apple juice has been exported from Argentina since 1978. Shipment is done in conventional containers without freezing (freezing is not economically feasible).

Fresh apple juice is almost transparent, but an oxidation and a nonenzymatic browning process quickly darkens the juice.

Up to now, the juice has been color graded by a honey color scale, and after browning, the product has not been commercially acceptable.

Our basic research on nonenzymatic browning may be directly applied to solve this problem.

It would be desirable to know the initial condition of the product and its storage conditions, in order to predict how long a particular parcel will last in good conditions. This is essential to guarantee a certain quality after shipment and to cover risks with adequate insurance.

Furthermore, it is necessary to control every element producing browning as well as migration of oxygen through the recipient walls, heat during transportation, absorption of radiation, and so forth to minimize them as much as possible. This work is now in the preliminary stage.

Corn

In Argentina, bad drying of corn produces losses of about 100 million dollars (U.S. dollars) a year. The main defect is overheating, which degrades the grain and gives rise to a browning process and in some cases to wrinkle of the shell.

The present work tries to establish the kinetics of browning with respect to time and temperature, in order to avoid defects in drying or at least to reduce them to a minimum.

Yerba Mate (South American infusion, *Ilex paraguariensis*, or *Ilex theazans*)

This product, which is extensively consumed in Argentina, Brazil, Paraguay, and Uruguay, has a processing program that includes long storage (about 9 to 10 months) to obtain an adequate flavor.

A new technique, with atmosphere and temperature control, will make it possible to reduce this time to 45 days. Product changes during this period include a color shift from green to yellow-green.

We are studying the "normal" or "ordinary" process and the "accelerated" one with respect to color changes and determining the correlation with time and "readiness for commercial use" evaluated in terms of organoleptic properties.

Conclusions

An extended research and development program on color of different articles of food has been and is being carried out.

Different problems are involved in each case, from basic research on nonenzymatic browning to the determination and construction of a color-test-

chart for classification of "Granny Smith" apples. We are dealing with the industrialization and commercialization of foodstuff, sometimes to control quality and sometimes to control the elaboration process.

This work originated with industrial needs and requirements for a scientific approach to the solutions of color problems. Changes in food color have many different causes, some of them more significant than others. Our investigations lead to knowledge of how to control procedures so as to meet requirements.

The results obtained up to now strengthen the feeling that food color control constitutes an important subject that can be scientifically and technologically applied to guarantee quality, reduce costs, and obtain the necessary competitiveness in the commercial market.

References

- [1] Lozano, R. D., "Estimación de blancura," *Proceedings 61th Meeting of the Argentine Physical Association*, Buenos Aires, Argentina, 1975.
- [2] Fago de Mattiello, M. L. and Lozano, R. D., "A Psychophysical Study of Whiteness," *Die Farbe*, Vol. 26, No. 1/2, 1977, pp. 47-61.
- [3] Lozano, R. D., "Los problemas de la medición de blancura en papeles," *Proceedings of the 1st Latinoamerican Technical Congress on Celulose and Paper*, Vol. 1, Buenos Aires, 1977, pp. 89-103.
- [4] Jungman, D. and Lozano, R. D., "Evaluación psicofísica de brillo," *Proceedings of the 4th Session of the Argentine Ill. Association*, Vol. 2, Tucumán, 1980, pp. 446-458.
- [5] Jungman, D. and Lozano, R. D., "Psychophysical Evaluation of Paper Samples," *Proceedings of the AIC Color 81*, Vol. 1, Berlin, 1981, p. 14.
- [6] Jungman, D. and Lozano, R. D., "La evaluación psicofísica de brillo. I-Prueba y selección del método," and "II-Muestras de papel," submitted for publication to *Optica Pura y Aplicada*, Madrid, Spain.
- [7] Lozano, R. D. and Priu, J. R., "The measurement of colour of retroreflective adhesive sheets used in road signs," *Proceedings of the International Conference on Photometry and Colorimetry*, Bulgarian Academy of Science, Varna, Bulgaria, 1973, p. 30.
- [8] Lozano, R. D., "Las láminas retrorreflectoras empleadas para señalización y los problemas de su medición. I Parte: Antecedentes y mediciones," *Luminotecnia*, Vol. 9, No. 1/2, 1974, pp. 21-27.
- [9] Lozano, R. D., "Observaciones a la Norma IRAM 10033- Señales de advertencia. Láminas reflectoras adhesivas," Publication INTI, pp23 (1974).
- [10] Lozano, R. D., "The problem of retroreflective materials," *Die Farbe*, Vol. 24, No. 1/6, 1975, pp. 167-180.
- [11] Lozano, R. D., "Las láminas retrorreflectoras empleadas para señalización y los problemas de su medición," *Proceedings of the 61th Session of the Argentine Physical Association*, Buenos Aires, Argentina, 1975, p. 19.
- [12] Lozano, R. D., "Measurement Standards Used in Road Signs," *Lighting Research and Technology*, Vol. 8, No. 2, 1976, pp. 107-112.
- [13] Lozano, R. D., "Las láminas retrorreflectoras empleadas en señalización y los problemas de su medición. II-Parte: Comparación entre distintas especificaciones y una propuesta de un método de control visual simple y económico," *Luminotecnia*, Vol. 10, No. 1/2, 1976, pp. 13-19.
- [14] Lozano, R. D., and Roig, D., Informe sobre la colocación de señales de advertencia en rutas de la Provincia de Buenos Aires," *Luminotecnia*, Vol. 11, No. 1/2, 1977, pp. 23-27.
- [15] Lozano, R. D., "Medición fotométrica de materiales retrorreflectores y catadióptricos," *Proceedings of the 4th Session of the Argentine Illumination Association*, Tucumán, Vol. 1, 1980, pp. 152-172.

- [16] Lozano, R. D., "La Norma IRAM 10033 y los requerimientos exigidos respecto del color y las propiedades fotométricas de los materiales empleados en señalización," *Proceedings of the 4th Session of the Argentine Illumination Association*, Tucumán, Vol. 1, 1980, pp. 226-253.
- [17] Lozano, R. D., "The Visibility, Colour and Measurement Requirements of Road Signs," *Lighting Research and Technology*, Vol. 12, No. 4, 1980, pp. 206-212.
- [18] Cogno, J. A., Etchehoury, E. M., and Lozano, R. D., "Problemas relacionados con las mediciones fotométricas y colorimétricas de triángulos de seguridad usados en las calles y rutas," submitted for publication to *Optica Pura y Aplicada*, Madrid, Spain.
- [19] Etchehoury, E. M., Jungman, D., and Lozano, R. D., "Medición de color y valores CIL de tachas reflectivas," Publication INTI, 1982, 83 pp.
- [20] Lozano, R. D., "El color y su medición," *Americalee*, Buenos Aires, 1978, 640 pp.
- [21] Petriella, C., Resnik, S. L., Chirife, J., and Lozano, R. D., "Cinética de la formación de color por pardeamiento no enzimático en sistemas modelos de alimentos," *Proceedings of the Symposium on Color on Foods*, INTI-CIC, Buenos Aires, Argentina, 1982, pp. 21-25.
- [22] Petriella, C., "Cinética de formación de color producida por reacciones de pardeamiento no enzimático en sistemas modelos líquidos con alta actividad de agua," M.A. thesis, University of Buenos Aires, 1983, 114 pp.
- [23] CIE, *Colorimetry*, CIE Publication 15.2, TC-1.3, 1982.
- [24] Lozano, R. D., "El color en las carnes. Un factor decisivo en las ventas," *Proceedings of the 2nd Symposium on Science and Technology of Meat*, INTI, Buenos Aires, 1978, p. 5.
- [25] Jungman, D., Lozano, R. D., and Melcón de Bellora, C., "Medición de color en corned-beef," *Proceedings of the 3rd Symposium on Science and Technology of Meat*, INTI, Buenos Aires, 1980, p. 3.
- [26] Fagotti, A. D., "Estudio sobre la influencia del tratamiento térmico en el oscurecimiento superficial del corned-beef," M.A. thesis, University of Buenos Aires, 1983, p. 102.
- [27] Lozano, R. D., Melcón de Bellora, C., Sanchez, J. J., and Trucco, R. E., "Measurement of colour as an indication of maturity of salted anchovy," *Proceedings of the 4th AIC Session*, Vol. 2, No. 5, 1981.
- [28] De Da Souza, E., Balseiro, C., Melcón de Bellora, C., and Jungman, D., "Variabilidad del color con el contenido de pigmento carotenoide en muestras de trigo durum de distintas zonas del país. Su estudio estadístico," submitted for publication to *Revista de la Alimentación Latinoamericana*.

Specifying the Appearance of Escalator Treads: How to Minimize the Disorientation Effect

REFERENCE: Cohn, T. E., "Specifying the Appearance of Escalator Treads: How to Minimize the Disorientation Effect," *Review and Evaluation of Appearance: Methods and Techniques. ASTM STP 914*, J. J. Rensilison and W. N. Hale, Eds., American Society for Testing and Materials, Philadelphia, 1986, pp. 69-77.

ABSTRACT: Escalator passengers sometimes experience a feeling of disorientation or dizziness while boarding or riding the machine. Prior work has shown that this perception may be due to a visual depth illusion caused by the appearance of the escalator tread. Measurements confirm that the escalator tread surface is a highly periodic visual stimulus exhibiting unusually high contrast as well as a spatial frequency matched to the preferences of the visual nervous system. Means of minimizing the depth illusion are explored. These center on disrupting the periodic structures of the tread surface. Expressions intended to serve as candidates for figure of merit for the tread appearance are developed. These take into account some properties of the visual nervous system including the decline with eccentricity of visual acuity and the bandpass character of spatial detail processing under light adapted conditions.

KEY WORDS: escalators, safety, appearance, visual illusion, depth perception

For many years there has been a justifiable concern with the parameters influencing the appearance of materials. Color, texture, and reflectivity to name several such parameters robustly govern ones ability to design esthetically pleasing, reproducible, human engineered, and safe materials. The constraints stem both from properties of materials as well as from properties of the visual nervous system. The visual nervous system, it is known, is forgiving to some extent. For example, because color vision is trichromatic [1] the designer has an enormous array of possible ways of achieving a particular color appearance. A material will appear "yellow" to a color normal person if it reflects a broad range of middle wavelengths or if it reflects only two wave-

¹ Professor, School of Optometry, University of California, Berkeley, CA 94720.

lengths, one green and one red. Such diverse formulations leading to the same appearance are called metamers, stimuli that look alike but are not, and their existence stems from an imperfect visual nervous system. The purpose of this paper is to examine another realm in which an imperfection of the visual nervous system supplies constraints, but in this case one stimulus, the escalator, can have more than one appearance. What results is ambiguous perceptions that can be dangerously unsafe. Means of specifying appearance that can be used to render the escalator less unsafe will be described.

History: The Evolution of the Design of the Escalator

In 1859 the inventor Nathan Ames patented his “Revolving Stairs” the forerunner of modern escalators [2]. In the early days of commercial implementation stairs were fashioned of wood and were moved continuously by means of rollers and gears. At the top and bottom landings, shunt structures resembling the bow of a boat were installed to firmly guide passengers off to the side of the machine and onto stationary surfaces. With many installations a major safety problem soon emerged. Shoes and fingers were getting caught between stair and shunt. Manufacturers solved this problem by constructing their stair treads with a cleat-slot arrangement. Cleats and slots were about 1 cm wide, covered the entire surface of the tread, and were oriented in the direction of travel. Tread surfaces meshed with a comb at both ends of the machine effectively preventing large objects from getting caught. Modern machines employ cast aluminum treads of the same design except that cleats and slots are smaller (about 2.5 and 5 mm wide, respectively) so that even the tip of an umbrella is unlikely to be caught between the moving tread and the stationary platform at the end of travel. Until recently, all treads were painted black after which the upper surface was machined smooth to give it a finished bright appearance. This practice has been termed “highlighting.” Thus in four stages the escalator tread surface has evolved from one identical in appearance to a wooden stair step to one characterized by a prominent array of parallel metallic dark and light stripes.

This evolution, brought about principally in the interests of safety, has had an unanticipated and undesirable side effect. The stripes have an unfortunate effect on the eye causing, as will be established below, a visual depth illusion.

Appearance of the Escalator Tread

To the eye, the escalator tread has a number of unique features as may be seen in Fig. 1. Its pronounced periodic nature is found rarely in our modern urban environment. At common viewing distances the critical dimensions of the pattern match certain features of the visual nervous system. Its contrast is uncommonly high. Its orientation is just appropriate to cause a visual depth illusion. Each of these points will be elaborated.



FIG. 1—*Passenger eye's view of an escalator.*

The appearance of periodicity stems from the repeating pattern (of cleats and slots) on the escalator tread surface. Causing the periodicity is the need for precise dimensions so as to afford a smooth combing action at the end of travel of the machine. To assess the pattern from this perspective, we have made measurements using a scanning photometer that assesses the luminance of small ($1/4$ - by 5-mm) areas across the tread face. The scanning slit was oriented parallel to the cleats and slots. Figure 2 shows a photograph of the subject material plus a plot of such measurements obtained from a heavily used piece of tread material. Illumination was oblique as would be the case in most installations. The luminance pattern is not a rectangular wave though that is essentially the underlying physical structure; rather, the waveform is more triangular manifesting the specular reflection from the worn edges of the tread cleats. Nonetheless, the pattern is strongly periodic, and this is one of its most important features. The pattern can be well-approximated as a sine-wave grating, for that is its fundamental component. The higher harmonic frequencies inherent in the pattern affect visibility only minimally as will be seen below.

Visual scientists use the term "spatial frequency" to describe the rate at which a pattern repeats itself in space. Given the physical dimensions of the

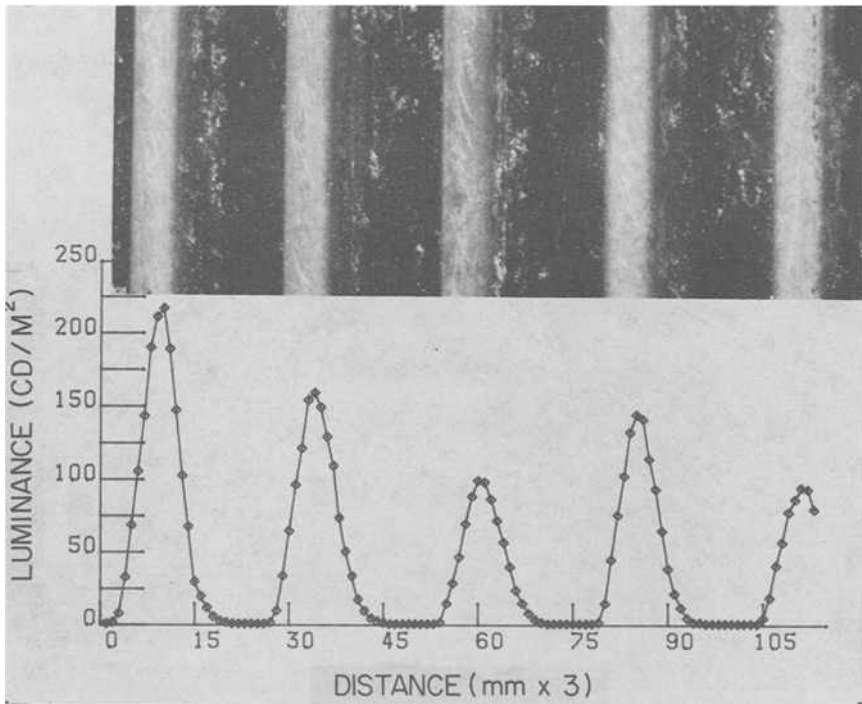


FIG. 2—(a) Photograph of a portion of a piece of escalator tread material under oblique illumination. Luminant was a tungsten lamp located 10 cm from left-most cleat in a plane 5 cm above the surface of the tread. Cleats appear as light vertical stripes about 2.5 mm wide. Grooves (or slots) are of approximately rectangular cross section, 5 mm wide and 10 mm deep. Sides and bottom of groove are painted black at the time of manufacture and, with use, accumulate dust and dirt which gives a grey caste in practice. (b) Plot of luminance integrated over a 0.25- by 5-mm slit oriented parallel to the cleats. Vertical axis is luminance in cd/m^2 . Horizontal axis is a numerical index of position where each unit is 0.33 mm. Maximum values of luminance for each cleat ranged from 105 to 220 cd/m^2 . Minimum values of luminance, characterizing the troughs, ranged from 0.6 to 1.5 cd/m^2 . Contrast thus always exceeded 99%. With more direct illumination the contrast was observed to decline to a value of about 98.3%.

repeating structures of the pattern (see above) at a viewing distance of 1.6 m, which is how far this pattern is from a typical adult observer when the observer is boarding an escalator, the fundamental spatial frequency of the pattern is about 340 cycles/rad. This frequency is at or near the peak of the contrast sensitivity function of a light adapted human observer [3] meaning that such a pattern is the best seen periodic pattern in the environment. Higher frequencies in the pattern are seen with far less sensitivity. For example, the sensitivity to 680 cycles/rad, the next harmonic component in the pattern, is about 3 dB less. "Best seen" refers to threshold conditions. We have recently established that the same spatial frequency is also best seen above threshold [4]. Additionally, the suprathreshold responses of physiological mechanisms

underlying detection of repeating stimuli are clearly optimized by spatial frequencies in this range [5].

Another important parameter governing the visibility of a stimulus is its contrast [6]. Contrast is defined as the ratio of the difference between maximum and minimum luminance in a pattern divided by twice the mean luminance. For the data shown in Fig. 1 contrast of the escalator tread is over 0.99 (1.00 being the maximum realizable value). Such a value is uncommonly high. Reflective objects rarely exhibit more than a 10:1 range of reflectivity, which would yield a contrast of 0.90. The high values recorded for the escalator tread are caused by a combination of factors including shadowing inherent in the cleat-groove structure, black paint in the grooves, and our choice of oblique lighting. By itself, the high value of contrast makes the tread a highly visible stimulus.

Finally, the orientation of the pattern presented by the tread is important. Consider the typical viewing situation as a rider is about to board the machine. The escalator rider is looking down at the tread face. Assuming that the eyes are located 1.5 m above the trailing edge of the 45 cm tread the spatial frequency at the front of the tread is about 4% higher than at the back. This is a negligible difference so effectively the tread may be approximated as lying in a fronto-parallel plane. Thus the stimulus is approximately a sine-wave grating, and it is oriented vertically, that is to say, in the vertical meridian of the field of view. In the next section the significance of the vertical orientation of the grating will be discussed.

Repeating Stimuli and Visual Depth Illusions

Above, we have analyzed the escalator tread appearance, concluding that it is a highly visible, approximately sinusoidal grating, oriented in the vertical meridian. How does this appearance translate to a visual depth illusion and from that to a health hazard? Part of the answer has been known since before the invention of the first escalator. In 1842, Sir David Brewster published the first English-language description of a visual depth illusion that occurs when the normal binocular observer looks at a repeating pattern [7]. The illusion, which since has come to be known as the "wallpaper illusion," comes about because, in its search for optimal congruence between the images falling in two eyes, the system of binocular fusion can be fooled. Within reasonable bounds any two vertical stripes can be fused. When different stripes are fused the result is a depth illusion, the stimulus appears ". . . to be where it's not and to not be where it is." [7]. The extent of the illusion can be large. For the viewing example cited above, each cleat width of error results in a 12 cm distance error. So for example, if two adjacent cleats are fused, the tread surface will appear to be 12 cm closer to the observer's eyes than it actually is. It has been hypothesized [8] that the depth error may lead to a postural instability

that could explain some of the 60 000 or so falls that occur yearly in this country [8].

Other Environmental Stimuli that Can Cause a Depth Illusion

The discoverers of the “wallpaper illusion” and subsequent researchers have noted [9] a number of common objects that can cause a comparable depth illusion. These include postage stamps, caned chair seats, fences, typewriter keys, and perforated acoustic tile. Other objects could theoretically cause depth illusions, but they have not been explicitly cited before. These are patterned carpet, floor tile, moving walkways, metal stair stamping as on airplane boarding stairs, and rubber floor mats as on transit bus floors. The significance of each of these is that falls might be the ultimate result of the depth illusion. Moreover, these objects, considered as stimuli, have varying qualities, particularly as regards the crucial appearance parameters of contrast and spectral purity. With appropriate research, it may be possible to specify the constellation of stimulus parameters that might be considered safe, thereby delimiting for users, standards setters, and manufacturers the acceptable bounds of appearance.

Specifying the Deleterious Features of the Tread

It has been established above that the visual depth illusion arises because nearby features of the tread surface can be erroneously fused with one another. There are a number of approaches to minimizing this aspect of tread design, some practical and some not. For example, the cleat-slot arrangement could be altered so that there no longer was a periodic pattern. This could be accomplished by adopting a graded or random spacing pattern while adhering to the constraints on minimum and maximum cleat and groove sizes as specified in code [10]. Such a solution would be expensive to implement because of the re-tooling costs. Another approach is to superimpose on the extant periodic cleat-groove pattern a competing nonperiodic pattern. Such a nonperiodic pattern could be implemented by machining, painting, etching, altered lighting, or by other measures. If this were to be attempted the designer would like to be able to predict the efficacy in practice of any proposed arrangement, hopefully without having to have a full-scale field test for each candidate improvement. To the end of minimizing the need for tests, the following ideas are advanced. Equations are developed below that should, based upon known principles of visual processing, enable designers to specify a figure of merit for any given pattern.

Two approaches will be presented. One arises from a simple linear systems model of visual perception, the other being relatively free of physiological assumptions and thus being simpler to implement. Neither has as yet been

tested, so for each an effort has been made to clearly state the underlying assumptions.

The first approach considers the visual system as a two-stage filter. In the first stage, a weighting function $h(x)$ describes the reduction with eccentricity x (measured in min arc) of the visual sensitivity for detail under light adapted conditions. For the present demonstration we have adopted an equation that closely fits the data of Green [11]. The equation is

$$h(x) = e^{-12.6x} \quad (1)$$

and says essentially that the ability of the visual system to signal detail information declines with distance of the target from the point of fixation. Such a filter may be thought of as the expression of the scarcity of connections from eccentric photoreceptors to central nervous system visual neurons. The output of this filter is the input for the second stage. The second filter stage expresses the known bandpass structure of the visual nervous system also under light adapted conditions. Here we have adopted the expression developed by Kelly [12]. Kelly's data are valid for 8-cycle/degree vertical targets, which completely cover the zone of sensitive detail vision. However, the implicit assumption that spatial frequency attenuation is independent of eccentricity is known to be a poor approximation [13], and it remains to be seen how serious an error this might introduce. The equation expressing the bandpass filtering characteristic is stated in the frequency domain as follows

$$C(s) = ks^2e^{-s} \quad (2)$$

where $C(s)$ is the attenuation of contrast at the frequency s , and k is a scaling constant. Now, a pattern of luminance specified by the function $L(x, y)$ is operated on by the two stages in cascade. Ignoring the mean luminance, the output of the first stage is $L(x) \cdot h(x)$. Call the spatial frequency transform of this quantity $L^*(s)$. Then the response function, $R(s)$ is simply $L^*(s) \cdot C(s)$. This yields finally the rather complex relation

$$R(s) = F[L(x)e^{-12.6x}]ks^2e^{-s} \quad (3)$$

where $F[]$ is the fourier transform operator.

Goodness Criterion

$R(s)$ can be used to define a measure of goodness by a number of methods once the goodness criterion is stated. For this argument, we adopt the criterion that the ideal response spectrum $R(s)$ is a constant. The most deleterious spectrum is $R(s') = K$ (where s' is the fundamental frequency defined by

the cleat-groove periodicity) and $R(s) = 0$ otherwise, for that would be a strictly periodic pattern. Consider the sum of energies at all integral multiples of frequency s' . Define this as R' . Let the figure of merit be defined as

$$f = E - R'/E \quad (4)$$

where E is the total energy (squared contrast) of the response pattern $R(s)$. If the pattern is white noise, no significant energy is found at s' , and so R' is negligible. Then $f = 1.0$. If all of the energy is at s' the pattern is strictly periodic and highly likely to produce ambiguous depth sensations. In that case $f = 0$ because $E = R'$.

Given any two patterns $L(x, y)$ and $L'(x, y)$, it is conjectured that if $f' > f$ then the superior pattern is L' .

The second approach to defining a figure of merit is to employ a sort of autocorrelation analysis and to ignore visual properties almost entirely. Begin with the same luminance distribution $L(x, y)$. Ignore variation in y . Define the luminance autocorrelation as

$$A(z) = \frac{1}{A} \int_{-A/2}^{A/2} L(x+z)L(x)dz \quad (5)$$

where z is a dummy variable with the units of x , and A is the tread width. The maximum of the function is at the origin [14]. A strictly periodic pattern will lead to an autocorrelation function that is also periodic with peaks at integral multiples of the fundamental period $1/s'$. A white noise pattern has an autocorrelation that dies to zero everywhere except at $z = 0$. Consider the energy within $\pm 1/2s'$ of the origin. This can be calculated by changing the integration limits in Eq 5. Denote this quantity A' . Energy outside this limit may be viewed as potentially deleterious if it can contribute to a similarity in the pattern $1/s'$ from the origin because that might lead to ambiguous fusion. Define the figure of merit as

$$f = A - A'/A \quad (6)$$

f has the property that it is zero for a periodic pattern because $A = A'$ and is unity for white noise, and as for the figure of merit advanced above, it is conjectured that a pattern with a large f is better than one with a small f . The reader will note that this figure of merit does "weight" regions close to fixation differently from those far away (as the eye also does) but in an all or none matter. By defining limits at $\pm 1/2s_0$, the definition is effectively laying greatest weight on the ambiguous percept that comes about from fusing adjacent cleats for example. The possibility of fusing cleats further than one removed from each other is ignored here. As with the figure of merit defined above, this one remains untested as yet. Moreover, both ignore the possibly impor-

tant contribution that could be made by color and the certainly important information present in the y -axis variation of the luminance pattern. The latter problem might best be dealt with by integrating the figure of merit f over the vertical extent of the pattern.

Conclusion

The appearance of a conventional escalator tread strongly favors an ambiguous depth percept because of a repeating structure across the horizontal meridian of the field of view. Approaches to minimizing the occurrence of the depth illusion by altering the appearance of the tread should be attempted. A figure of merit for tread appearance would be a useful construct with which to compare several alternative appearance designs. Two such figures of merit have been suggested. To varying degrees, they take account of the relevant properties of the human visual apparatus.

Acknowledgments

I thank Daniel Greenhouse for assistance in luminance measurements. Apparatus was kindly supplied by the Vision and Lighting Laboratory of the Lawrence Berkeley Laboratory. Research was supported in part by the Institute for Transportation Studies, and by a research grant (EY 02830 to TEC) and a Core Center grant (EY 03176 to Jay M. Enoch), both from the National Eye Institute.

References

- [1] Wyszecki, G. and Stiles, W. S., *Color Science*, Wiley, New York, 1962.
- [2] Fruin, J., *Pedestrian Planning and Design*, Metropolitan Association of Urban Designers and Environmental Planners, New York, 1972.
- [3] Campbell, F. W. and Green, D. G., *Journal of Physiology*, Vol. 181, 1965, pp. 576-593.
- [4] Hamer, R. D. and Cohn, T. E., *Investigative Ophthalmology and Visual Science*, Supplement to Vol. 26, 1985, p. 142.
- [5] Movshon, J. A., Thompson, I. D., and Tolhurst, D. J., *Journal of Physiology*, Vol. 283, 1978, pp. 101-120.
- [6] Stromeyer, C. F., III, and Klein, S., *Vision Research*, Vol. 14, 1974, pp. 1409-1420.
- [7] Brewster, D., "On the Knowledge of Distance Given by Binocular Vision," *Philosophical Magazine and Journal of Science (London)*, Vol. XXX, May 1847, pp. 305-315.
- [8] Cohn, T. E., *Investigative Ophthalmology and Visual Science*, Supplement to Vol. 25, No. 3, 1984, p. 293.
- [9] Ittleson, W. H., *Visual Space Perception*, Springer, New York, 1960.
- [10] *Safety Code for Elevators and Escalators*, ANSI/ASME A17.1-1981, American Society of Mechanical Engineers, New York, 1981.
- [11] Green, D. G., *Journal of Physiology*, Vol. 270, 1970, pp. 351-356.
- [12] Kelly, D. H., *Vision Research*, Vol. 15, June 1975, pp. 665-672.
- [13] Daitch, J. M. and Green, D. G., *Vision Research*, Vol. 9, Sept. 1969, pp. 947-952.
- [14] Lee, Y. W., *Statistical Theory of Communication*, Wiley, New York, 1960.

Visual Color Technology Development for Industrial Applications

REFERENCE: DeGross, J. T., "Visual Color Technology Development for Industrial Applications," *Review and Evaluation of Appearance: Methods and Techniques*, ASTM STP 914, J. J. Rennilson and W. N. Hale, Eds., American Society for Testing and Materials, Philadelphia, 1986, pp. 78-91.

ABSTRACT: There has been a need for a visual method of generating a color without preparing a sample standard or finished product. This styling and reference capability is required to generate new colors and review their visual appearance during the development of new products or restyling old lines. In the majority of visual approaches, a color chip or other reference has been used as a guide, which must then be matched with colored materials on a manual basis. Even with the utilization of an automated computer color system, the visual appearance of many materials cannot be fully duplicated until the actual product materials are available.

Applied Color Systems' staff approached the question, "Is it possible to create a device that can simulate the finished product color and appearance that can be duplicated in the final product?" several years ago with a technology review and came to the conclusion that a mechanical/electrical approach could supply many of the answers to solve this need. As part of the technology review, we studied projection systems, video graphics, and the integration of spinning disks. Of all of the currently available technologies, we found that only the spinning disk based on the Maxwell technique solves both the color and appearance problems and gives reproducible results that can generate predictable colorant formulations.

The device developed from the basic Maxwell disk concept is a solid state fully integrated system that creates visual color simulations that duplicated a range of typical industrial product finishes. It is apparent that many exciting new things can be accomplished with such a device. By adding visual modifications to the disks, the operator can visualize various loadings of white or create a metallic "look" to simulate metal loadings of paint or ink finishes. He can then take the data output from this device and convert them by computer into colorant formulas on a fully automated basis. This same data can be used to communicate color data from one location to another and be able to see the actual color in the second location.

Industry may also be able to use such a device as a merchandising aid to help the customer to visualize the finished product color, whether it be on an industrial product surface, a contractor's building, or an interior decorating scheme.

¹Formerly, marketing director, Applied Color Systems, Inc., Princeton, NJ 08543.

Based on performance in a number of industrial installations, we now feel confident that the Visual Color System can be an important aid to industry in the styling, communications, and merchandising of colored products. The device has the potential to open up new development areas in color technology to allow the manufacturer to have better control of color specification and a visual understanding of the color component of his product.

KEY WORDS: color specification, color formulation, visual color response, Maxwell disk, standard observer, metamerism colors, standardized lighting, color communication

When a designer/specifier of industrial products requires a supplier to produce products with a surface finish of exact color and appearance, the present method is to actually prepare a sample simulating that product finish to act as a guide to the producer. This physical standard serves both the purchaser of the materials and the producer of the product as the basis for manufacture, purchase, and color specification. The manufacturer may purchase the finish colors and be required to have his vendor match the color standard and prepare samples of the actual colorant (that is, paints, inks, or textile dyelot) being produced to compare the actual product against a colorant standard. Visual comparisons and the experience of colorists in the color producing industries are most often utilized to produce acceptable products on a commercial basis [1].

Defining the Color Communication Problem

Industry currently requires physical standards to determine color approvals for parts submission to customers and production as well as for the styling requirements of finished product to visualize the effect of the color and the process. Industry has developed several techniques for color specification. Typically, the colorant supplier (paint, ink, plastic compound, and textiles), and the parts fabricator must prepare sample plaques with the actual coloring materials in a laboratory process similar in nature to the final process. Samples prepared in this manner are time consuming, costly, and often tend to change color over time. Sample preparation techniques may vary widely compared to production confusing the issue: "What is the acceptable color standard?"

A second technique is to use a specification reference system, such as the Munsell color book, the Swedish "Natural Color" system, or the German Deutsche Industrie Norm (DIN) color system. These systematized, well defined color references can frequently be used as a first approximation to a color specification. The weakness of all of these color systems, however, is that even with several thousand colors the exact specified color and appearance cannot be finalized without the preparation of an actual product sample. Also, the commercially prepared samples in each of the color and appearance reference systems have a tendency to deteriorate over time and serve as

questionable references unless updated and tied in with actual product samples.

Because the human observer differs in the ability to judge color [2] and the judgment may vary in the use of the proper colorant materials to correct the batch [3], instrumental devices have become standard tools for industrial color control. Colorimeters (color difference meters) are devices used to measure batch against standard and assure a dependable evaluation of standard versus batch. A more sophisticated instrument, the spectrophotometer, can provide detailed colorimetric reflectance data. Tied to a computer, the spectrophotometer allows the colorant supplier to produce the lowest cost formulation and limit the choice of colorants in the correction of the final colorant batch. Fast batch correction improves utilization of the colorant manufacturing plant while assuring an acceptable product for the end product manufacturer.

Spectrophotometers and colorimeters are successfully used in the laboratory and colorant manufacturing plant for quality control and formulation. These devices do not solve the color communications problem between levels of trade, that is, colorant manufacturer to fabricator to color stylist. There has been a growing need for a technique to specify new colors quickly, change specifications, and communicate color specifications between specifier, fabricator, and colorant suppliers. The techniques should provide data to automatically calculate color formulations for a variety of industrial coloring techniques including paints, printing, plastic fabricating, and textile dyeing and printing. Styling of color, the most subjective part of material specification, depends on the human eye of the parties to the business arrangement, requiring agreement between specifier and producer.

The technique should allow a designer/specifier to observe a wide number of colors and then, when the correct color has been chosen, to quickly and easily communicate that specification to the supplier and allow the supplier of colorant to use that specification as the basis for colorant manufacture. The transaction between designer/specifier and product fabricator and colorant supplier could be simplified and speeded. In addition, a great deal of the risk of producing an acceptable batch of colorant to be used in coloring a product would be reduced.

Color Communications Concept Development

Applied Color Systems (ACS) approached the industrial color communications problem beginning in 1975 with a technology review of color simulation techniques. In the review of the various state-of-the-art techniques available, systems were studied utilizing projection of colored image techniques, color video displays, and the integration of color based on the Maxwell spinning disk.

In the technology review, Color Graphic video and photo projection devices were identified, which are excellent for design applications that had color styling possibilities, especially in the area of presentation and stylist interaction. These graphic systems and projection systems were interesting for the designer; however, they all had major flaws in color reproducibility and color gamut when compared to the needs of the wide range of industrial colors. We also discovered that color video terminals increased viewer metamerism by a very high factor. Of all available technologies, it was our opinion that only the Maxwell spinning disk solved both the color and appearance problems and gave colorimetrically reproducible results that could generate predictable reflective color simulations on a repeatable basis [4,5]. In 1978 the decision was made to move ahead in the development of a practical device based on the Maxwell spinning disk.

Product Concept

In the period of the 1860s, J. Clark Maxwell, a former professor of experimental physics at Cambridge University, used rotating disks in studies of color [6,7]. He showed that by varying the relative size of the colored sectors, a variety of color simulations could be made when the disks were spun. The concept, although scientifically interesting, did not achieve commercial use and remained an academic teaching curiosity.

During the last 20 years, a number of simulation devices have been attempted using the spinning disk principle. In 1962, Color Corporation of America introduced a product that was driven by mechanical wires. It had minimum color gamut and was based on nonrepeatable lighting sources. The output was mechanically read and the pastel gamut was narrower than the paint colors that it attempted to simulate. This product did not succeed commercially, and no others have been seriously attempted since.

In order to develop a successful commercial color simulation product, it became clear that four elements of design would be required:

1. The lighting source must be repeatable and create a highly predictable light source evenly across the disks and provide a narrow range of color temperature on a predictably long-term basis.
2. The device must be fully automated with the operator able to control colored disk area as the device spun.
3. The area of each of the colored disks must be read automatically and calculated by computer means.
4. The output of the device must be repeatable from unit to unit and be suitable as base data for computer calculated colorant formulation development.

Product Development

An initial prototype was designed and numerous tests run to develop colored disk preparation techniques, controllable light sources, and techniques to capture device data. Several prototypes were built and by early 1980 a demonstratable unit gave results of sufficient quality to assure that a final design could be developed [8].

A panel of colorant and fabrication manufacturers was asked to review the unit and to make comment. A wide variance of opinion was given. However, the general attitude was positive, indicating that if technical problems could be overcome the product would have practical application in the industrial world.

A decision was made in 1980 to go to commercial design and bring the Visual Color System (VCS) product to market. The task proved formidable since it required the development of six separate subsystems; these became the final product. Development projects in specialty lighting, high-speed photo-optic bar code reading, power distribution and micro-motor drive, the development of a micro-readout and operator control system, the development of a pigmentation application system for wide color gamut and long-term stability, and the development of a mechanical movement and control system to assure disk movement at high-speed rotation were conducted. Each of these projects proved successful and the final product design was completed by the summer of 1982.

Two production prototype units were built based on this design, and reproducibility and repeatability studies were begun. The results of these studies proved that dependable, repeatable colors could be simulated. The areas representing these colors were illuminated with a light source that had excellent color distribution in the daylight simulation area (6900 K) and reproducibility from instrument to instrument. The final design prototype was shown to key representatives from industry and product stylist/specifiers during 1982. During 1983, units were installed in key accounts to develop practical results correlating the color seen on the VCS with actual colors of colorant materials and parts produced with color formulas predicted, based on VCS data.

Software has been developed that converts the additive color output of the Visual Color System to colorimetric reflection data. Formulation correlation has been developed for plastics, coatings, textile dyes, and a variety of Ink Systems. Results to-date in actual industrial environments indicate that the data output of the Visual Color System can be reliably used in the production of practical colorant formulas. In a similar way, it has been shown that a colored sample can be read by a computerized spectrophotometer, converted to VCS area readings that can then be entered on the Visual Color System, and the color will represent the computer generated color in a visually acceptable way under the predicted viewing conditions.

VCS Design Elements

The detail of the VCS design can be broken down into three basic elements: the lighting system, the object, and system operation and logic.

The Lighting System

The development of the lighting system required the production of an overhead and a light source that would create a natural viewing environment with a well diffused daylight simulation lamp. Further, the lamp must fire in such a way that strobing was not caused on the spinning disks. It was also important that long-term lamp life give a predictable, even color temperature to provide a technically dependable lighting source. Specifications were developed and submitted to key producers of light sources. Several prototype lamps were tested. The final vendor of the lighting source was Duro-Test, Inc., of North Bergen, NJ. Jointly, a final acceptable lamp was developed and tested. A pair of lamps were mounted in an overhead that was coated neutral gray to provide a nonconflicting viewing environment. The two lamps are mounted in opposing positions, providing even illumination across the spinning disks. Both short-term and long-term lighting tests indicate that we had developed a superior lighting system for viewing the integrated color of the spinning disks. (See Table 1.)

In addition to the daylight simulation lamps, a set of tungsten lamps have been added to the lighting system with a separate switch, to give an indication of metamerism for visual consideration. However, it is normally suggested that specification data be read only under daylight simulation, since this data can be converted to other illumination predictions by color formulation software.

The Object

The object, in the case of the Visual Color System device, is the disks themselves. It was important that a mechanically stable disk be constructed that could be automatically controlled while moving at visual integration speeds in excess of 1600 rpm. The mechanical construction of the disks was attempted with a variety of materials. The final choice was a lamination of a stainless steel backing with a polycarbonate base substrate. The disks are mounted mechanically around a hub in sets of three segments of 120° each. The movement of each disk set is done by a gearing system driven by a micro DC-powered motor mounted on the turning shaft. Each of six moving disks has a dedicated DC motor that is powered through a commutator from the central power core. The conversion from the control switches to power distribution is controlled by microprocessor.

TABLE 1—*Long-term lamp test.*

Date	Continuous Hours On	Color Temperature, K ^a
3/4	45	6936.45
3/10	167	6916.78
3/17	357	7002.67
3/24	528	6939.70
4/27	1338	6950.07
5/17	1819	6874.63
7/7	3047	6766.57
7/27	3522	7018.37
8/17	4032	6919.00
8/31	4368	6844.83
10/4	5184	6925.77
11/9	6042	6804.08
12/2	6597	6733.84
1/12	7585	6780.15

Equipment

VCS-10 simulator apparatus
 2 lamps illuminant I-14WT12 daylight simulation
 E G & G Spectroradiometer Model 555-66

Procedure

Two lamps chosen at random from manufacturers batch. Lamps mounted in VCS-10 apparatus and turned on March 2, 1982. Lamps were left on continuously during test period through 1/12/83. An E G & G Spectroradiometer was aimed at the lamps and read at least every 2 months during the test period.

^aAverage color temperature = 6886.64.

A variety of disk coloring techniques was attempted, including coating systems, printing systems, and laminations of plastic film. We found that the most practical reproducible technique was screen printing using inks with pigments of stability to withstand more than 1000-h QUV artificial weathering exposure. The following pigment types were chosen:

Yellow—Pigment Yellow 93

Green—Pigment Green 7

Violet—Violet 23

Blue—Pigment Blue 15

Red—Pigment Red 104 blend with pigment Red 149

Orange—Pigment Red 104

A quality control technique for the printed disks has been developed which provides excellent color reproducibility from set to set (Table 2). All disk quality control is accomplished under spectrophotometric control. For each set of three disks, a batch centroid is located and a chromatically balanced pair, based on lightness/darkness, is chosen. The set of three, when spun,

TABLE 2—Visual Color System disk set color calculations.

CIELAB	ILL	X	Y	Z	L*	a*	b*	C*
1. COMPARE SEGMENTS TO STANDARD								
Green standard	I	17.33	33.85	11.20	64.84	-61.78	46.99	77.62
Green disk-centroid	I	16.49	32.56	10.70	63.81	-62.03	46.60	77.58
Green disk-lighter	I	18.34	35.36	11.83	66.03	-61.41	47.34	77.54
Green disk-darker	I	17.22	33.69	11.13	64.71	-61.87	46.96	77.76
CIELAB	ILL	DL*	Da*	Db*	DE*	DC*	DH*	
Green RO/16	I	-1.04	-0.25	-0.40	1.14	-0.04	0.47	
Green RO/16	is	1.04						
		darker than Green RO/10						
Green RO/16	is	0.04						
		duller than Green RO/10						
Green R1/20S	I	1.18	0.36	0.35	1.29	-0.07	-0.50	
Green R1/20S	is	1.18						
		lighter than Green RO/10						
Green R1/20S	is	0.07						
		duller than Green RO/10						
Green R2/112	I	-0.13	-0.09	-0.03	0.16	0.05	0.08	
Green R2/112	is	0.13						
		darker than Green RO/10						
Green R2/112	is	0.05						
		brighter than Green RO/10						
2. COMPARE AVERAGE READINGS OF SEGMENT SET TO STANDARD								
CIELAB	ILL	X	Y	Z	L*	a*	b*	c*
Green standard	I	17.33	33.85	11.20	64.84	-61.78	46.99	77.62
Green/average of all three disks	I	17.35	33.87	11.22	64.86	-61.75	46.96	77.58
CIELAB	ILL	DL*	Da*	Db*	DE*	DC*	DH*	
Green/O11	I	0.02	0.03	-0.03	0.04	-0.04	0.01	
Green/O11	is	0.02						
		lighter than Green RO/10						
Green/O11	is	0.04						
		duller than Green RO/10						

create a repeatability as a set of less than one delta E CIELab. This quality control technique, based on ACS colorimetric experience, indicated that each set of disks can be dependably supplied, providing reproducible results from instrument to instrument.

The pigments chosen and the additive effect of the disks have created a wide color gamut in simulated daylight. This gamut can be represented in the CIE diagram which, although it only represents a slice through color space, is an indication of how broad the gamut is. As an initial review of the system, we reviewed various color palettes. Shown in Fig. 1 is a typical architectural paint pigment colorant palette superimposed within the gamut of the VCS disk

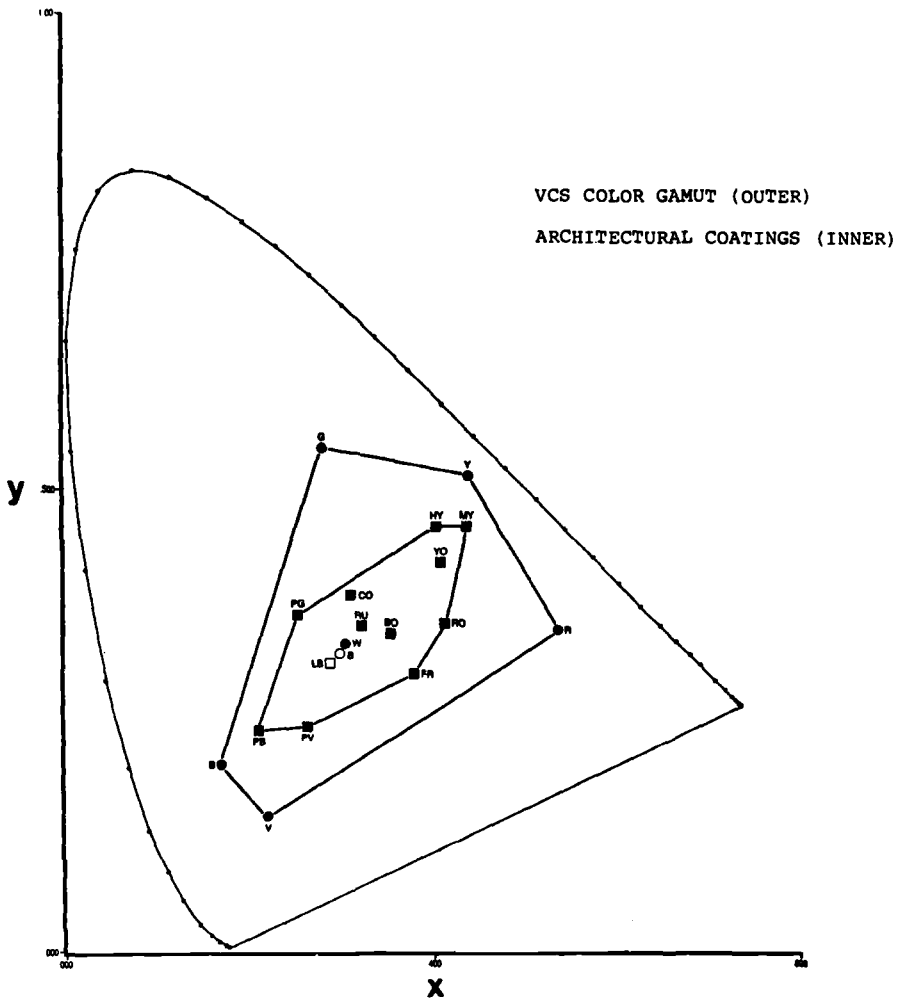


FIG. 1—CIE chromaticity diagram.

gamut. The present disk sets will provide styling capability for most industrial colorant palettes. However, since all real colorants have limitations in visual appearance, there will be some colors that cannot be simulated. In these cases, additional colors or modifications to the disks may be required.

We initiated studies using area modification and masking techniques to provide simulations to give the effect of metallic systems, high/flat gloss, and other visual appearances. Continued development work is expected in these areas to provide the broadest gamut of color simulation capabilities. Software factors have also been developed so that one color simulation can be used to create color simulation data for products having the same color but various gloss levels. It was found that samples of several gloss levels must be simulated separately to give the proper visual representation. The computer calculation of the colorant formula, however, is achieved in the same manner for both high and flat gloss levels.

VCS Operation and Logic

When the VCS is turned on, the main drive motor spins the complete disk pack. As the drive motor comes to full speed, the viewer light system is turned on automatically. Each set of segments has a distinctive bar code located on the outer edge of the segments. These bar codes are arranged in such a manner that their location identifies disk color. Three optical reading heads are mounted at 120° intervals around the circumference of the disk pack. As the pack spins, each of the optical sensors reads a section of the bar codes. A microprocessor samples the output of these devices and automatically identifies each of the segments exposed and calculates the exposed area. This data, sampled several times a second, is displayed at the operator's keyboard (Fig. 2). Thus, as the disks are moved by the planetary gear motors and drive gear mechanism, the operator will see both the color change and change of the area data as response to his motion of the control switches. The significance of reading the actual area exposed compensates for any possible mechanical malfunction in the movement of the disks; that is, the unit reads only the actual disk area being viewed by the operator. Complete operation, electronic distribution, and the display mechanism are fully automated. The miniaturization of the components and the consolidation of the micro controls allows the device to be offered in a practical size for most styling and industrial quality control laboratory locations.

The control panel is engineered to allow the operator to change the area of each of the colors in the disk pack and is provided with a jog switch that allows minute step-by-step color changes to see exacting color modifications. The operator sees the actual color and is able to compare and contrast that color to color chips or other actual sample materials. The Visual Color System thus simulates real color to the observer and yet captures the colorimetric data output on a repeatable and reproducible basis. Software is available that



FIG. 2—VCS with system operator.

will convert the data output of the Visual Color System and calculate reflectance curves that can be inputted to formulation systems, colorant search programs, or batch correction programs. The complete product package includes the Visual Color System and color software for ACS Chroma-Pac licensees.

VCS Performance

The three major elements, that is, lighting, disk elements, and logic, when brought together, were tested in a number of ways. The actual versus calculated device output was measured by a spectroradiometer aimed at the spinning disks and then calculating the theoretical ratio between various settings of the disks. We found the correlation coefficient between calculated and

measured to be 0.9995. The reliability of the device to perform across the full area of the disk settings is highly predictable.

Further tests were run using sample colored panels, measuring them on a spectrophotometer, taking the calculated VCS settings directly from an ACS Color Control System, and setting them up on the Visual Color System. A panel of observers indicated that the first settings were within a visual match of the panels provided. Both trained and random observers tested a broad range of samples in this manner.

Similar tests have been accomplished by generating VCS data and calculating colorant formulations, preparing material samples of the formulations, creating a product/sample, and comparing the formed sample to the VCS disk appearance at the calculated settings. Continued field testing is in progress on a wide number of industrial applications to assure the correlation be-

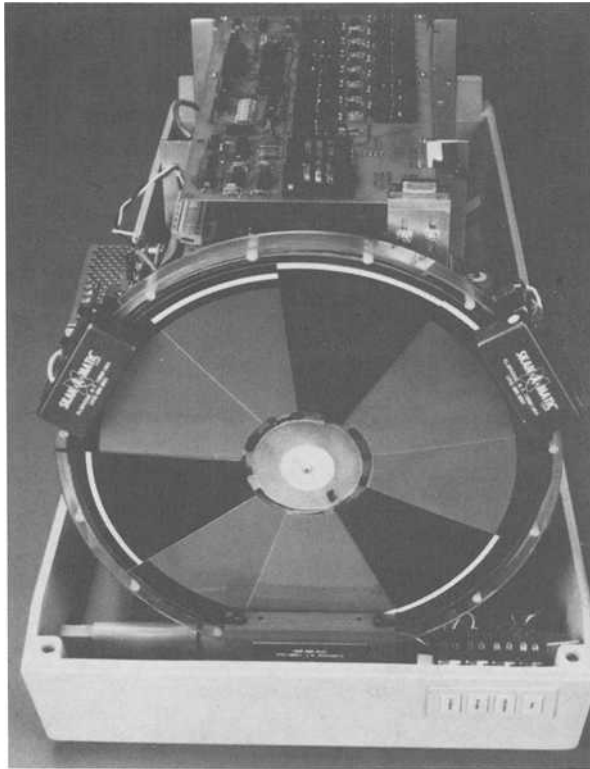


FIG. 3—A frontal view of the interior of the Visual Color System. Showing the disk pack and the optical sensors, positioned at 10:00, 2:00, and 6:00. The optical sensors "read" the length of the white bars along the circumference of the disk pack.

tween the color appearance of the Visual Color System and actual production of colored materials.

Practical Use of the System

It has been indicated that the Visual Color System can allow a product designer/stylist to generate millions of colors of great color gamut and to repeatedly see these colors on one device, and when giving the same data to

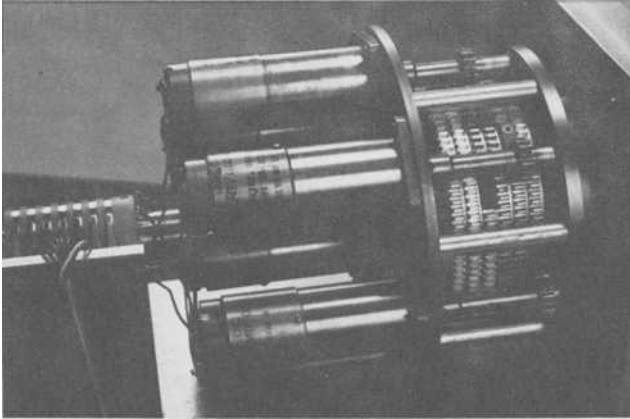


FIG. 4—Close-up of planetary gear motors and gearing mechanism. These motors control the operation of the gears, which control operation of the individual disk segments.

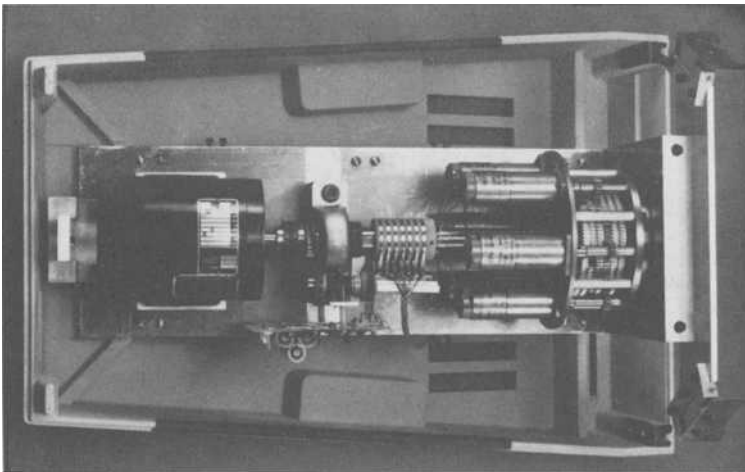


FIG. 5—Overhead view of the interior of the system, showing main motor at rear, dedicated planetary gear motors and gearing mechanism.

another operator, see the same color on a second device. This capability is already providing the basis for color communications in multi-plant operations, and is being utilized to create color standards between designer/specifier, manufacturer, and colorant suppliers. It is being tested to be utilized to store color standards and serve as a replacement for initial sample preparation. The device is also useful in the development of new colors for new product lines or special custom colors. The device (Figs. 2 through 5) is seriously being tested in the development of new sales concepts for merchandising paints, inks, textiles, and plastic compounds.

This concept is currently used by the appliance, automotive, textile, and coatings industries in choosing colors and formulating these colors for specific products. As a color development product, a communications product, and a merchandising product, the device seems to have broad significant practical potential in many industries. We feel that this device offers the first opportunity for a colorist to create visually real colors under reproducibly automatic viewing conditions that can simulate actual production applications. The invention has been created; the usefulness is now being proven by a large variety of industrial users.

References

- [1] Rodriguez, A. B. J., "Total Instrumentation In Color Manufacture," *Journal of Coatings Technology*, Vol. V51, No. 648, 1979.
- [2] Beck, J., *Surface Color Perception*, Cornell University Press, Ithaca and London, 1972.
- [3] Kawakami, G., "The Appearance of Color Differences Under Varying Conditions of Viewing," *Acta Chromatica*, Vol. 3, No. 2, 1978, pp. 87-92.
- [4] Chamberlin, G. J. and Chamberlin, D. G., *Color, Its Measurement, Computation and Application*, Hayden & Sons, Ltd., London, Philadelphia, Rheine, 1980, pp. 24-26.
- [5] Judd, D. B. and Wyszecki, G., *Color in Business, Science and Industry*, 3rd ed., John Wiley & Sons, New York, 1975, pp. 66-68.
- [6] Mac Adam, D. L., *Color Measurement, Theme and Variations*, Springer-Verlag, New York, 1981, pp. 48-49.
- [7] Maxwell, J. C., "On the Theory of Compound Colors and the Relations of the Colors of the Spectrum," *Proceedings of the Royal Society*, London, Vol. 10, No. 404 484, 1860, and *Philadelphia Magazine*, Vol. 4, No. 21 141, 1860, Scientific Paper, pp. 149.
- [8] Worn, P. R., Stanzola, R. A., and Hall, D. R., "Reflected Color Simulator," United States Patent 4,310,314, 1980.

William B. Cowan¹

On the Specification of Heterochromatic Brightness

REFERENCE: Cowan, W. B., "On the Specification of Heterochromatic Brightness," *Review and Evaluation of Appearance: Methods and Techniques, ASTM STP 914*, J. J. Rensilison and W. N. Hale, Eds., American Society for Testing and Materials, Philadelphia, 1985, pp. 92-102.

ABSTRACT: For many years it has been known that luminance, the CIE quantity best correlated with perceived brightness, does not work well for many colors. Consequently, the CIE charged a technical committee to find a better solution. The National Research Council of Canada, responding to the committee, has produced a function that can be used to correct luminance to produce predictions for brightness matches. This function, which is empirical, based on the extensive data that have been taken on brightness, is summarized in this report.

KEY WORDS: luminance, brightness, colors

This paper reports some results from a project that has occupied many years of manpower over the last decade at the National Research Council of Canada (NRCC). The purpose of this project has been to find a method whereby the brightness judgments (for example, which of two stimuli is the brighter?) of human observers can be predicted. The NRCC project, which has involved many scientists (the author, C. Ware, G. W. Wyszecki, M. E. Breton, and D. Alman, to name only those directly involved) has been part of a larger effort, coordinated by the Heterochromatic Brightness technical committee of the Commission Internationale de l'Eclairage (CIE). This paper summarizes some aspects of a proposal for an interim solution to the problem of specifying brightness judgments, which has been presented by the NRCC to the CIE. In it we will try to go through the reasoning that led us to the particular solution that has been proposed, and then to give the details of the solution, and how it is to be used.

¹Associate research officer, Division of Physics, National Research Council of Canada, Ottawa, Ontario, Canada K1A 0R6.

This report is intended only to be an informal summary of the work that has been carried on at the NRCC. Readers who wish to know more about this work may contact the NRCC to get a copy of the technical report [1], which gives full details of the procedure and results of this project, and which also contains a complete collection of references on the problem of specifying heterochromatic brightness.

Why Brightness is a Problem

Brightness judgments are psychophysical judgments. What this means is that a physical stimulus, for example, a lighted area, gives rise to a psychological response, the sensation of brightness. The brightness judgment represents a correspondence between a physical quantity and a psychological quantity. An adequate brightness specification is a method that, given the physical specification of the stimulus, will generate the relevant brightness attributes. A simple way of doing this is to use a human observer, showing him the stimuli in question, and asking him what his judgment is. The convenience and limitations of such a solution are too obvious to mention. As a complement or replacement or both for the human observer we would like to find a method whereby one or more photodetectors can be used to analyze the physical properties of the stimulus, and a calculation based on those measurements can be used to specify brightness. There are two fairly obvious methods for doing this, neither of which is successful, and before discussing the method we settled on, we will briefly mention their drawbacks.

Luminance

It has long been known that the CIE 1924 luminance specification is fairly well correlated with human brightness judgments. That is, if two stimuli S_1 and S_2 have the same chromaticity, then their relative brightnesses are the same as their relative luminances. To be specific, if $Y(S_1)$ is the luminance of stimulus S_1 , then S_1 is brighter than S_2 if and only if

$$Y(S_1) > Y(S_2)$$

and S_1 is equally bright as S_2 if and only if

$$Y(S_1) = Y(S_2)$$

It is tempting to extend this to lights that differ in chromaticity, defining brightness by means of luminance, so that brightness relationships are determined by luminance relationships, as in the two equations above. Using luminance like this has several significant advantages:

1. The definition of luminance through the CIE 1924 $V(\lambda)$ function is already in wide use.

2. Luminance is additive. The luminance of the additive mixture of two stimuli is the sum of the luminances of the two stimuli

$$Y(S_1 + S_2) = Y(S_1) + Y(S_2)$$

3. Because luminance is additive it may be calculated from a luminous efficiency function that specifies the luminous efficiency of each wavelength of a stimulus.

$$Y(S) = K_m \int V(\lambda) S_\lambda d\lambda$$

where S_λ is the spectral power distribution of the stimulus S , and $V(\lambda)$ is the CIE 1924 luminous efficiency function.

4. Because photodetectors integrate their input signal with respect to a sensitivity function, and because luminance is defined by integration it is possible to build inexpensive meters to measure luminance. This is done using filters to modify the sensitivity function of the photodetector until it matches $V(\lambda)$.

Luminance has, however, one important disadvantage. Stimuli equal in luminance do not appear equally bright when they differ in chromaticity. This difference is small when the lights are close in chromaticity, but gets large when the chromaticities are very different. For example, a yellow or white light must be twice as luminous as a saturated red light in order to appear equally bright. This is about as large as the discrepancy gets, so that luminance is adequate as a measure of brightness when errors as large as factors of two or three may be neglected.

A Brightness Efficiency Function

The advantages of luminance, listed above, suggest that it might well be worth trying to find a "brightness efficiency function" analogous to the luminous efficiency function. Thus, if the brightness efficiency function were $\hat{B}(\lambda)$, then we could calculate

$$\hat{B}(S) = \int \hat{B}(\lambda) S_\lambda d\lambda$$

and have lights ranked in brightness according to the value of \hat{B} calculated for them. This system shares several advantages with the use of luminance, to wit:

1. It is easy to calculate brightness once the brightness efficiency function is known.

2. Inexpensive meters can be built using filters and photodetectors to emulate the brightness efficiency function.

The problem is that brightness is not additive. That is, if $B(S)$ is a function defined so that all lights S that are judged to be equal in brightness have the same $B(S)$ value, then $B(S)$ cannot be defined so that

$$B(S_1) + B(S_2) = B(S_1 + S_2)$$

The integral form determined by the brightness efficiency function has just such a property, so that we can be sure that the brightness efficiency function is inadequate as a description of human brightness judgments.

The Specification Problem

To go beyond the unsuccessful attempts discussed previously, it is necessary to consider theories, models, and data: what they are, and how they interact to produce answers to specification problems, such as the brightness one.

Theories

A theory is a description of the system under consideration, its parts, and their interactions. The terms of the theory refer to the system as it actually exists. That is, they refer to real objects. For example, a theory of brightness might encompass:

1. An image—consisting of photons, having a spectral power distribution, and so on.
2. The eye—consisting of optics, photoreceptors, and so forth, and having such important properties as spectral sensitivity and so on.
3. The optic nerve—having coding properties for color, such as opponent colors.
4. The brain—taking input from the optic nerve, and producing sensations such as motion, hue, brightness, and so on.

The theory would refer to such objects, doing its best to describe their properties and their interactions, in so far as they contribute to the behavior that is of interest to the theory.

Models of Theories

A model of a theory is a particular description of the theory, one which produces a correspondence between parts of the theory and a formalism, usu-

ally mathematical, which can be used to make concrete theoretical properties. For example, a mathematical model of the above theory would consist of

1. A spectral distribution corresponding to each point in the image, $P_\lambda(x)$ where x refers to position in the visual field.

2. Cone spectral excitations, $R(x)$, $G(x)$, $B(x)$, defined in terms of cone sensitivity functions $\bar{r}(\lambda)$, and so forth

$$R(x) = \int \bar{r}(\lambda) P_\lambda(x) d\lambda$$

The excitations vary from point to point in the visual field. Equivalently, tristimulus values, $X(x)$, $Y(x)$, $Z(x)$, defined in terms of color matching functions, could be used.

3. Equations for an opponent colors representation, which might be something like the following three:

An achromatic channel

$$A(x) = R(x) + G(x)$$

A red/green channel

$$R/G(x) = R(x) - G(x)$$

A yellow/blue channel

$$Y/B(x) = A(x) - B(x)$$

Note that the model specifies exactly how to calculate channel excitations at each point in the visual field.

4. Equations that describe the process whereby the brain determines brightness from the channel excitations.

$B(x)$ = the result of some calculation involving $A(x)$ and so forth

A structure such, as the one just described, is called a model because numbers (and functions, and so forth) stand for real things, such as photons or cones.

Clearly, a correct theory, and an accurate model of the theory is the perfect solution to the specification problem. The model will produce numbers that reflect human brightness judgments just because it is imitating the process whereby those judgments are produced in the human visual system. And the model is the ultimate solution, since it will change only in the unlikely event that the human visual system changes.

Unfortunately there is no successful model that explains the working of the visual system to the level of brightness. In fact, there are many models, none of which is widely accepted, and none of which remains constant from year to year. This suggests that vision scientists are still groping in the dark when trying to explain brightness, and it is impossible to know whether a successful theory will be available next year or next century. It is possible to give a few reasons why a good theory of brightness may not be forthcoming in the near future:

1. Brightness is part of color appearance, as are color constancy, adaptation, induction, and so on, and there is little theorizing that comes successfully to terms with much of this body of phenomena.
2. Brightness depends on spatial properties of stimuli. How bright an object looks depends not only on the amount of light it emits, but also on the amount of light neighboring objects emit. This suggests that zone theories of color vision, which are the best current attempts at visual theorizing, may not be adequate to explain brightness.
3. There is large variability in brightness judgments, both from person to person and from day to day.
4. Brightness has many meanings: brilliance, gloss, luminosity. We may well need a tighter definition (or definitions) before a good theory can be constructed. The multiple meanings of brightness may well be connected with the variability noted above.

Data

Accepting the likelihood that the immediate future will not produce a theory of the visual system that is adequate to explain brightness, we turned to the data, to see if there was a possibility of producing an interim solution that would be useful until such a time as there is a good theory to explain brightness. There is a considerable body of data that has been taken on this topic over the last 25 years or so. In general, the data come from experiments where several test stimuli of varying chromaticity were matched in brightness to a reference stimulus. What is available from such an experiment is

- (1) the chromaticity of the test stimulus x, y ,
 - (2) the luminance of the reference stimulus at the brightness match L_B ,
- and
- (3) the luminance of the test stimulus at the brightness match L_0 .

Among the studies that we were able to obtain, there were over 6000 data points of this form, an impressive number. But it would be unlikely that any particular light(s) of which a user wished to know the brightness would be among those 6000. Thus we need to model the data in some way.

A Model of the Data

A model of the data is created in a manner analogous to the way that a theory is modelled. That is, the data are described by mathematical functions that can be calculated at any point in color space. To do this it is necessary to make one assumption, that the data sample the underlying function densely enough that data points that could be derived between existing data points would be reasonably fit by interpolation. We can then fit a curve through the data whereupon a result can be derived for any value of the parameters. The result derived is designed to conform as closely as possible with the existing data; it is not the reflection of any theory of the system, since the only assumption involved in the modelling process is that the data should sample the parameter space densely enough that they actually show us all the irregularities that a measurement of every single point would reveal.

Models of data may be very simple or very complicated. They tend to be simple when the data in question depend on only a few different variables (degrees of freedom) and when the data vary slowly and smoothly as the variables change. They tend to be complicated when the data depend on many variables, and when it varies quickly and irregularly when the variables change.

Our Model of the Brightness Data

The purpose of our model of the data is to predict the equivalent luminance L_B , given the colorimetric specification of a stimulus L_0 and x, y . This prediction gives us the results of brightness matches, since two stimuli are equally bright if they are equivalent in brightness to the reference stimuli of the same luminance. We will consider L_B to be a multiple of L_0 , and try to predict how this ratio varies as the colorimetric coordinates of the test stimulus vary. The data show that over a wide range of luminance the ratio does not depend on luminance. Thus, we can define the conversion function $C(x, y)$ by

$$C(x, y) = \log(L_B/L_0)$$

Our objective was to find a parametric form for the conversion function. Noting that it varies slowly as the chromaticity coordinates change, we decided to form an expansion of the function in terms of x and y .

$$C(x, y) = a_{00} + a_{10}x + a_{01}y + a_{20}x^2 + a_{11}xy + a_{02}y^2 + \dots$$

The problem was then to find the coefficients a_{ij} , which best represent the 6000 data points. To do so, we

(1) collected as much data as we could find. We did a literature search, and conducted a mail survey to authors of papers that turned up in the search.

(2) reduced all the data to give L_B , L_0 , x , and y . Not all data could be so reduced because some studies gave inadequate colorimetric specification of their stimuli. At this point we had over 6000 data points.

(3) checked the data for consistency, to find a set of viewing conditions for which the coefficients a_{ij} do not depend on noncolorimetric parameters of the stimulus. After finding the conditions, given in detail below, we kept all points from studies which used viewing conditions that fulfilled the conditions. At this point we had more than 3000 points.

(4) did a least squares regression, varying the coefficient values to find the ones that best fitted the data.

(5) minimized the number of coefficients, consistent with the object of faithfully reproducing the data.

More details of this data reduction process are available in a technical report available from the author of this paper [2].

The Conversion Function

Recollecting some definitions, x , y , and L_0 are the chromaticity coordinates and the luminance of a stimulus for which brightness relations are desired, and L_B is the luminance of a reference stimulus that is equal in brightness to the colored stimulus. The luminance conversion function is defined so that

$$L_B = L_0 10^{C(x,y)}$$

or, in terms of the logarithms

$$\log(L_B) = \log(L_0) + C(x, y)$$

We call $C(x, y)$ the conversion function, and its value, which is used to make a particular conversion, the conversion factor. After performing the regression, as described above, we determined the conversion function to be

$$C(x, y) = 0.256 - 0.184y - 2.527xy + 4.656x^3y + 4.657xy^4$$

The function is normalized at D_{65} , so that the conversion factor for a stimulus of the same chromaticity as D_{65} is 0.0.

For practical use we show in Fig. 1 a contour diagram, where the conversion factor is shown for different chromaticities. Actually, the figure shows contours of $10^{C(x,y)}$, since those values, which multiply the luminance, are probably more useful. The conversion factor for a given stimulus can be determined either by evaluating the equation for $C(x, y)$, or by interpolating between contours on the diagram.

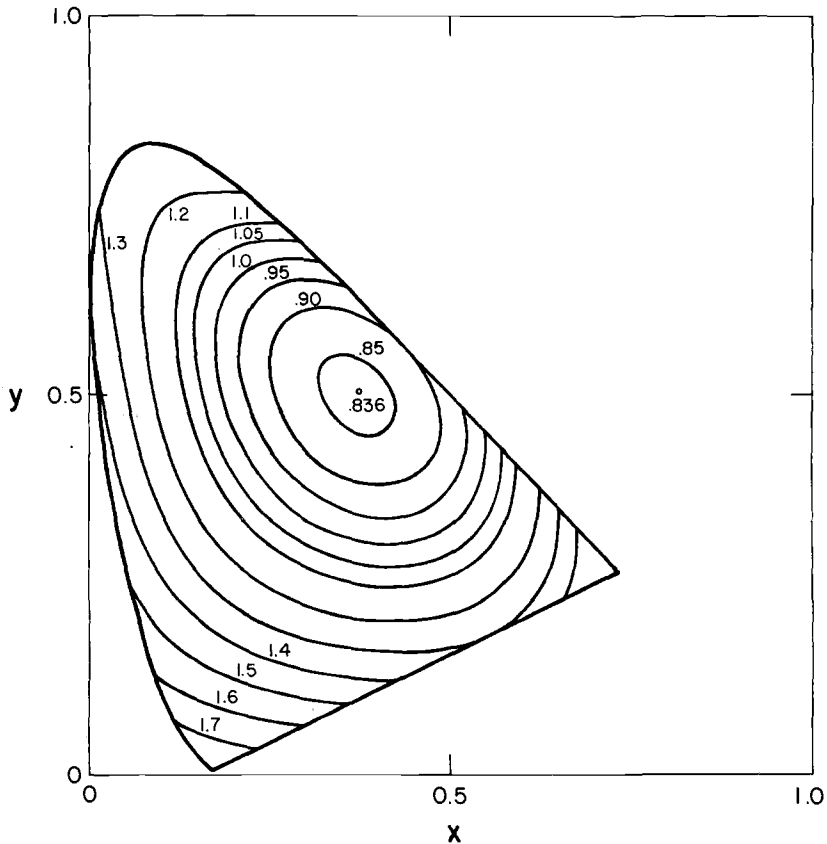


FIG. 1—A contour plot showing the variation of the conversion factor as a function of chromaticity. What is plotted is actually $10^{C(x,y)}$. This is the factor that multiplies the luminance to generate equivalent luminance so that brightness comparisons can be made.

The conditions under which the factor so determined is valid are

- (1) size of stimulus between 0.5 and 3.0° ,
- (2) luminance of stimulus greater than 2.0 candelas/ m^2 ,
- (3) stimuli that are to be compared in brightness have similar colored surrounding areas,
- (4) the ambient illumination is neutral, and
- (5) the y value of the chromaticity coordinates of the stimulus is greater than 0.02 . This is necessary because data are sparse in this region of color space, and the function changes rapidly, so that it is dangerous to interpolate.

To give an example of the use of the conversion function, here is the procedure for determining which of two color stimuli is the brighter.

1. Determine the colorimetric coordinates (x , y , and L_0) of each stimulus.
2. Calculate the conversion factor $C(x, y)$, using the conversion function or the contour diagram.
3. Calculate

$$L_B = L_0 10^{C(x,y)}$$

for each stimulus. Alternatively, $\log(L_B)$ can be calculated if it is more convenient.

4. Whichever stimulus has the greater value of L_B , or $\log(L_B)$, will be seen to be brighter by the average observer.

Unresolved Questions

The conversion factor discussed in this report does not totally solve the problem of calculating the brightness of colored stimuli. There is, to begin with, the question of finding a good theory that will explain how brightness perception is accomplished by the visual system. The resolution of this problem, as has been mentioned, is most likely many years in the future. It awaits, in our opinion, the existence of a good (and comprehensive) theory of color appearance, and it ought to produce, not only a brightness ranking, as the conversion function does, but also a brightness scale. Such a theory contains many unsolved puzzles, such as color constancy, simultaneous contrast, and many others, and must become, in the years ahead, of more and more importance to scientists who study color. For an interesting example of this, more ambitious, approach to the brightness specification problem see Ref 2, which includes further references to this type of modelling.

In the meantime, the work that produced the conversion function indicates that there are significant gaps in the present brightness data. More data are desirable examining the variation of brightness judgments as the following degrees of freedom are varied:

1. *Field Size*—The conversion function handles stimuli from 0.5° to 3.0° . Smaller stimuli seem to have brightness that follows luminance exactly, but data from nonspectral stimuli are needed to confirm that finding, and data at varying field sizes are needed to allow some kind of interpolation between the present conversion function and luminance. For larger stimuli there is just enough data to show that the conversion function must be altered. The relation between large field brightness data and the ten degree color matching functions must be examined.

2. *Low Light Levels*—It is well known that brightness judgments change at low light levels, presumably because rods begin to have an influence. Significant amounts of data are needed before we can consider building a conversion function that takes this effect into account.

3. *Adaptation/Induction Effects*—There is little data which takes adaptation or induction or both into account for brightness judgments. The number of degrees of freedom involved here is large, and the quantity of data needed to extend the conversion function to include these effects may well be unmanageable. If so, theoretical understanding of these effects may be needed before brightness judgments can be systemized for these degrees of freedom.

One final issue must be addressed in further investigations of brightness. It is: "What is brightness used for?" The data used in the present work are all taken under conditions where observers see two extended stimuli at the same time and match them with respect to their perceived brightness. In practice, an observer is likely to be doing some task, for example, looking for colored lights on a display. The display designer really wants to know how to calculate how well the observer will be able to use the stimuli to do the task he has to do. This is often called the visual salience of the stimulus. In using brightness he is assuming that brightness and visual salience for his task are the same thing, but they may not be at all. Research in this field must begin to look at the question of visual salience and how it varies from task to task. Such study is necessary to discover when it is relevant to use the present conversion function, and whether others may be needed.

Acknowledgments

The work done in this report has been done in the Optics Section of the Division of Physics of National Research Council (NRC) under the continuous direction and encouragement of the late Gunter Wyszecki. Colin Ware was a collaborator on the work that produced the conversion function, and much of the data that were used in the study were produced by earlier Research Associates in our laboratory, of whom Dave Alman and Michael Breton are the most notable.

References

- [1] Ware, C. and Cowan, W. B., "Specification of Heterochromatic Brightness Matched: A Conversion Factor for Calculation Luminances of Stimuli Which are Equal in Brightness," National Research Council of Canada Technical Report, Ottawa, Ontario, Canada, 1984.
- [2] Bartleson, C. J., "Measures of Brightness and Lightness," *Die farbe*, Vol. 28, 1980, pp. 132-148.

Author Index

B-D

Billmeyer, Fred., Jr., 3, 14-32
Cohn, Theodore E., 4, 69-77
Cowan, William B., 3, 93-102
DeGross, James T., 4, 79-91

G-J

Glicksberg, Susan, 40-48
Hale, W. N., editor, 1-4
Hauch, Laurie A., 40-48
Hunter, Richard S., 2, 5-13
Johnson, Norbert L., 3-4, 49-61
Jungman, David, 4, 62-68

K-M

Kwan-Nan Yeh, 40-48
Lozano, Roberto D., 4, 62-68
Melcón de Bellora, Cristina, 4, 62-68

O-R

O'Donnell, Francis X. D., 3, 14-32
Rennilson, Jay J., editor, 1-4
Robertson, Alan R., 2-3, 33-39

Subject Index

A

- Adaptation effects, 102
- Air contamination, evaluation of, 1
- ANLAB color difference formula, 37
- Aperture, 5; illustration, 6
- Appearance
 - evaluation of, 1
 - of food colors, 62-68
 - measurement principles, 2, 50
 - modes, 5-13
 - aperture, 5; illustration, 6
 - illuminant, 6; illustration, 6
 - object, 6-7; illustration, 6; table, 8
 - and perception, 1-2, 14-32
 - of retroreflectors, 49-61
 - use of technology in minimizing disorientation effect, 69-77
- Application-oriented
 - goniophotometry, measuring appearance of retroreflectors by, 49-61
- Application parameter, 52, 53, 55, 69, 70-73
- Applied Color Systems (ACS), 80
- ASTM standards
 - D 1729: 1
 - D 523: 3, 26
 - D 2244: 3
 - D 3134: 3
 - E 167: 51
 - E 179: 51
 - E 808: 51, 54; illustration, 54
 - E 809: illustration, 57

- ASTM Standards on color and Appearance Measurement, 2
- Autocorrelation analysis, 76

B

- Brightness, 97
 - heterochromatic, 92-102; illustration, 100
 - relationship between luminance and perceived, 3, 92-102; illustration, 100
 - visual judgment of, 14
- Brightness efficiency function, 94-95
- Brightness judgments, 92, 93, 97, 101

C

- Cartesian coordinate system, 52
- Chroma, weighting of, 36-37
- Chromaticity coordinates, 54
 - in CIE system of colorimetry, 33
- CIE
 - on color difference evaluation, 33-39
 - on heterochromatic brightness, 92-102
- CIE chromaticity diagram, 33
- CIELAB formula, 34-35, 36, 38
- CIELUV formula, 34-35, 37, 38, 63-64
- Coefficient of retroreflection, illustration, 57

- Color(s) (*See also* Gloss)
 appearance modes, 2, 5-13; illustration, 6, 11, 12; table, 8
 application of technology in, to industrial and agricultural situations, 1, 3, 78-91; illustration, 86, 88, 89, 90; table, 84, 85
 development of scales, 1
 evaluation of, 2, 5-13
 formulation of, 10, 13, 78-81
 judging brightness of, 92-102; illustration, 100
 measurement of
 on foods, 1, 4, 62-68
 surface, 9-10
 metamerism, 83
 order system, 3
 specification reference system, 79-80
 standard observation of, 80
 tolerance specification, 2-3, 33-39
- Color communications, 79-80
 concept development, 80-81
- Color Corporation of America, 81
- Color difference
 CIE work on evaluation, 33-39
 formulae, 34-35
 perception, 35-36
 specification, 3
- Colorimetry, 80
 CIE work on, 33-39
 and dye analysis of polyester fabrics, 40-48; table, 41, 42, 44, 45, 46, 47
- Committee E-12 on Appearance of Materials, 4
- Committee on Color Difference Evaluation (CIE), 2-3, 34, 35, 38
- Computer
 in appearance analysis, 50, 80
 formation of color by, 10, 13, 80
 in development of visual color technology, 78-91; illustration, 86, 88, 89, 90; table, 84, 85
- Contrast, 73
- Contrast gloss, 15
- ## D
- Deflection factors, 5-13
- Depth perception, and minimization of disorientation effect, 69-77
- Diffuse color measurements, 13
- Diffuse reflection, 7
 $D/0^\circ$ /geometry versus $0^\circ/45^\circ$ for, 9-10; table, 8
- Directionality, 15
- Disorientation effect, use of appearance technology in minimizing, 69-77
- Disperse dyes, use of, in dyeing polyester fabrics, 40-48; table, 41, 42, 44, 45, 46, 47
- Distinctness-of-image gloss, 15
 $D_{SEX}/0^\circ$ geometry, 10, 13
 $D_{SIN}/0^\circ$ geometry, 10, 13
- Duro-Test, Inc., 83
- Dye(s)
 accuracy of extraction, 40-41
 analysis of polyester fabrics, 40-48; table, 41, 42, 44, 45, 46, 47
 and color quality control, 4
- ## E
- Entrance angle, 51
- Escalator treads
 appearance of, 70-73; illustration, 71, 72
 evolution of design of, 70
 use of appearance technology in minimizing disorientation effect on, 4, 69-77

F

- Fabric dyeing (*See* Dyes)
- Filters, appearance of, and air contamination, 1
- Fish, measurement of color on, 64
- Fluorescents, 2
- Foods, measurement of color on, 4, 62-68
- Fruits, measurement of color on, 65-66

G

- German Deutsche Industrie Norm (DIN) color system, 79
- Gloss, 3 (*See also* Specular reflection)
 - evaluation of, 1, 2, 5-13
 - experimental verification of color relationships, 10, 12; illustration, 11, 12
 - psychometric scaling of, 3, 14-32; illustration, 18, 20, 21, 22, 23, 24, 28, 29; table, 19, 25, 27
 - types of, 14-15
 - visual scale of, 31
- Glossimetry, 26-27, 30-31
- Goniophotometry
 - application-oriented, 51-52
 - traditional, 51
- Goodness criterion, 75-77
- Grains, measurement of color on, 64-65

H

- Helmholtz reciprocal relation, 9
- Heterochromatic brightness, 92-102; illustration, 100
- Highlighting, 70
- Hue indices, weighting of, 36-37

I

- Illuminant, 6; illustration, 6 (*See also* Luminance)
- INDSCAL, use of, in analysis of gloss data, 17-18, 20, 21, 22, 26; illustration, 21, 23, 24; table, 19, 25
- Induction effects, 102
- Industrial applications, of visual color technology, 78-91; illustration, 86, 88, 89, 90; table, 84, 85
- Internal reflection, 7
- International Commission on Illumination (*See* CIE)

J-K

- JPC79, 37
- KYST, use of, in analysis of gloss data, 17, 18, 20-21, 22; illustration, 18, 22, 23; table, 19, 25

L

- Lightness, weighting of, 36-37
- Local coordinate system, 52, 53-54
- Luminance
 - pattern of, in escalator tread, 71; illustration, 72
 - relationship between perceived brightness and, 3, 92-102; illustration, 100
 - sign, 55, 60; illustration, 59
- Luminance autocorrelation, 76
- Luminance conversion function, 99
- Luster, 15

M

- Macroscopic surface properties, 15
- Maxwell spinning disk, 4, 80-81

Meats, measurement of color on, 63-64
 Metamerism, 83
 Metamers, 70
 Methods for Instrumental Evaluation of Color Differences of Opaque Materials (D 2244), 3
 MINISSA-1 (M), use of, in analysis of gloss data, 17, 21-22
 Multidimensional scaling (MDS), 17
 (*See also* INDSCAL; KYST; MINISSA-1(M); PINDIS)
 Munsell color book, 79

N

National Institute of Industrial Technology (INTI), measurement of color on foods at, 62-68
 Nondestructive tests, use of, in dye analysis, 40-41
 Nonenzymatic browning, 63, 66

O

Object mode, 6; illustration, 6; table, 8
 submodes of, 6
 Observation angle, 51
 Orange peel, 15

P

Packaging, selecting colors for, 4
 Perception, and appearance, 1-2, 14-32
 Periodicity, 71
 Photodetectors, 94
 Photoelectric instruments, use of, in appearance evaluation, 1
 PINDIS, use of, in analysis of gloss data, 17; illustration, 22, 24, 28-29; table, 19, 25

Polyester fabrics, colorimetric determination of dye content on, 40-48; table, 41, 42, 44, 45, 46, 47
 Psychometrics, 14-32
 Psychometric scaling, of gloss, 3, 14-32

R

Recommended Practice for Selecting and Defining Color Gloss Tolerance of Opaque Materials for Evaluating Appearance (D 3134), 3
 Reflected light, 7
 Reflection (*See also* Diffuse reflection; Specular reflection)
 geometric conditions for the measurement of color, 7, 9
 Reflection haze, 15
 Replicate option, 17-18
 Retroreflectance. *See* Retroreflectors
 Retroreflection (*See* Retroreflectors)
 Retroreflectors
 measuring appearance of, by application-oriented goniophotometry, 3-4, 49-61
 visual appearance of, 55-60
 coefficient of retroreflection, illustration, 57
 headlamp angle, illustration; 58
 headlamp luminous intensity, illustration, 59
 measuring angle, illustration, 55, 56, 57
 sign luminance, illustration, 59
 Retroreflector measurement geometry, 54
 Rotation angle, 51

S

- Safety, use of appearance technology in minimizing disorientation effect on escalator treads, 4, 69-77
- Sensory Evaluation of Appearance of Materials, 2
- Sheen, 14
- Sign luminance, 55, 60; figure, 56-59
- Soxlet extractions, of dyes, 40-41
- Spatial frequency, 71-73
- Spectrophotometry, 80
 - and color analysis, 80
 - and dye analysis, 40-48
- Spectral reflection, 50
- Spectral responsivity, 50
- Spectrophotometer geometry illustration 3, 11
- Specular gloss, 14
- Specular reflection, 3, 7, 10, 14; table, 8
- Standard observation of color, 80
- STP 297, 5
- Swedish "Natural Color" system, 79

T

- Textiles, role of color as marketing factor, 4
- Texture, 15
- Tristimulus values, in CIE system of colorimetry, 33

U

- Uniform diffusion, 9

V

- Vegetables, measurement of color on, 66
- Visual Color System (VCS), 82, illustration, 88, 89, 90
 - design elements, 83-88
 - lighting system, 83; table, 84
 - object, 83-87; illustration, 86; table, 85
 - operation and logic, 87-88
 - performance, 88-90
 - practical use of, 90-91
- Visual color technology, industrial applications of, 78-91; illustration, 86, 88, 89, 90; table, 84, 85
- Visual depth illusion, 70, 73-75
- Visual gloss scales, 1, 3
- Volume-color mode, 7

W-Y

- Wallpaper illusion, 73, 74
- Yerba Mate, measurement of color on, 66

ISBN 0-8031-0480-4